

A 32 SUB-BAND/TRANSFORM CODER
INCORPORATING VECTOR QUANTIZING
FOR ADAPTIVE BIT ALLOCATION

by

Courtney D. Heron

Submitted to the
DEPARTMENT OF ELECTRICAL ENGINEERING AND COMPUTER SCIENCE
in partial fulfillment of the requirements
FOR THE DEGREES OF
BACHELOR OF SCIENCE
and
MASTER OF SCIENCE
at the
MASSACHUSETTS INSTITUTE OF TECHNOLOGY
February 1983

(c) Courtney D. Heron, 1983

The author hereby grants to MIT permission to reproduce and to
distribute copies of this thesis document in whole or in part.

Signature of Author

Department of Electrical Engineering and Computer Science,
October 8, 1982.

Certified by

Thesis Supervisor (Academic)

Certified by

Company Supervisor (VI-A Cooperating Company)

Accepted by

Chairman, Departmental Committee on Graduate Students

Archives
MASSACHUSETTS INSTITUTE
OF TECHNOLOGY

MAY 27 1983

LIBRARIES

**A 32 SUB-BAND/TRANSFORM CODER
INCORPORATING VECTOR QUANTIZING
FOR ADAPTIVE BIT ALLOCATION**

by

Courtney D. Heron

**Submitted to the Department of Electrical Engineering and
Computer Science February 1983 in
partial fulfillment of the requirements for the Degrees of
Bachelor of Science and Master of Science in
Electrical Engineering**

ABSTRACT

Recently frequency domain techniques for coding digital voice have received considerable attention. Sub-band coding (SBC) with 2 to 12 frequency bands and a relatively low computational complexity is at one end of the scale. Adaptive transform coding (ATC) with 128 to 256 bands and relatively high computational complexity is at the other end of the scale. At coding rates of 16 kb/s ATC is generally rated to be superior in quality to SBC. In this thesis the middle range of complexities and channel bandwidths between those of SBC and ATC have been investigated by experimenting with new techniques for 32 band sub-band/transform coding at 16 kb/s. Dynamic bit assignment and adaptive quantization of the sub-band signals have been accomplished with a new spectral side information model consisting of a switched source of all-pole spectral templates in accordance with recent concepts of vector quantizing and clustering methods. Two new designs for 16 kb/s 32 band sub-band/transform coders which were simulated on a general purpose digital computer are presented.

Informal listening tests were carried out to compare the quality of these coders with previous SBC and ATC designs. The coders were also compared on the basis of computational complexity. The overall results appear promising, indicating that the new coders have a quality similar to ATC with about three times the complexity of 4 band SBC. Suggestions are made for further research of these middle range techniques.

**Academic Thesis Supervisor: Dennis H. Klatt
Title: Senior Research Scientist**

**Company Thesis Supervisor: Ronald E. Crochiere
Title: Member of Technical Staff, Bell Laboratories**

ACKNOWLEDGMENTS

I wish to express my sincere gratitude to my advisor at Bell Laboratories, Dr. Ronald E. Crochiere, for his guidance, encouragement, and helpful suggestions. Further special thanks is due to Dr. Richard V. Cox for his continued advice and enthusiasm. His assistance in software development and in the learning of the computer system has been invaluable. I owe special thanks to Dr. Lawrence R. Rabiner for providing the software for the clustering algorithm used for generation of the spectral templates. I am also particularly indebted to Dr. James L. Flanagan of Bell Laboratories for inviting me to work in his department and for providing all the necessary facilities, and to Dr. Dennis H. Klatt of MIT for agreeing to be my thesis supervisor.

I would like to thank Dr. Ronald E. Crochiere, Dr. Ronald E. Sorace, Dr. Richard V. Cox, and Dr. Dennis H. Klatt for their helpful and thorough comments on earlier versions of this manuscript. Special thanks is also due both the the Word Processing and the Drafting Departments of Bell Laboratories for their fine work.

I would like to thank the National Consortium for Graduate Degrees for Minorities in Engineering for their fellowship support. I am also grateful to John Tucker and the MIT 6-A program for giving me the wonderful opportunity to work for Bell Telephone Laboratories.

Finally, I am sincerely thankful to my parents, Ivanhoe and Violet Heron, for their continuing love, support, and encouragement.

TABLE OF CONTENTS

TITLE PAGE.....	1
ABSTRACT	2
ACKNOWLEDGMENTS.....	3
TABLE OF CONTENTS.....	4
LIST OF FIGURES AND TABLES.....	6
I. INTRODUCTION	9
1.1 A Brief Description of the 32 band sub-band/transform coder algorithm.....	13
1.2 The Scope of the Thesis.....	16
II. A 32-BAND QUADRATURE MIRROR FILTER BANK IMPLEMENTED WITH A PARALLEL STRUCTURE.....	18
2.1 Introduction.....	18
2.2 Principles of Tree Decomposition	18
2.3 Derivation of the Parallel Structure from the Tree Structure	20
2.4 The Implementation	25
2.5 Filter Bank Transfer Function.....	26
2.6 Observations.....	27
III. A SPECTRAL SIDE INFORMATION MODEL FOR SPEECH SIGNALS.....	29
3.1 Introduction.....	29
3.2 Derivation of the Spectral Templates.....	29
3.2.1 The clustering algorithm for generating the templates	30
3.3 A dynamic Template Selection Scheme	31
3.4 An Evaluation of the Tradeoffs between the Spectral Accuracy and Complexity of the Template Model	34
3.4.1 Observations.....	37
IV. A BIT ASSIGNMENT SCHEME FOR SPECTRAL NOISE SHADING.....	40
4.1 Introduction.....	40
4.2 Bit Assignment for Flat Noise Power.....	40
4.3 Bit Assignment for Noise Shaping.....	42
4.4 Observations.....	48
V. ADAPTIVE QUANTIZATION OF NARROW BAND SUB-BAND SIGNALS.....	49
5.1 Introduction.....	49
5.2 A Review of Adaptive Quantization Schemes for Frequency Domain Speech Coding.....	50

5.3	An Adaptive Quantization Scheme for Coding the Outputs of the 32-Channel Analysis Filter Bank	58
5.3.1	Observations	66
5.4	A dynamic Pre-Emphasis/De-Emphasis Scheme for Adaptively Quantizing the Outputs of the 32-Channel Analysis Filter Bank	67
5.4.1	Observations	71
VI.	AN ANALYSIS OF THE PERFORMANCE AND COMPLEXITIES OF BOTH 32 SUB-BAND/TRANSFORM CODERS	73
6.1	Introduction	73
6.2	Results of an Informal A versus B Comparison Test	73
6.3	The Complexity Performance Trade-offs	77
VII.	SUMMARY AND RECOMMENDATIONS FOR FURTHER RESEARCH	81
7.1	Summary	81
7.2	Suggestions for Further Research	81
	REFERENCES	83
APPENDIX I	QUADRATURE MIRROR FILTERING	86
APPENDIX II	FOURTH ORDER LPC TEMPLATES FOR 1,2,3,4, AND 5 BIT CODEBOOKS	98
APPENDIX III	THE BIT ASSIGNMENT USED FOR GENERATING THE BIT ASSIGNMENT CODEBOOKS	105
APPENDIX IV	THE D.S.P.	108
	BIOGRAPHICAL NOTE	110

LIST OF FIGURES AND TABLES

FIGURES

1.1	Block diagram of a sub-band coder.....	11
1.2	32 band sub-band/transform coder algorithm	13
2.1	2 band QMF filter bank.....	19
2.2	Tree structure implementation of a 32 band QMF filter bank	21
2.3	Parallel structure implementation of a 32 band QMF filter bank	22
3.1	Flowchart of template generation procedure	32
3.2	Relationship between the accuracy and complexity of the spectral side information model.....	36
3.3	Superimposed input and template spectra for two complexity extremes	38
4.1	Bit assignment rule for a flat noise spectrum	43
4.2	Example template and derived bit assignment for a flat noise spectrum	44
4.3	Frequency weighted bit assignment rule	46
4.4	Bit assignments and quantization noise for flat noise spectrum and for flat SNR	47
5.5.1	General feed forward adaptive quantizer with a time-varying gain	51
5.1.2	General feedback adaptation of the time-varying gains	52
5.2	Block diagram of LPC vocoder driven adaptive transform coder	55
5.3	Block diagram of a modified LPC vocoder driven adaptive transform coder.....	56
5.4	Homomorphic side information model.....	57
5.5	Illustration of the quantizer output ranges and input levels for 8 template 4th order LPC modelling.....	61
5.6	Illustration of the increased accuracy of coding with a 32 template 10th order LPC side information model.....	62
5.7	Distortion Performance of vector quantizing for a 1024 template 10th order LPC analysis	64
5.8	Subjectively optimized quantizer output ranges and input levels for 32 template 10th order LPC modelling.....	65

5.9	32 band sub-band/transform coder algorithm with dynamic preemphasis.....	68
5.10	Subjectively optimized quantizer output ranges of preemphasized input levels for 32 template 10th order LPC modelling	70
5.11	Illustration of quantizer "underloading" and overloading	72
6.1	Assessment of coder performance versus complexity	79
I.1	Composite frequency responses of the 32 band-pass QMF filters	96
I.2	Magnitude ripple of the 32 band analysis/synthesis filter bank	97
II.1a	1 bit 4th order LPC template codebook	99
II.1b	2 bit 4th order LPC template codebook	100
II.1c	3 bit 4th order LPC template codebook	101
II.1d	4 bit 4th order LPC template codebook	102
II.1e	5 bit 4th order LPC template codebook.....	103,104
III.1	Flowchart of the bit assignment rule for a flat noise spectrum	106
IV.1	Block Diagram of the BTL Digital Signal Processor	109

TABLES

6.1	Percent preference of coders in an informal A versus B Comparison Test.....	75
6.2	Ranking of coders according to the percent of A versus B votes received.....	76
I.1	Z-Transforms of Analysis Filters.....	89
I.2	Filter coefficients, Frequency Response, and QMF Ripple for the filters $H_1(z)$, $H_2(z)$, $H_3(z)$, $H_4(z)$, $H_5(z)$	91,92,93,94,95

CHAPTER I

1. INTRODUCTION

Recently, there has been considerable interest in applying digital technology to a broad range of applications in communications and coding. This technology offers important advantages such as flexible processing, increased transmission reliability, and error resistant storage — to mention a few. A variety of digital signal processing techniques, which exploit known properties of speech production and perception to varying degrees, has been proposed and studied for the purpose of reducing the required transmission bit rates or storage requirements for such "digital voice" applications [1]. These signal processing techniques range from low to high computational complexity designs which offer a corresponding tradeoff between complexity and performance.

Historically, speech coders have been divided into two broad categories, waveform coders and vocoders. Waveform coders attempt to reproduce the original speech waveform in accordance with some fidelity measure whereas vocoders model input speech according to a speech production model that separates the sound sources and vocal-tract filtering functions for resynthesizing the speech. Waveform coders have been more successful at producing good quality, robust speech, but require higher bit rates (in excess of 8 kb/s). Vocoders are more dependent on the validity of the speech production model and tradeoff voice quality for lower bit rates (2-5 kb/s) [1-2].

In order to reduce the bit rate of waveform coders, much effort has been devoted to frequency domain methods where the speech is encoded separately in different frequency bands. These methods permit control over the number of bits/sample and therefore the accuracy that is used to encode each frequency band. This enables different bands to be encoded with different accuracies according to their information content. The basic systems which have been studied extensively are sub-band coding and transform coding.

Sub-band coding, which exploits the quasi-stationarity and non-uniformity of the short-time spectral envelope of speech, is based on a 2 to 12 band division of the speech spectrum by means of a filter bank. In this scheme the number of bits/sample allocated for quantizing each frequency band is fixed at a certain value. The quantizer step sizes in each band are independently self-adapted according to a first order predictive technique after Jayant [32] which exploits the sample-to-sample amplitude correlation in each band. In general sub-band coding offers moderate complexity with moderate quality.

Transform coding, which exploits redundancies in the short-time speech spectrum, is based on a 128 to 256 band division of speech by means of a block transform analysis [2,3]. In this technique the input speech is blocked into frames of data and transformed by an appropriate fast transform algorithm. The transform coefficients are then encoded and inverse transformed into blocks of coded speech. The number of bits/sample allocated for quantizing the signal in each band and the step size of the quantizer in each band are dynamically updated on the basis of a "spectral side information model" of the incoming speech [2,3]. Transform coding offers better performance than sub-band coding but is far more complex.

An area not previously explored has been the middle range of techniques such as systems with 16 to 64 frequency bands which have complexities ranging between those of sub-band and transform coding methods. We have sought to answer the question of how effectively these systems will perform and the complexities involved for coding digitized voice at bit rates in the range of 16 kb/s. Such systems are of interest from the standpoint of digital speech transmission systems for use over standard telephone lines. These transmission systems require fairly high quality speech at 4.8 kb/s to 16 kb/s in a transmission environment which is not error free. This thesis reports on the study of 32 band sub-band/transform coding techniques at bit rates in the 16 kb/s range.

A block diagram of an N band sub-band coder is shown in Fig. 1.1. The input speech $s(t)$ is low-pass filtered to its Nyquist frequency $\Omega_s/2$ then sampled at Ω_s yielding $s(n)$ — the

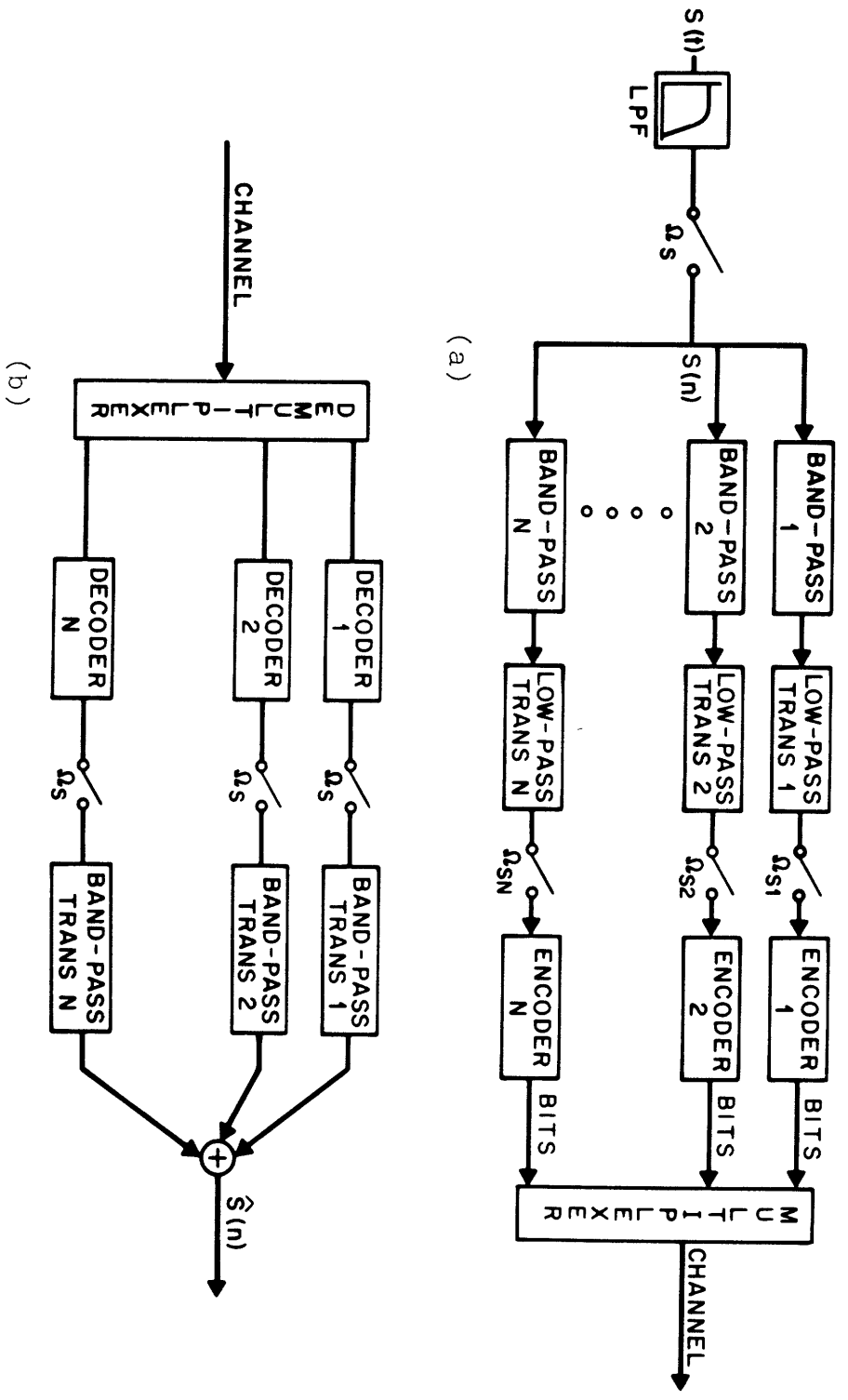


Fig. 1.1 A block diagram of a sub-band coder; (a) receiver section; (b) transmitter section.

discrete time representation of a bandlimited signal which has been sampled at the Nyquist rate. This discrete time signal is split into N contiguous sub-band signals by the bank of bandpass filters. Each sub-band signal is translated down to the base-band and then decimated to the Nyquist rate for that sub-band by discarding $N - 1$ out of every N samples (these steps are often combined in practice for computational savings). The bandpass filtering, base band translation, and decimation operations comprise the analysis filter bank. These base-band signals are separately encoded using an adaptive PCM scheme. The bits from each of these encoders are multiplexed, and then transmitted. The transmitted bit stream is demultiplexed and decoded by the receiver. The sub-band signals are interpolated to the original sampling rate Ω_s , by inserting $N - 1$ zeros between each sample. The interpolated signals are band pass translated to the proper frequencies, and then added, to produce $\hat{s}(n)$ a coded version of the input signal $s(n)$. This comprises the synthesis filter bank.

For the coders that were implemented as part of this thesis: N was 32, the sampling frequency was 8 kHz, and the sub-bands were of equal frequency width. Although designs incorporating non-uniform sub-bands can be considered, these designs are known to be less efficient in terms of their algorithm complexities and have not been pursued in this thesis. By independently adapting the quantizers' step sizes in each band according to the signal level in that sub-band, adaptive pulse code modulation (APCM) quantization exploits the quasi-stationarity and non-uniformity of the short time spectral envelope of speech. Use of APCM quantization for each band maintains a constant signal-to-noise ratio (SNR) over a large range of signal levels in any band [28]. By coding each sub-band separately, the quantization error from a band will be constrained to be in that band. Thus signals in one sub-band will not be masked by the quantizing noise produced in another sub-band. The number of bits allocated for coding each band, and hence the SNR of each band, can be set according to perceptual criteria [2] while maintaining a constant total bit rate by keeping the total number of bits constant. Dynamic bit allocation schemes can periodically update the bit allocation and hence the spectral shape of the quantizing noise — according to the spectral content of the input

speech.

1.1 A Brief Description of the 32 band sub-band/transform coder algorithm

Fig. 1.2 is a block diagram for the basic 32 band sub-band/transform coder design that is studied in this thesis. The division of the voice signal into sub-bands is achieved by a 32-channel quadrature mirror filter (QMF) bank [13-16] which is described in Chapter Two. Each sub-band signal (represented in the figure as y_1 through y_{32}) is independently coded and decoded using an APCM scheme incorporating a dynamically varying bit assignment and quantizer step size in each band. As in the case of transform coding, the bit assignment and quantizer step size vectors (represented in the figure as \hat{b}_i and $\hat{\Delta}_N$ respectively) for encoding and decoding the sub-bands are provided by a spectral model of the incoming speech.

A new spectral model utilizing recent concepts of vector quantizing [17,19] has been employed in the new coder designs for representing the time-varying spectral envelope of the speech signal at a modest cost in computational complexity. The input speech is represented by a all-pole spectral model that is dynamically selected from among a small collection of such models. This concept has been referred to in the literature as a "switched source of all-pole spectral models" [18]. We have experimented with a set of spectral models ranging from 4 to 32 in number in which each model is represented by the LPC vector $1/A_i(z)$. Since each segment of incoming speech is quantized to one of a set of LPC vectors without explicitly performing a standard LPC analysis, the method can be thought of as a technique for quantizing input LPC speech vectors. Each spectral model (defined in the figure by the codeword (C_i) , which can be selected from the set, defines a one-to-one mapping to a bit assignment pattern in the bit assignment codebooks for encoding and decoding incoming speech. Generally speaking, the bit assignments have been computed so that the majority of the available bits are assigned to bands where the signal is estimated to be the strongest.

The best LPC model for each 16 msec segment of speech is selected from the collection of LPC vectors so as to minimize the log likelihood ratio distortion measure [22] between the

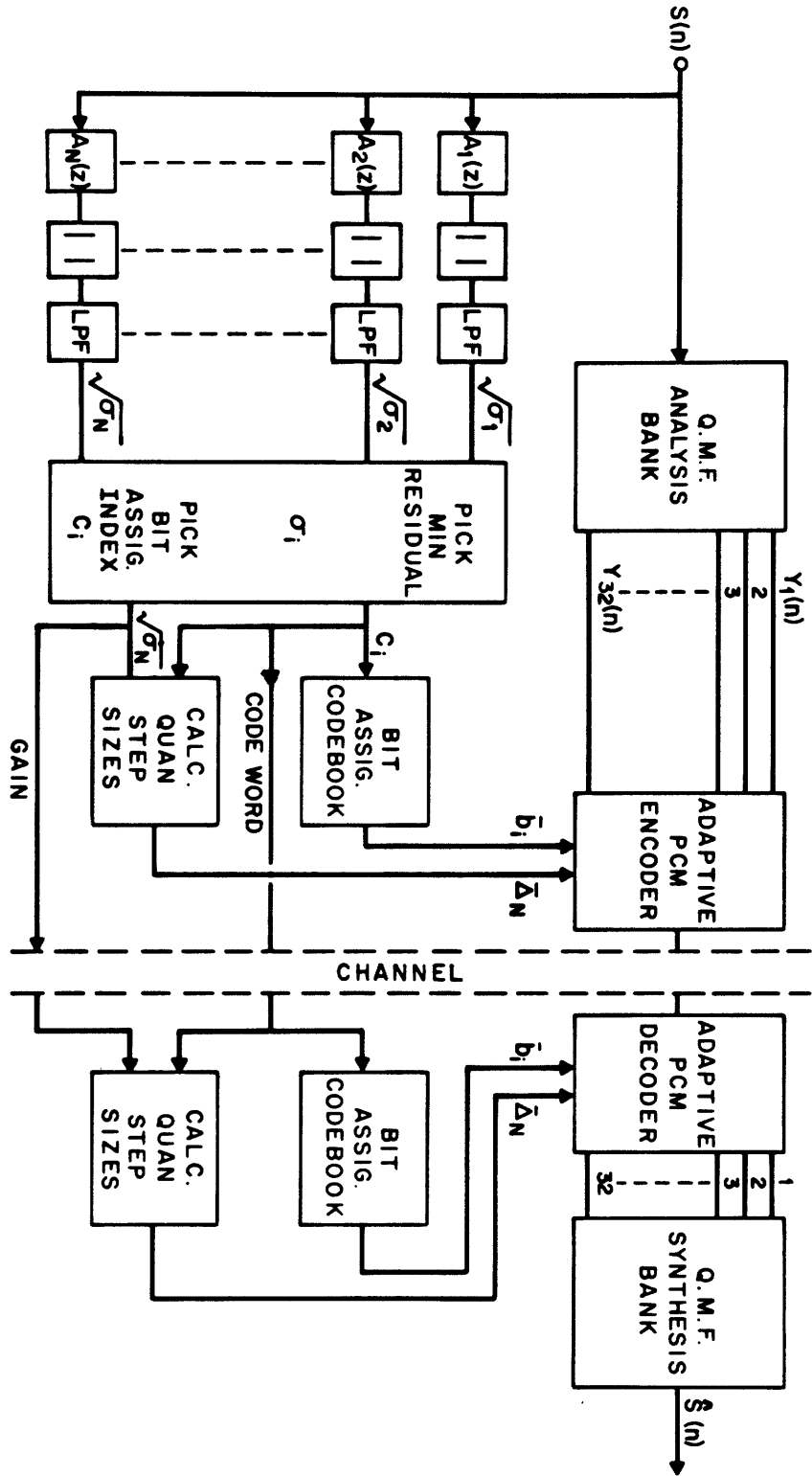


Fig. 1.2 32 band sub-band/transform algorithm

speech and template spectra. This LPC model yields the minimum residual energy of the signals obtained from filtering the input speech segment with each inverse LPC filter $A_i(z)$. The square root of the minimum residual energy, $\sqrt{\sigma_i}$, is the gain term of the best LPC template (or model) [28] and is used with that template for setting the quantizer step sizes for encoding and decoding each band.

Since the number of LPC template vectors used to represent the input speech is very small, if the vectors are reasonably chosen, the spectral distances between any two of these vectors will necessarily be "large" in order to encompass a variety of speech sounds. This has been an important consideration for developing a simple and efficient method for selecting the minimum energy residual necessary for the template codeword and gain selection. The lower left hand corner of Fig. 1.2 depicts such a method. The square root of the N th residual energy, $\sqrt{\sigma_N}$, is estimated by low-pass filtering the absolute value of the N th residual signal. This signal is obtained from filtering a speech segment with the N th inverse template filter $A_N(z)$. These computations are executed for each of the N inverse template filters for each segment of speech. The best template is selected to have the minimum gain estimate $\sqrt{\sigma_i}$.

The LPC spectral templates are generated with the aid of a clustering method previously applied to speech recognition [24,25] and vector quantizing for LPC vocoders [17-19]. The procedure identifies a set of LPC template vectors as cluster centers such that the average (log likelihood ratio) spectral distortion measure from all input vectors to their best match in the template vector collection is minimized [19,20].

In order that the speech coder be speaker independent, the clustering program inputs a large set of autocorrelation training vectors derived (based on a frame by frame analysis) from a speech database including a wide variety of talkers. The majority of the silence (background noise) must be eliminated from this database to ensure that numerous shades of background noise are not represented by the input training vectors.

In summary, the algorithm of Fig. 1.2 has incorporated a hybrid of ideas from both sub-

band coding and transform coding techniques. The structure accomplishes a 32-band decomposition of speech in which the bit assignment patterns and step sizes for encoding and decoding each sub-band are dynamically updated on the basis of a new spectral model. This model is based on recent concepts of vector quantizing in conjunction with known clustering methods. Since the new spectral model is much simpler and requires less side information* than recent spectral models that have been applied to ATC algorithms (such as models based on homomorphic analysis [3] and standard LPC analysis [34]), the approach taken in Fig. 1.2 appears inviting.

1.2 The Scope of the Thesis

This thesis reports on the study of two new techniques for 32 band sub-band/transform coding at 16 kb/s rates. Both coders have been implemented and tested on a general purpose digital computer. The proposed coding schemes offer good quality reconstructed speech at complexities that occupy the middle range between simpler sub-band and more complex adaptive transform coding techniques. Recent concepts of vector quantizing in conjunction with clustering methods have been employed for modeling speech with a switched source of all-pole spectral templates for dynamic bit assignments and adaptive quantization. An important objective of this thesis is to gain insight into the performance — complexity tradeoffs involved in these middle range schemes. The thesis is structured so that the fundamental components of the algorithm in Fig. 1.2 are separately discussed, prior to presenting a review of our findings in Chapters 5 and 6. The thesis is organized as follows:

Chapter 2 describes a 32-band quadrature mirror filter bank implemented with a parallel structure (utilizing a technique proposed by Esteban and Galand [14]) for sub-band decomposition of the speech signal. A derivation of the structure is given along with a discussion of its implementation and performance.

* side information is information that is separately transmitted across the channel to establish the bit assignments and quantizer step sizes for the decoder. This corresponds to the "codeword" and "gain" of Fig. 1.2.

Chapter 3 is concerned with the spectral side information model for the speech signal. The chapter begins by describing how the spectral templates were derived from a training speech data base and is followed by a discussion of the model for template picking and gain computation. The chapter concludes with an evaluation of the tradeoff between the accuracy and complexity of the template model for various LPC orders and numbers of templates.

Chapter 4 presents the bit assignment algorithm used for generating the bit assignment codebooks. Bit assignment methods for a flat noise spectrum as well as spectral shaping of the quantization noise are discussed.

Chapter 5 is concerned with adaptive quantization of narrow band signals for coding the 32 sub-bands. The chapter begins with an overview of adaptive quantization techniques that have been applied to sub-band and transform coding. Two techniques for quantizer step-size adaptation corresponding to both coders are developed and discussed.

Chapter 6 presents the results of an informal comparison test for quality which was performed in order to compare the effectiveness of the coder designs presented in Chapter 5 with simpler sub-band and more complex transform coding methods. The overall performance/complexity trade-offs of the 32 band coders are evaluated relative to these methods.

Chapter 7 concludes the thesis with a summary of major results and some suggestions for further research.

CHAPTER II

2. A 32-BAND QUADRATURE MIRROR FILTER BANK IMPLEMENTED WITH A PARALLEL STRUCTURE

2.1 Introduction

Since the design of efficient filter bank techniques in the midrange of 16 to 64 bands has not been well established, we have utilized concepts of quadrature mirror filters based on earlier sub-band work. This design has provided a good filter-bank analysis and synthesis framework for algorithm study in spite of its large storage and processing requirements for a 32 band design.

Sub-band decomposition based on a tree arrangement of quadrature mirror filters (QMF's) has been applied at low bit rates, and has been shown to avoid aliasing effects due to finite filter transition bandwidths and decimation [13]. The filter bank described in this chapter was derived from a 5 level tree structure QMF bank utilizing a technique proposed by Esteban and Galand [14]. Although it is strictly equivalent to the tree approach, the parallel approach allowed additional implementation simplicity although extra coefficient storage is necessary.

2.2 Principles of Tree Decomposition

Fig. 2.1 shows the classical 2 band QMF filter bank for decomposition of the signal $x(n)$ into 2 contiguous sub-bands. In this implementation $x(t)$ is lowpass filtered to its Nyquist frequency $\Omega_s/2$ then sampled at Ω_s , yielding $x(n)$. The signal $x(n)$ is filtered by a lowpass filter $H_1(\omega)$, and a highpass filter $H_2(\omega)$. Since the spectra of $x_1(n)$ and $x_2(n)$ occupy only 1/2 the Nyquist bandwidth the sampling rate can be decimated by a factor of 2. This results in the signals $y_1(n)$ and $y_2(n)$ obtained from decimating $x_1(n)$ and $x_2(n)$ respectively. In the receiver the signals $y_1(n)$ and $y_2(n)$ are interpolated by a factor of 2 and filtered by $K_1(\omega)$ and $K_2(\omega)$ respectively. These signals are then added to produce the reconstructed signal $s(n)$. Since in practice $H_1(\omega)$ and $H_2(\omega)$ will have finite transition widths the decimation operation of

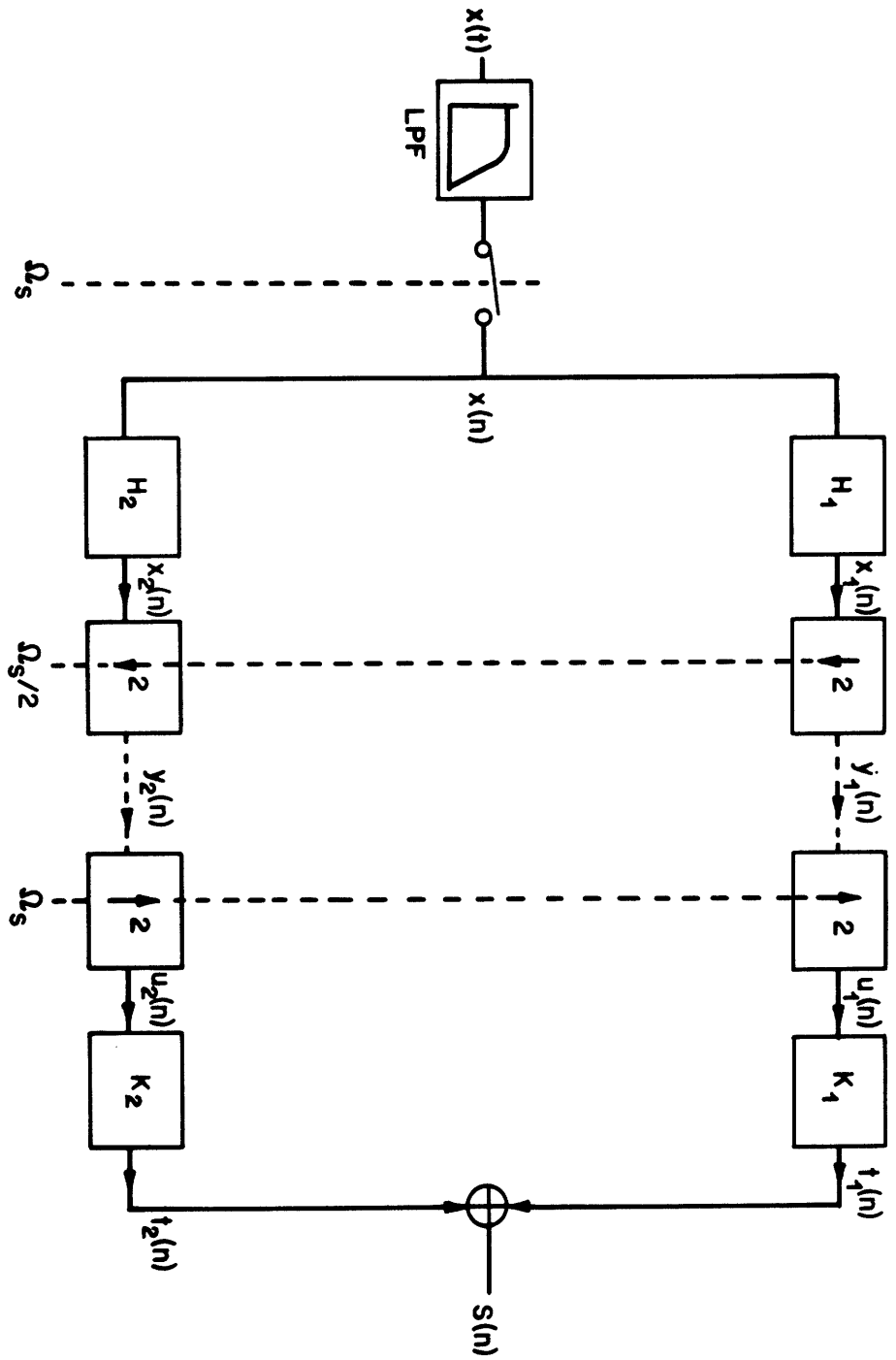


Fig. 2.1 Principle of 2 sub-band splitting by use of QMF filters. (After Esteban and Galand).

Fig. 2.1 will result in aliasing terms. It has been demonstrated [13] that these terms are cancelled by choosing $H_1(\omega)$, $K_1(\omega)$, $H_2(\omega)$, $K_2(\omega)$ such that the following conditions hold:

1. $H_1(\omega)$ is a symmetrical FIR filter of even order N .
2. $H_2(\omega) = H_1(\omega + \pi)$.
3. $K_1(\omega) = H_1(\omega)$.
4. $|H_1(\omega)|^2 + |H_1(\omega + \pi)|^2 = 1$.
5. $K_2(\omega) = -H_2(\omega)$.

In this case $s(n) = \frac{1}{2} x(n - N + 1)$. That is, the output signal is a replica of the input signal (neglecting the gain factor of $1/2$) with an $N - 1$ sample delay. A derivation of this result and the above five conditions is presented in Appendix I.

This decomposition can be extended to more than two sub-bands by highpass and lowpass filtering the signals $y_1(n)$ and $y_2(n)$ and reducing the sampling rate accordingly. In the general case the input signal, $x(n)$, is split into 2^M sub-band signals sampled at $\Omega_s/2^M$ by a M -stage tree arrangement of decimated filters. The sub-band signals are reconstructed to form the output by a symmetric tree arrangement of interpolation filters. Fig. 2.2 shows this for $M = 5$.

2.3 Derivation of the Parallel Structure From the Tree Structure

Fig. 2.3 depicts the parallel structure implemented for decomposition of the signal $x(n)$ into 32 contiguous sub-bands. This is achieved by filtering with a bank of 32 contiguous bandpass filters $F_i(z)$ uniformly covering the frequency range $0 \leq \omega \leq \pi$. Since the resulting spectra $X_i(\omega)$ occupy only $1/32$ of the Nyquist bandwidth, the sampling rate is then decimated by a factor of 32 to yield the signals $y_i(n)$. These signals occupy the full Nyquist bandwidth as a result of the frequency domain translation and stretching operations achieved by decimation. The reconstructed signal $s(n)$ is obtained by interpolating the signals $y_i(n)$ by a factor of 32, then by re-filtering and summing the outputs.

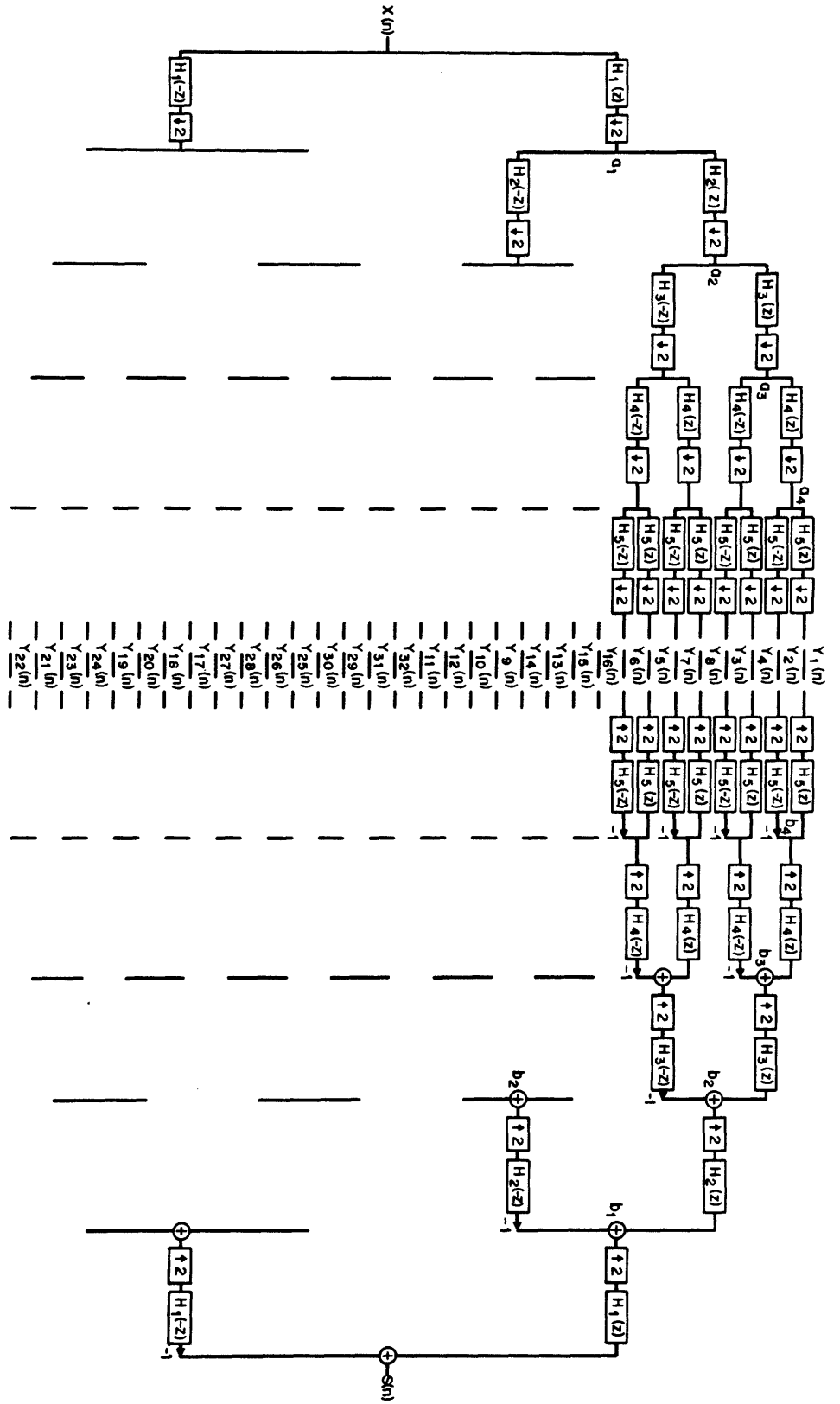


Fig. 2.2 Five stage QMF Tree structure for 32 sub-band splitting.

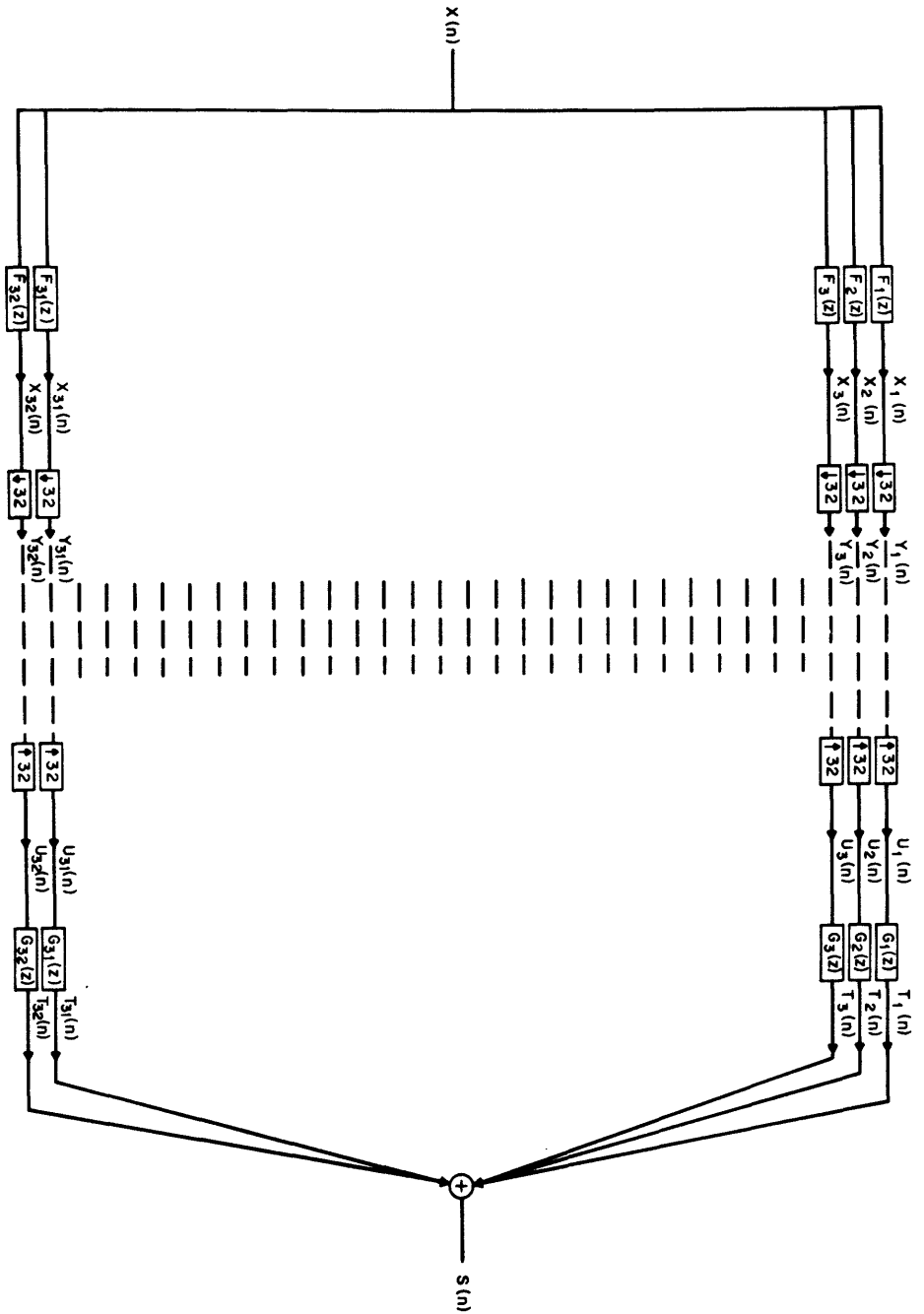


Fig. 2.3 QMF parallel structure for 32 sub-band splitting.

We can derive a set of 32 conditions which are necessary to insure the perfect reconstruction of $s(n)$ (without aliasing). The z -transforms of $x_i(n)$ are given by

$$X_i(z) = F_i(z)X(z) . \quad (2.1)$$

The z transforms of the decimated signals $y_i(n)$ are [11]

$$Y_i(z) = \frac{1}{32} \sum_{l=0}^{32-1} X_i(e^{-j\frac{2\pi}{32}l} z^{1/32}) . \quad (2.2)$$

Interpolating 2.2 results in

$$U_i(z) = Y_i(z^{32}) . \quad (2.3)$$

Final filtering results in

$$T_i(z) = G_i(z)U_i(z) , \quad (2.4)$$

$$S(z) = \sum_{i=1}^{32} T_i(z) . \quad (2.5)$$

Combining equations (2.1) through (2.5) yields

$$S(z) = \frac{1}{32} \sum_{i=1}^{32} G_i(z) \sum_{l=0}^{31} \left[F_i(e^{-j\frac{2\pi}{32}l} z) X(e^{-j\frac{2\pi}{32}l} z) \right] . \quad (2.6)$$

Elimination of the aliasing terms in (2.6) requires that

$$S(z) = \frac{1}{32} X(z) \sum_{i=1}^{32} G_i(z)F_i(z) , \quad (2.7)$$

$$\sum_{i=1}^{32} G_i(z)F_i(e^{-j\frac{2\pi}{32}l} z) = 0 , \quad 1 \leq l \leq 31 . \quad (2.8)$$

By identifying the z -transforms of the sub-band signals for the parallel and tree structures it is possible to determine the relationship between the coefficients of both structures.

For the parallel implementation, the first sub-band signal $y_1(n)$ is given from Eqs. (2.1) and (2.2) by

$$Y_1(z) = \frac{1}{32} \sum_{l=0}^{31} F_1(e^{-j\frac{2\pi}{32}l} z^{1/32}) X(e^{-j\frac{2\pi}{32}l} z^{1/32}) . \quad (2.9)$$

Referring to figure (2.2) we can derive the expression for the first sub-band signal of the tree structure

$$A_1(z) = \frac{1}{2} [X(z^{\frac{1}{2}})H_1(z^{\frac{1}{2}}) + X(-z^{\frac{1}{2}})H_1(-z^{\frac{1}{2}})] \quad (2.10a)$$

$$A_2(z) = \frac{1}{2} [A_1(z^{\frac{1}{2}})H_2(z^{\frac{1}{2}}) + A_1(-z^{\frac{1}{2}})H_2(-z^{\frac{1}{2}})] \quad (2.10b)$$

$$A_3(z) = \frac{1}{2} [A_2(z^{\frac{1}{2}})H_3(z^{\frac{1}{2}}) + A_2(-z^{\frac{1}{2}})H_3(-z^{\frac{1}{2}})] \quad (2.10c)$$

$$A_4(z) = \frac{1}{2} [A_3(z^{\frac{1}{2}})H_4(z^{\frac{1}{2}}) + A_3(-z^{\frac{1}{2}})H_4(-z^{\frac{1}{2}})] \quad (2.10d)$$

$$Y_1(z) = \frac{1}{2} [A_4(z^{\frac{1}{2}})H_5(z^{\frac{1}{2}}) + A_4(-z^{\frac{1}{2}})H_5(-z^{\frac{1}{2}})] \quad (2.10e)$$

Equating equations 2.9 and 2.10e gives

$$F_1(z) = H_1(z)H_2(z^2)H_3(z^4)H_4(z^8)H_5(z^{16})$$

with repetition of the pattern in other bands. A complete listing for all the analysis filters $F_l(z)$ is given in Table 1 of Appendix I.

The synthesis filters $G_l(z)$ can be obtained by an analogous procedure. For the signal $t_1(n)$ of Fig. 2.3 we can write

$$T_1(z) = Y_1(z^{32})G_1(z) . \quad (2.11)$$

Referring to figure 2.2 we can write

$$B_4(z) = Y_1(z^2)H_5(z) , \quad (2.12a)$$

$$B_3(z) = B_4(z^2)H_4(z) , \quad (2.12b)$$

$$B_2(z) = B_3(z^2)H_3(z) , \quad (2.12c)$$

$$B_1(z) = B_2(z^2)H_2(z) , \quad (2.12d)$$

$$T_1(z) = B_1(z^2)H_1(z) . \quad (2.12e)$$

Equating equations (2.11) and (2.12e) reveals

$$G_1(z) = F_1(z) .$$

It is shown more generally that

$$G_i(z) = (-1)^{(i-1)} F_i(z) . \quad (2.13)$$

The equations for the analysis (and hence the synthesis) filters in Table 1 of Appendix I suggest a straightforward filter implementation procedure. Consider for example the implementation of the fourth analysis filter described by the z -transform

$$F_4(z) = H_1(z)H_2(z^2)H_3(z^4)H_4(-z^8)H_5(z^{16}) . \quad (2.14a)$$

The corresponding impulse response can be expressed as

$$\begin{aligned} f_4(n) = & h_1(n) * h_2\left(\frac{n}{2}\right) \omega_2(n) * h_3\left(\frac{n}{4}\right) \omega_4(n) \\ & * (-1)^{\frac{n}{8}} h_4\left(\frac{n}{8}\right) \omega_8(n) * h_5\left(\frac{n}{16}\right) \omega_{16}(n) \end{aligned} \quad (2.14b)$$

where the sequence $\omega_L(n)$ is defined to be nonzero only at integer multiples of L : that is

$$\begin{aligned} \omega_L(n) = & 1 , \quad n = 0, \pm L, \pm 2L, \dots \\ & = 0 , \quad \text{otherwise} . \end{aligned}$$

Equation (2.14b) is the result of first forming the sequences $h_1(n)$, $h_2(n)$, $h_3(n)$, $(-1)^n h_4(n)$, and $h_5(n)$, then interpolating these sequences by factors of 1, 2, 4, 8, and 16, respectively; and convolving the results to obtain $f_4(n)$.

2.4 The Implementation

Examination of the z -transforms of the filters in Table 1 of Appendix I reveal symmetries which can be exploited to minimize coefficient storage space. By noting that

$$F_1(z) = F_{32}(-z), F_2(z) = F_{31}(-z), \dots, F_{16}(z) = F_{17}(-z)$$

it is seen that the upper 16 filters can be obtained from the lower 16 filters by a shift of π radians which amounts to alternating the sign of every other filter coefficient in the time domain. Furthermore it can be seen that the odd numbered filters $F_1(z), F_3(z), \dots$ are all symmetric, and the even numbered filters $F_2(z), F_4(z), \dots$ are all anti-symmetric. A direct result of these properties is that all the filter coefficients can be derived from storing only the

first half of the first (or last) 16 filters.

The actual quadrature mirror filters used for this implementation were designed by J. D. Johnston using the Hooke and Jeaves optimization algorithm [16]; 64 tap, 32 tap, 24 tap, 16 tap, and 12 tap filters were used in the first, second, third, fourth and fifth splits respectively. A list of coefficients for these five filters ($h_1(n)$, $h_2(n)$, $h_3(n)$, $h_4(n)$, $h_5(n)$) is given in Table 2 of Appendix I together with plots of frequency response and QMF ripple. Figure I.1 (of Appendix I) depicts the magnitude response of the 32 bandpass filters $F_1(z)$ through $F_{32}(z)$ which were designed using the above five filters.

The filter bank was implemented in computer simulation on a general purpose computer, a Data General AP130, using an array processor. The analysis, filtering, and decimation operations of figure 2.3 was achieved using a direct form structure of an M to 1 decimation [12]. Interpolation operations and synthesis filtering were achieved using a standard polyphase filter structure [12].

2.5 Filter Bank Transfer Function

It is possible to derive an expression for the transfer function of the analysis/synthesis filter bank of figure 2.3, which can be interpreted in terms of a magnitude ripple in the frequency domain. By substitution of Eq. (2.13) into (2.7) we obtain

$$S(z) = \frac{1}{32} X(z) \sum_{i=1}^{32} F_i(z) (-1)^{(i-1)} F_i(z). \quad (2.15)$$

Re-arranging terms gives

$$S(z) = \frac{1}{32} X(z) \left\{ [F_1^2(z) - F_{32}^2(z)] + [-F_2^2(z) + F_{31}^2(z)] + [F_3^2(z) - F_{30}^2(z)] + \cdots + [-F_{16}^2(z) + F_{17}^2(z)] \right\}. \quad (2.15a)$$

Since $F_{32}(z) = F_1(-z)$, $F_2(z) = F_{31}(-z)$, $F_{30}(z) = F_3(-z)$, ..., $F_{16}(z) = F_{17}(-z)$, (2.15a) becomes a sum over odd indices

$$S(z) = \frac{1}{32} X(z) \left\{ [F_1^2(z) - F_1^2(-z)] + [F_{31}^2(z) - F_{31}^2(-z)] + [F_3^2(z) - F_3^2(-z)] + \cdots + [F_{17}^2(z) - F_{17}^2(-z)] \right\}. \quad (2.15b)$$

$S(z)$ can be expressed more compactly by summing over odd terms as

$$\frac{1}{32} X(z) \sum_{\text{odd } j=1}^{31} [F_j^2(z) - F_j^2(-z)] = S(z). \quad (2.16)$$

For $F_i(z)$ a symmetric FIR filter of even order it can be shown that (see Eq. I.13b of Appendix I)

$$\left|_{z=e^{j\omega}} [F_i^2(z) - F_i^2(-z)] \right| = \left[|F_i(\omega)|^2 + |F_i(\omega+\pi)|^2 \right] e^{-j(N-1)\omega}. \quad (2.17)$$

Evaluating (2.16) on the unit circle yields

$$S(\omega) = \frac{1}{32} X(\omega) \sum_{\text{odd } j=1}^{31} \left[|F_j(\omega)|^2 + |F_j(\omega+\pi)|^2 \right] e^{-j(N-1)\omega}. \quad (2.18)$$

Since

$$F_2(\omega) = F_{31}(\omega+\pi), F_4(\omega) = F_{29}(\omega+\pi), F_6(\omega) = F_{27}(\omega+\pi),$$

the Fourier transform of the output signal is given by

$$S(\omega) = \frac{1}{32} X(\omega) e^{-j(N-1)\omega} \sum_{i=1}^{32} |F_i(\omega)|^2. \quad (2.19)$$

Ignoring the gain term and the delay of $N - 1$ samples, perfect reconstruction of the input signal requires that

$$\sum_{i=1}^{32} |F_i(\omega)|^2 = 1. \quad (2.20)$$

This term is plotted in figure I.2 of Appendix I on a magnified dB scale indicating a peak-to-peak ripple of less than 0.074 dB.

2.6 Observations

The plot of Fig. I.1 confirms the performance of the filter bank design of this chapter for limiting the amount of internal aliasing between the bands of the analysis filters (the worst case is down 15 dB). The internal aliasing cancellation properties of the design is evidenced by the

"flat" frequency response shown in Fig. I.2. Time domain testing has confirmed also that the filter bank is linear and shift invariant within practical limits. It is worth pointing out that because of the good frequency resolution of the analysis and synthesis filters their impulse responses are long in time (514 samples). The interpretation of these observations are postponed until Chapter 5.

CHAPTER III

3. A SPECTRAL SIDE INFORMATION MODEL FOR SPEECH SIGNALS

3.1 Introduction

A switched source of all-pole spectral templates is used for modeling incoming speech in order to achieve efficient dynamic bit assignment and quantizer step size adaptation for encoding the sub-band signals. These templates (which are represented as LPC vectors) are derived through an iterative process called a clustering algorithm which involves spectral comparisons on a large set of LPC training vectors derived by autocorrelation analysis on a speech database [24,25]. Once the templates comprising the vector codebook have been derived, it is necessary to dynamically select that template which best models the incoming speech.

The beginning of this chapter discusses the speech database and clustering algorithm for template generation. This is followed by the template selection scheme and an analysis of the tradeoffs between the accuracy and complexity of the spectral template model.

3.2 Derivation of the Spectral Templates

In order to generate a set of spectral templates, a training database was first established. The database was comprised of speech by 7 speakers, 4 male and 3 female. Each speaker contributed about 19.6 seconds of speech by uttering the same 10 phonetically balanced sentences. This resulted in a 137 second database. Forty-two seconds of silence was eliminated from this database to ensure that numerous shades of background noise did not occupy valuable space as spectral models.

The speech used was high quality microphone speech bandpassed from 100 Hz to 3500 Hz, sampled at 8 kHz, and quantized to 16 bits/sample. An LPC analysis using the autocorrelation method [28] was then performed on the data using an analysis window (Hamming window) of

length 256 samples (or 32 ms).^{*} This window was shifted by 256 samples at a time generating about 3,000 vectors. Each vector was stored as a gain-normalized autocorrelation sequence, $\{R_{xx}(n)/\alpha_M, n = 0,1,2,\dots,M\}$, where M is the order of the LPC analysis and α_M is the residual energy resulting from passing the windowed input segment through its corresponding LPC inverse filter.

This analysis was performed for LPC orders of 10,8,6,4 and 2 for 1,2,3,4, and 5 bit template codebooks^{**} in order to select the LPC order and number of templates resulting in the best tradeoff between spectral modeling and the amount of "side information" required. As an example, figure II.1 of Appendix II shows frequency domain plots for 1,2,3,4 and 5 bit template codebooks derived from a fourth order LPC analysis.

3.2.1 The clustering algorithm for generating the templates

The clustering algorithm used to generate spectral templates was developed by B. H. Juang [19] and implemented by L. R. Rabiner [20]. These templates were selected such that an average spectral distortion measure — in this case the log likelihood ratio [22,23] — from all input vectors to their best match in the template vector collection was minimized [17,19]. A number of spectral distortion measures have been discussed by Gray and Markel [21] and Gray et al. [23]. In theory, any of these distortion measures can be used in the clustering algorithm. However, for LPC vector quantizing, the distortion measure should be consistent with the residual energy minimization concept of the LPC analysis process [19]. Three distortion measures have been found with this property [23]: the Itakura-Saito measure, the Itakura measure, and the likelihood ratio measure. Because of practical considerations such as computation, storage complexity and variations in the input gain level, the likelihood ratio measure has been found to be more appropriate for LPC vector quantization [19].

^{*} This is a standard size analysis window for speech [28].

^{**} A b bit template codebook contains 2^b templates.

Briefly, the procedure taken by the clustering algorithm was as follows [19].

1. Start at 1 bit with 2 initial codewords.
2. For each gain normalized autocorrelation vector in the training database, perform an exhaustive search over all available codewords to find its nearest neighbor (using the log-likelihood spectral distance measure) and then assign the input to the corresponding cell.
3. Update each cells centroid by solving the LPC equation corresponding to the average autocorrelation sequence and use the new centroids as the current codewords.
4. Repeat steps 2) and 3) until the change in average distortion drops below a preset threshold.
5. If the maximum desired number of bits is reached, stop the process; if not, proceed to 6).
6. Initialize codewords for the next bit stage by perturbing each centroid.

A flowchart of this procedure is given in figure 3.1 [19].

3.3 A Dynamic Template Selection Scheme

Once the LPC order and the number of templates comprising the vector codebook have been selected, it is necessary to dynamically select that template which best models each incoming speech frame of 4 ms (32 samples). This template is chosen to minimize the log likelihood ratio distance measure between the best (gain-normalized) LPC model of the speech spectra, and the template spectra. This measure compares two gain-normalized model spectra giving the best spectral match possible over all gain values [21].

Let $X(z)$ be the z -transform of a frame of speech and let $\sqrt{\sigma_M}/A_M(z)$ be the optimal M th-order LPC model of $X(z)$. The squared gain term σ_M is the residual energy resulting from inverse filtering $X(z)$ with $A_M(z)$. Also, let $1/A_i(z)$ be any M th order, gain-normalized all-pole filter from the vector codebook. Inverse filtering $X(z)$ with $A_i(z)$ results in a residual σ_i , $\sigma_i \geq \sigma_M$. σ_i is given as:

$$\sigma_i = \frac{1}{2\pi} \int_{-\pi}^{\pi} |X(\omega)A_i(\omega)|^2 d\omega \quad (3.1)$$

The Log-Likelihood Ratio measure between the optimum (gain normalized) LPC model of the speech spectra $1/A_M(z)$, and the template spectra $1/A_i(z)$ is defined as [17,19,22]:

$$d_{LR} \left(\frac{1}{A_M}, \frac{1}{A_i} \right) = \log \frac{\sigma_i}{\sigma_M} = \log \left[\frac{1}{2\pi} \int_{-\pi}^{\pi} \frac{|A_i(\omega)|^2}{|A_M(\omega)|^2} d\omega \right] \quad (3.2)$$

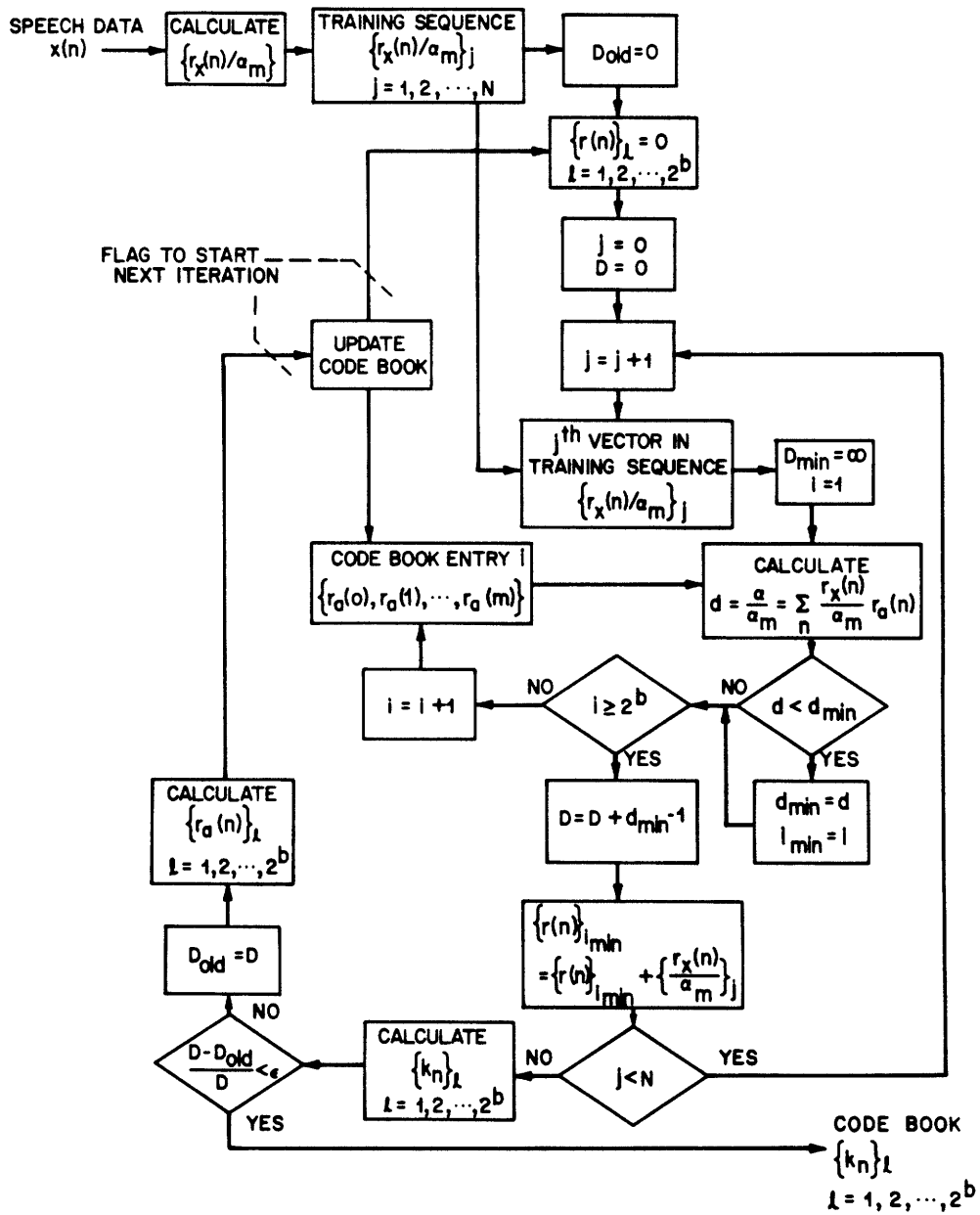


Fig. 3.1 Flowchart of codebook generation procedure. Juang et al.: Distortion Performance and LPC Voice Coding

Clearly, minimizing d_{LR} is equivalent to minimizing the residual energy σ_i since the optimal (minimum) σ_M is fixed for a given input frame.

Figure 1.2 illustrates a scheme for computing $\sqrt{\sigma_i}/A_i(z)$, the best template model of the speech — represented by the gain $\sqrt{\sigma_i}$ and the template number (or bit assignment index) C_i . According to this scheme the input speech $s(n)$ is processed frame by frame to result in a template selection and gain computation every 16 ms. Since speech is approximately stationary over 16 ms intervals, the bit assignment pattern and quantizer step sizes for coding the sub-band signals need only be updated every four, 4 ms frames, hence the side information (consisting of the gain and bit assignment index) need only be transmitted every 4 frames.

In principle the optimum spectral template for modeling a particular frame of speech should be chosen such that the residual energy resulting from inverse filtering a windowed speech segment of $s(n)$ with the inverse FIR filter $A_i(z)$ is minimized. The windowed speech segment corresponding to the ℓ -th (32 sample) frame can be conveniently expressed as

$$s_\ell(n) = s(n+32\ell) \cdot \omega(n) \quad (3.3)$$

where $\omega(n)$ is a finite length window (e.g. a Hamming window) that is identically zero outside the interval $0 \leq n \leq N - 1$. The residual energy σ_i which results from inverse filtering $S_\ell(z)$ with $A_i(z)$ can be expressed in the time domain as:

$$\sigma_i = \sum_{n=-\infty}^{+\infty} \left[S_\ell(n) * a_i(n) \right]^2 = \sum_{n=0}^{N-1+M} e^2(n) \quad (3.4)$$

where $e(n) = S_\ell(n) * a_i(n)$ and M is the LPC order of the templates. The minimum residual σ_i is the squared gain estimate for the template model.

We have mentioned in the first chapter that by employing a small number of LPC templates in the vector codebook we are doing a "course" spectral modeling of the input speech. Although the scheme of figure 1.2 for computing the best template model is not strictly equivalent to the method described above, its performance and computational efficiency for implementation on a digital signal processing chip justify its implementation. In this method

the input signal $s(n)$ is not windowed. The spectral template is chosen by minimizing an estimate for $\sqrt{\sigma_i}$, the square root of the residual energy. This minimum estimate has been found to be proportional to the gain of the optimal template model. The absolute value of the residual signal $|\hat{e}(n)| = |s(n) * a_i(n)|$ is LP filtered with a 1-pole IIR filter with unit sample response

$$h(n) = G(1-\beta)\beta^n U(n) \quad (3.5)$$

to compute the estimate of $\sqrt{\sigma_i}$; where G , β , and U are defined below. This estimate

$$\sqrt{\sigma_i} \cong \sum_{k=0}^{\infty} |\hat{e}(k)|h(n-k) \quad (3.6)$$

is evaluated for selecting the template and gain every 128 samples (16 ms).

An explanation of the parameters of the model is now given. G is the proportionality constant chosen to optimize the gain estimate. β is selected to control the exponential time constant of the impulse response of $h(n)$ and hence the number of samples of $|\hat{e}(n)|$ which are averaged in Eq. (3.6) to form the gain estimate of $\sqrt{\sigma_i}$. β is set to .98 corresponding to a time constant of approximately 50 samples (6.25 ms). U is the unit step function.

3.4 An Evaluation of the Tradeoffs between the Spectral Accuracy and Complexity of the Template Model

The complexity of the spectral side information model developed in this chapter is proportional to the LPC order and the number of templates employed in the gain and template selection scheme of figure 1.2. Since the amount of processing required for template and gain picking (the number of multiplications and additions performed by the hardware for each template selection) varies proportionally with the complexity of the model, some tradeoffs need to be made between the accuracy in modeling the speech spectrum and the amount of processing required by the scheme in figure 1.2.

In order to select the LPC order and the number of templates for computation of the side information, an experimental relationship has been derived between the number of templates,

their LPC orders, and the spectral accuracy of the model. An evaluation of the spectral accuracy of the template model was based on spectral distance measurements (calculated every 4 ms frame) between the template spectral model and a standard 14th order LPC analysis spectrum of the input.

Both spectra were represented by 1024 point DFT's of gain normalized LPC spectra. A 256 point Hamming analysis window was shifted 32 samples at a time for computing the LPC spectrum of the input — the template model was the output of the template picking procedure discussed in the previous section.

Three spectral distance measures corresponding to the first, second, and fourth L_p norms were calculated in the log-domain (in bits) for every 4 mS frame of input speech. These distance measures are given for the p th norm as*

$$E_p(n) = \left[\frac{1}{513} \sum_{k=1}^{513} \left\{ \log_2 |S_{A_n}(k)| - \log_2 |S_{T_n}(k)| \right\} \right]^{1/p} \quad (3.7)$$

where $S_A(k)$ and $S_T(k)$ are 1024 point DFT's of the gain normalized actual and template LPC spectra respectively. This error measure was calculated in the \log_2 domain because the bit assignment in any band is proportional to the log magnitude of the optimum template in that band. Further details of this are considered in Chapter 4.

Each error measure E_p was averaged over time — using a speech file which contained no silence — to compute an average spectral error. This was done for various LPC orders and numbers of the templates.

The functional relationship discovered between the number of templates, their LPC orders, and the spectral accuracy of the model is plotted in figure 3.2 for $p = 2$ **

* The subscript n is a reminder that the DFT's are functions of time as well as frequency.

** The same plots for $p = 4$ and 1 show the same trends but assign greater and lesser emphasis, respectively, to the spectral peaks.

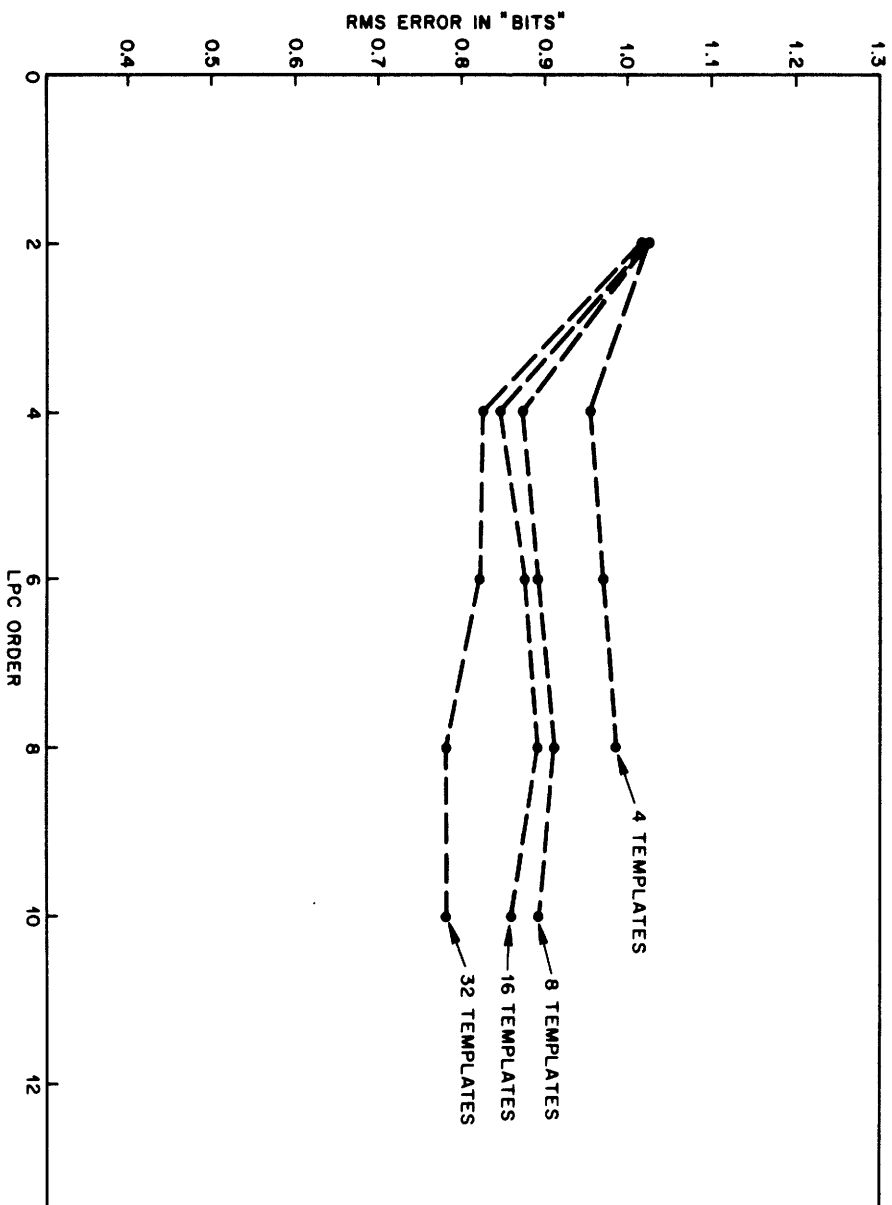


Fig. 3.2 Experimental relationship between the number of templates, their LPC order, and the accuracy of the spectral model.

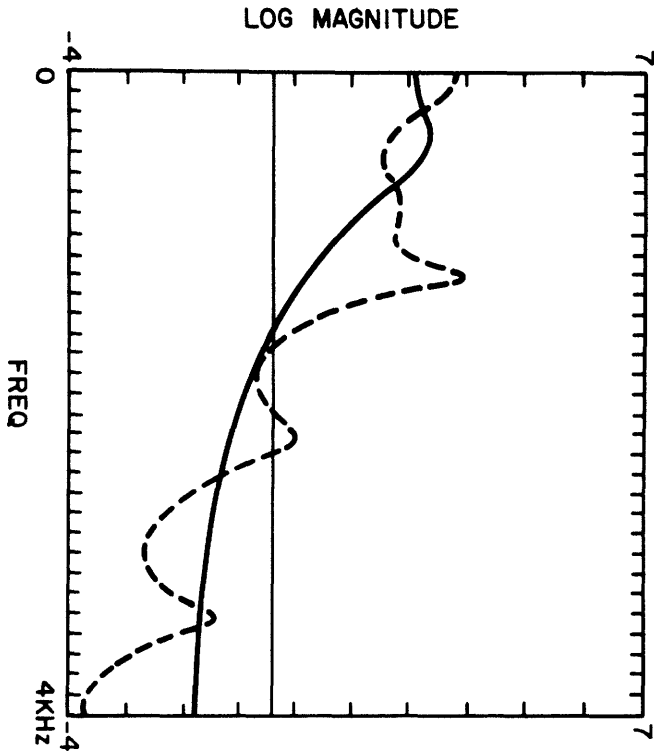
These plots need some explaining. From an intuitive standpoint we expect that for a given number of templates the spectral error should decrease monotonically as the LPC order of the templates increase. This intuition is only correct if there are enough templates, or cluster centers, for the clustering algorithm to form sufficiently "tight" clusters to properly model all the different speech sounds. Only with 32 templates (or more) do we observe monotonically decreasing spectral error with increasing LPC order. When fewer templates are used the spectral error increases when the LPC order exceeds 4.

Figure 3.3 shows an example of the accuracy of the template model for two complexity extremes. The figure shows log magnitude plots of an actual LPC spectrum (the dotted line) superimposed over the best template LPC spectrum (the solid line) for the case of a four template 2nd order LPC analysis (shown in Fig. 3.3a) and a 32 template 10th order LPC analysis (shown in figure 3.3b).

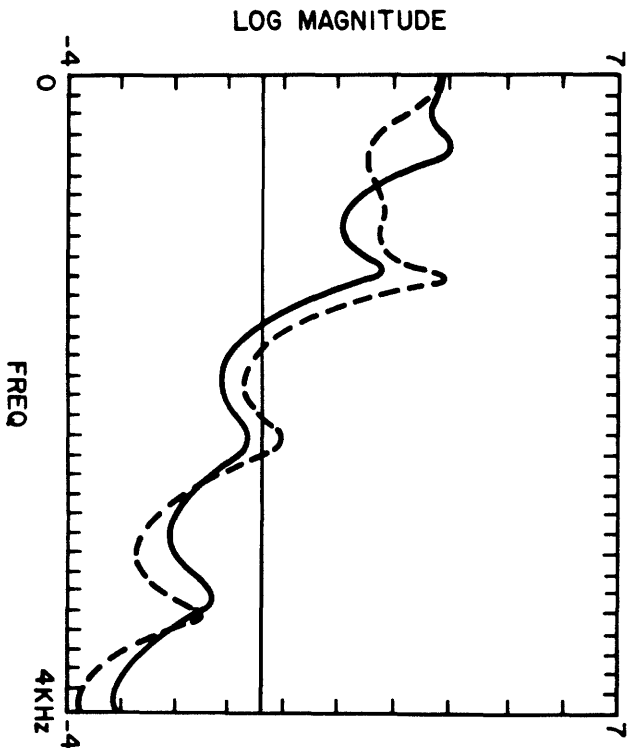
Eight, fourth order LPC templates were selected as a first cut tradeoff between the amount of processing and the accuracy of the resulting spectral model. This choice results in approximately 40 multiplies and adds (in the implementation of Fig. 1.2) which are required per frame for selection of the template and gain term, and an average RMS error in bits of less than one.

3.4.1 Observations

Tests have been performed over a wide range of complexities of the template side information model. These tests are in general agreement with the experimentally derived relationship between the LPC order of the templates, the number of templates, and the accuracy of the model. For example, the four best sounding coding schemes were obtained using 32 spectral templates of 10th, 8th, 6th, and 4th order LPC with qualities from highest to lowest in this order. Listening tests later performed with side information complexities of up to 128 templates with 10th order LPC yielded only differential improvements in speech quality over the 32 template model.



(a) RMS error (in bits) = 1.094
A 4 template, 2nd order LPC analysis.



(b) RMS error (in bits) = .708
A 32 template 10th order LPC analysis.

Fig. 3.3 The LPC spectrum of the input (the dotted lines) superimposed over the LPC template spectrum (the solid lines) for 2 side information complexities.

It is worth pointing out that although the time averaged RMS spectral error in figure 3.2 ranges over only a quarter of one bit the corresponding audible range of coded speech quality varies quite vastly. In general, higher order L_p norm error measures increase the error spread because they give more weight to the peak errors in the spectral model. Nevertheless, the error norm order must exceed 4 to get error spreads in excess of only three tenths of one bit.

CHAPTER IV

4. A BIT ASSIGNMENT SCHEME FOR SPECTRAL NOISE SHAPING

4.1 Introduction

The bit assignment scheme determines the number of bits that are allocated for quantizing each sub-band signal of the QMF analysis filter bank. The algorithms presented in this chapter are used for off-line calculation of the bit assignment codebooks of Fig. 1.2. The bit assignment decision is based on a local estimate of the amplitude variance of the signal in each sub-band as obtained from the spectral template used to represent the speech. The i th sub-band is uniformly quantized with quantizer size Δ_i and 2^{b_i} quantizer levels.

This chapter discusses a bit assignment technique for achieving a quantizing noise power which is flat in frequency, as well as a technique for achieving a noise power which "follows" the spectral amplitude of the speech signal for auditory masking of the noise [2]. The techniques presented in this chapter are valid subject to the assumptions that:

1. The spectral side information model provides a good estimate of the amplitude variance of the sub-band signals.
2. The quantizer step sizes Δ_i are well adapted to the amplitude variance of the signal in each sub-band.

Under these assumptions the number of levels assigned for quantizing the sub-band signal in any channel will determine the "coarseness" of the quantization in this channel, and hence the SNR obtained for quantizing that channel.

4.2 Bit Assignment for Flat Noise Power

Let us assume that the sub-band output sequence $y_i(n)$ of the i th sub-band is a sequence of statistically independent, stationary, Gaussian random variables with zero mean and variance σ_i^2 . The estimate of σ_i^2 is provided by the template estimate of the spectral magnitude in band i . If an average mean-squared quantization error D^* is minimized, the optimal bit assignment for the i th sub-band signal is given by [29]

$$b_i = \delta + \frac{1}{2} \log_2 \frac{\sigma_i^2}{D^*}. \quad (4.1)$$

The second term is the lower bound rate given by rate distortion theory for independent, Gaussian, r.v.'s with variance D^* [1]. δ is a correction term that accounts for the performance of practical quantizers; it depends on the type of quantizer and the PDF of the signal to be quantized. The dependence of b_i on δ will be neglected [29]. D^* , the average mean-squared distortion or quantization noise variance is defined as

$$D^* = \frac{1}{32} \sum_{i=1}^{32} \sigma_e^2(i) \quad (4.2)$$

where $\sigma_e^2(i)$ is the quantization noise variance as a result of quantizing the i th output y_i . The parameter D^* of Eq. (4.1) must be chosen such that

$$B = \sum_{i=1}^{32} b_i. \quad (4.3)$$

The sum of the bits available for quantizing each channel is equal to the total number of bits available for quantizing each (32 sample) frame. At a 16 kb/s coding rate there are 250 frames/second and hence B is roughly 64 (neglecting requirements for transmission of side information of gain and template number). It has been shown [29] that the above bit assignment rule leads to a flat noise distribution in frequency, i.e., $\sigma_e^2(i) = D^*$ for all i .

For practical implementation Eq. (4.1) can be modified as

$$b_i = \lfloor \log_2 \sigma_i - D \rfloor \quad (4.4)$$

where the operation $\lfloor \cdot \rfloor$ is defined as

$$\lfloor u \rfloor = \begin{cases} 0, & \text{if } u < 0 \\ \text{greatest integer } \leq u, & \text{if } 0 \leq u < b_{\text{MAX}} \\ b_{\text{MAX}}, & \text{if } u \geq b_{\text{MAX}} \end{cases} \quad (4.5)$$

where b_{MAX} is the maximum number of bits allowed for quantizing any channel output, and $D = \frac{1}{2} \log_2 D^*$ (the quantization noise in bits). An algorithm for implementing the above bit assignment scheme is given in Appendix III.

An intuitive explanation of why this bit assignment rule, based on a minimum mean-square error over the frame, leads to a flat noise distribution in frequency can be seen in fig. 4.1 [2]. The horizontal dashed lines represent decision thresholds, λ_i , for choosing the bit allocation b_i . As an example, if the i th log spectral output $\log_2 \sigma_i$ falls between λ_2 and λ_3 , then 3 bits are allocated for that coefficient. The thresholds are spaced 6 dB apart. Recall that for a uniform quantizer with proper loading the SNR is given by

$$SNR(\text{dB}) = 6B + [4.77 - 20 \log_{10} \frac{X_{\text{MAX}}}{\sigma_x}] \quad (4.6)$$

where σ_x is the standard deviation (RMS level) of the signal, and $X_{\text{MAX}} = \Delta \cdot 2^{B-1}$ the maximum quantizer level. Hence for every 6 dB that σ_i is increased, one more bit, or 6 dB of signal-to-noise-ratio is added to the quantizer. Thus, the noise power remains flat across the frequency bands. Exceptions to this occur when $\log_2 \sigma_i < \lambda_0$ and when $\log_2 \sigma_i > \lambda_4$. These cases correspond to the minimum and maximum bit assignments of 0, and say, 5 bits respectively. If the total number of bit assigned in this way is less than B — the number of bits available for quantizing the frame — then the level of the thresholds λ_i (proportional to D^*) are uniformly reduced. The threshold levels are uniformly increased if the total number of bits is greater than B . An example bit assignment using this scheme for $B = 61$ is illustrated in Fig. 4.2b by the solid line. The dashed line of Fig. 4.2a depicts the log magnitude of a 4th order LPC template (taken from an 8 template set) model of input speech $\log_2 \left[\frac{1}{A_i(z)} \right]$. The corresponding amplitude scale "in bits" is indicated on the figure.

4.3 Bit Assignment for Noise Shaping

We have noted that the previous bit assignment scheme minimizes the noise variance $\sigma_e^2(i) = D^*$ and results in a flat noise power across the spectrum that is proportional to λ_0 . It is known from perceptual criteria that minimum mean-square error or a flat noise distribution is sub-optimal for masking the quantization noise in each frequency band. The distribution of quantization noise across the frequency channels can be controlled by a modified bit assignment

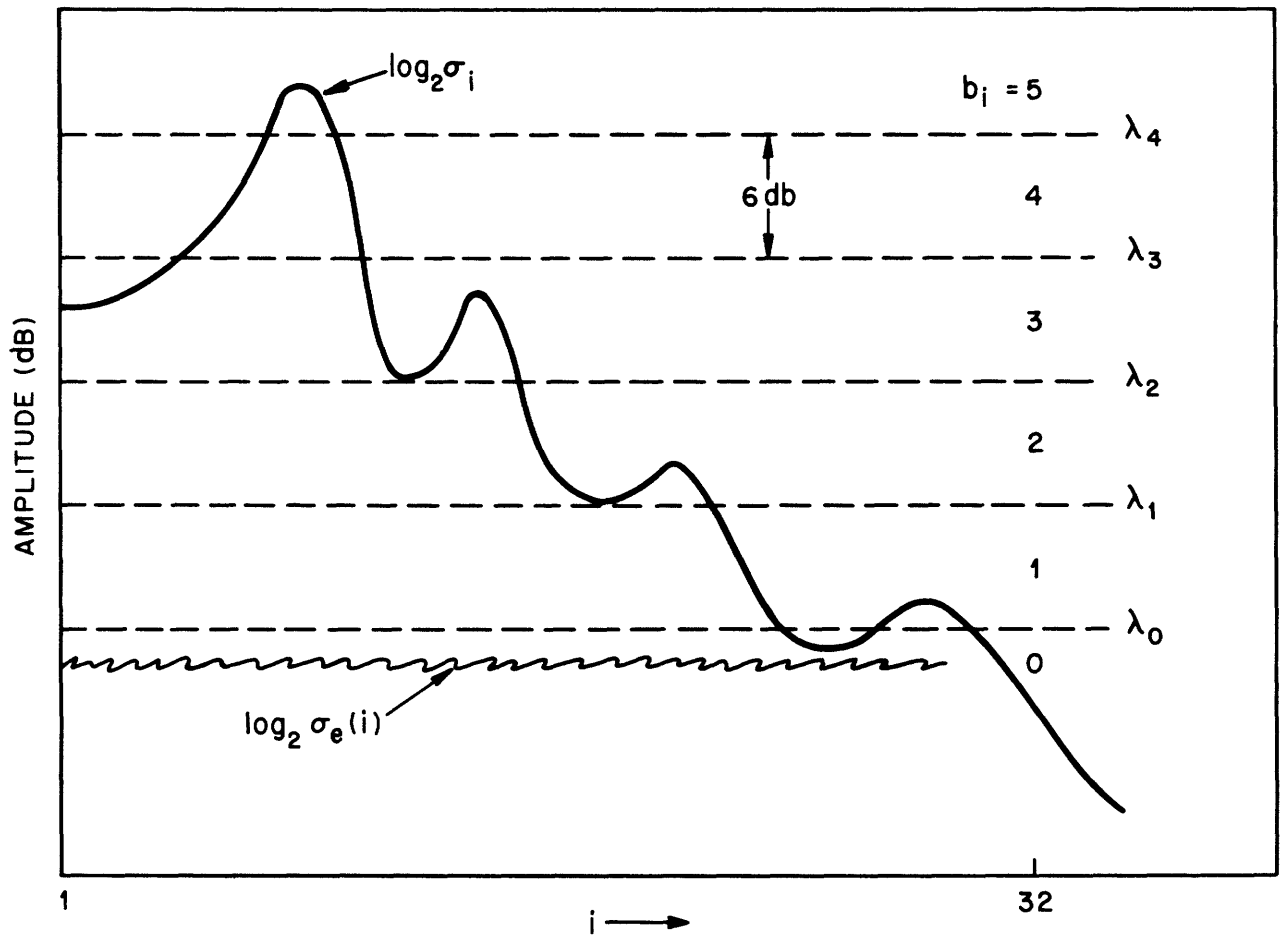


Fig. 4.1 Bit assignment rule for a flat noise spectrum.
 Tribolet and Crochiere et al.: Frequency Domain Coding Of Speech.

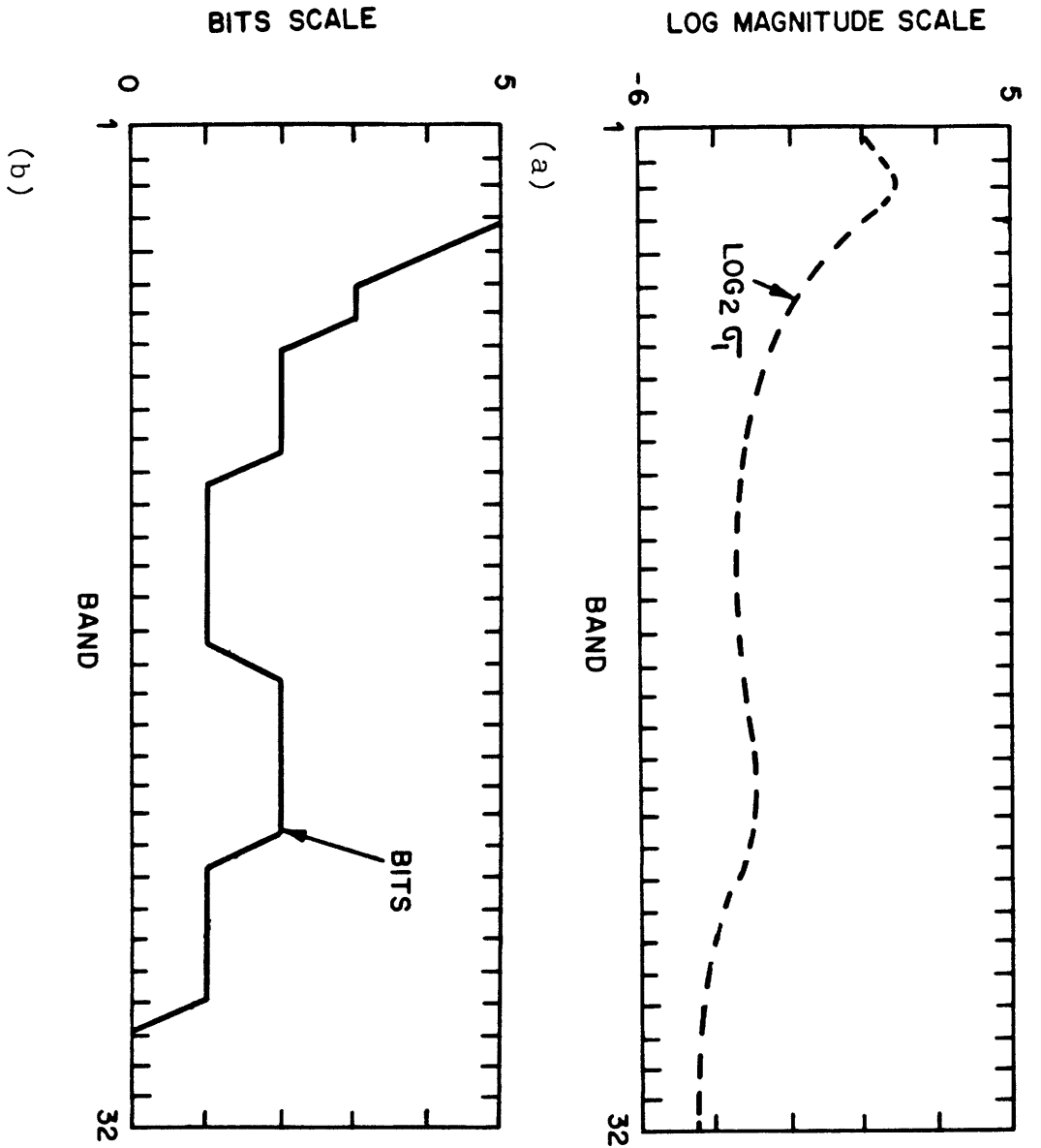


Fig. 4.2 (a) LPC template, (b) derived bit assignment for a flat noise spectrum.

rule [2]

$$b_i = \delta + \frac{1}{2} \log_2 \frac{W_i \sigma_i^2}{D^*} \quad i = 1, 2, \dots, 32 \quad (4.7)$$

where W_i is a positive weighting function. This bit assignment minimizes the frequency weighted distortion measure

$$D^* = \frac{1}{32} \sum_{i=1}^{32} W_i \sigma_e^2(i) \quad (4.8)$$

resulting in a noise variance given by

$$\sigma_e^2(i) = C \cdot W_i^{-1} \cdot D^* \quad i = 1, \dots, 32 \quad (4.9)$$

where C is a constant. Figure 4.3 provides an interpretation of this frequency weighted bit assignment where the thresholds are now $\lambda_i - \frac{1}{2} \log_2 W_i$. Viewed another way we have pre-emphasized σ_i^2 to $W_i \sigma_i^2$, and used the flat thresholds of figure 4.1.

The weighting function should be chosen in a manner in which the quantization noise is best masked by the speech signal [30]. The weighting function

$$W_i = \sigma_i^{2(\gamma-1)} \quad (4.10)$$

belongs to a class of functions which provide a wide range of control over the shape of the quantizing noise relative to the shape of the speech spectrum by experimentally varying γ . The case where $\gamma = 1$ (uniform weighting) has already been discussed. This case yields a flat noise spectrum and the bit assignment obtained is such that the signal-to-noise-ratio has the shape of the spectrum. The case where $\gamma = 0$ (inverse spectral weighting) leads to a flat bit assignment. Here the noise spectrum follows the input spectrum, and the signal-to-noise-ratio is constant as a function of frequency. The quantization noise distribution "in bits" given approximately by

$$\log_2 \sigma_e \cong \log_2 \sigma_i - b_i + 1 \quad (4.11)$$

is depicted by the dashed lines in figures 4.4a and 4.4b for $\gamma = 1$ and $\gamma = 0$ respectively. In general, as the value of γ is gradually varied between these two extremes ($0 < \gamma < 1$), the noise spectrum will change from one that precisely follows the speech spectrum to a flat distribution.

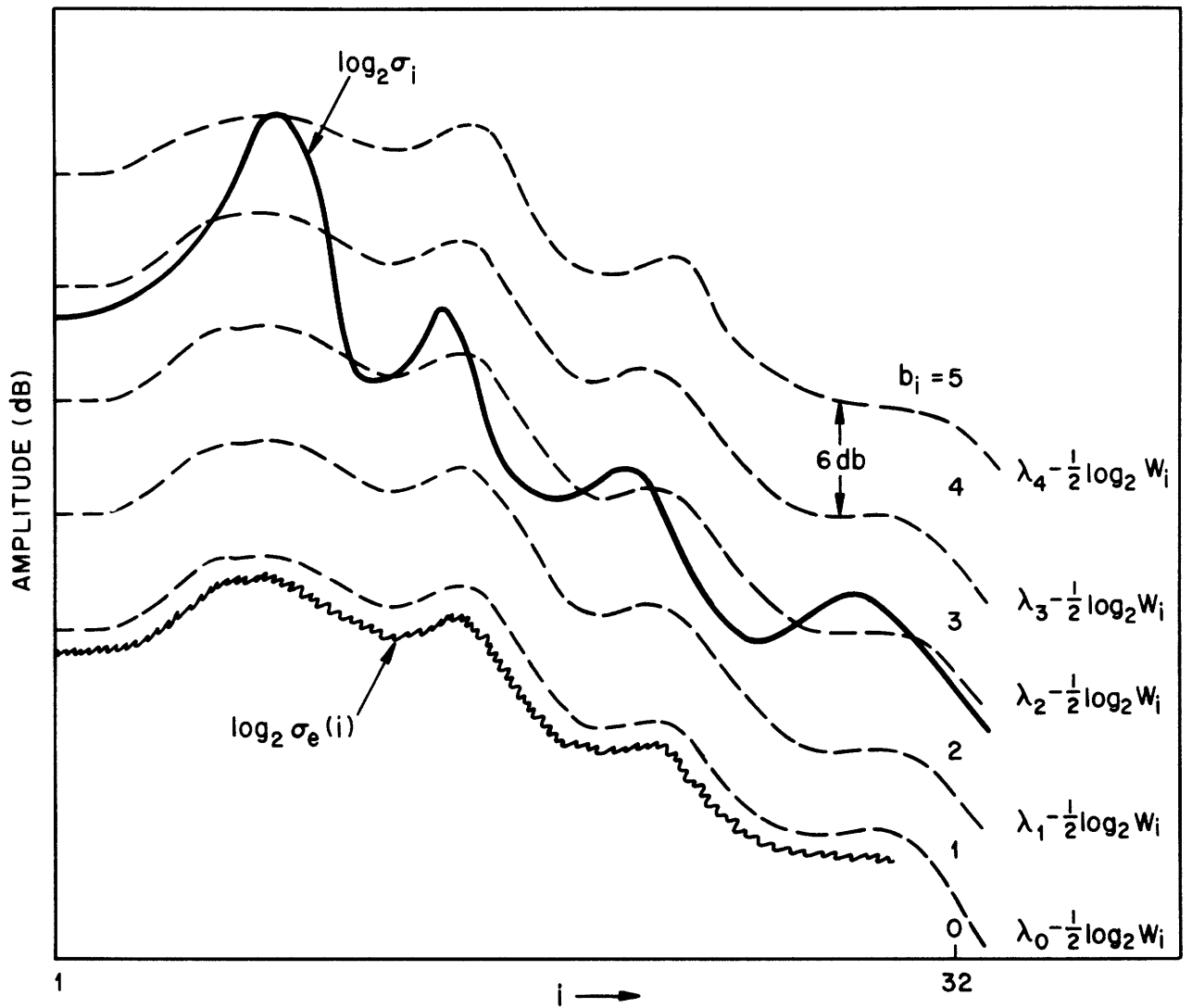


Fig. 4.3 Frequency weighted bit assignment rule.
 Tribolet and Crochiere et al.: Frequency Domain Coding Of Speech.

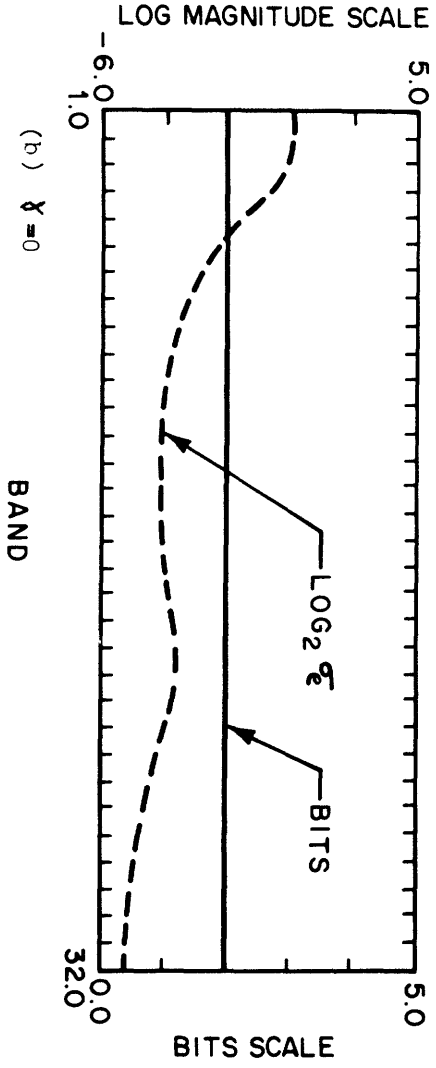
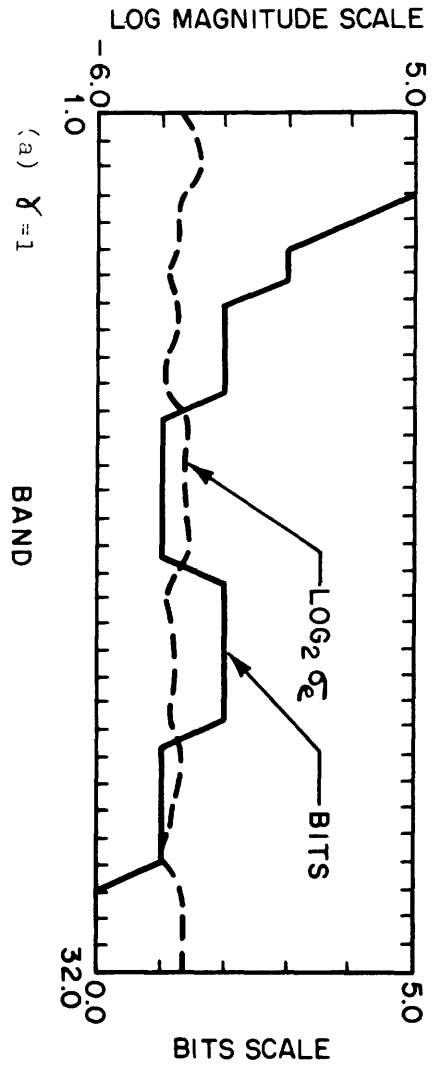


Fig. 4.4 Bit assignments and quantization noise (solid lines and dotted lines respectively) for flat noise spectrum and flat SNR .

4.4 Observations

In this chapter we have discussed a bit assignment scheme which enables us to experiment with bit assignment codebooks computed with an arbitrary amount of noise shaping — or control over the degree to which the spectral shape of the quantization noise follows the spectral envelope of the speech. Additional details of the bit assignment procedure are presented in Appendix III.

CHAPTER V

5. ADAPTIVE QUANTIZATION OF NARROW BAND SUB-BAND SIGNALS

5.1 Introduction

In quantizing the sub-band signals we are faced with the problem of adaptively setting the quantizer step sizes for uniformly quantizing the outputs of the 32 channel QMF analysis filter bank. On the one hand we want to choose the quantization step size large enough to accommodate the maximum peak-to-peak range of the signal to avoid quantizer overloading. On the other hand we would like to make the quantization step size small so as to minimize quantization noise due to "underloading". This is compounded by the nonstationary nature of the speech signal as well as the speech communication process. The amplitude of the speech signal can vary over a wide range within a given utterance, from voiced to unvoiced sections, and for different talkers.

In order to adapt the step sizes to utilize the full range of the quantizers, a local estimate of the time-dependent variance of the speech is required in each band. If the signal variance is known, the quantizer levels (or step size for a uniform quantizer) can be chosen to minimize the quantization error variance, or mean squared error for a zero mean signal. The quantization noise variance is defined as

$$\sigma_e^2 = E[e^2(n)] = E[(\hat{x}(n) - x(n))^2] \quad (5.1)$$

where $x(n)$ is the input, $\hat{x}(n)$ is the quantized output and the error signal $e(n)$ is assumed to have zero mean. Minimization of the quantization error variance corresponds to maximization of the signal to quantization noise ratio defined as

$$SNR = \frac{\sigma_x^2}{\sigma_e^2} = \frac{E[x^2(n)]}{E[e^2(n)]} \quad (5.2)$$

when the input signal is assumed to be zero mean. The problem of quantizing for minimum mean-squared quantization error was studied by Max [31] who has published tables for "optimum" quantizers with both equally and non-equally spaced levels under the assumption of

a normally distributed input signal. Although it is known that mean squared error criteria is perceptually sub-optimal, it is a good first cut criteria.

To state the problem again in more precise terms; the problem of adapting the quantizer step sizes is the problem of computing a "good" local estimate of the variance of the speech signal in each channel at a modest cost in computational complexity, while keeping the amount of side information to a small fraction of the total information rate of 16 kbs. This is consistent with algorithm study in which the complexities involved have been restricted to the middle range between those of simpler sub-band and more complex transform coding techniques.

5.2 A Review of Adaptive Quantization Schemes for Frequency Domain Speech Coding

The technique of varying the quantizer step size in proportion to the standard deviation of the input signal is known as adaptive quantization. There are two basic categories encompassing such techniques — feed forward adaptation and feedback adaptation. In both cases the step size is made proportional to the standard deviation of the signal, or the gain applied to the input of a uniform fixed quantizer can be made inversely proportional to this standard deviation.

Block diagrams of the two schemes are shown in Fig. 5.1.1 and Fig. 5.1.2. In feed-forward adaptation a gain term is calculated from the input, quantized, and sent as "side information" along with the encoded signal $c(n)$. In feedback adaptation the gain term is calculated from the codewords and no side information is required. Although feedback adaptation requires no side information there is increased sensitivity to transmission errors, since such errors imply both codeword and step size errors. On the other hand, side information requirements for sub-band coding with many bands can become excessive with feed-forward adaptation. For sub-band coding with a small number of bands (2-4) step size adaptation has been effectively dealt with using both forward and backward adapting techniques.

Jayant [32] has developed a backward adapting technique where the step size of a uniform quantizer is adapted at each sample time by the formula

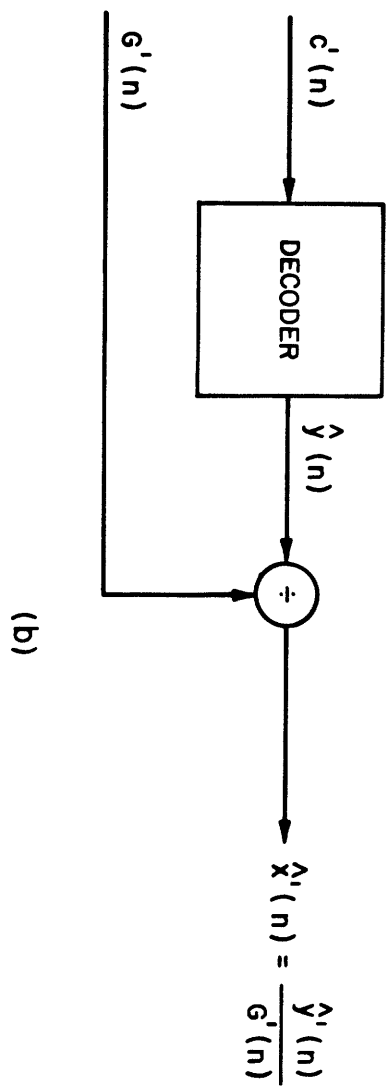
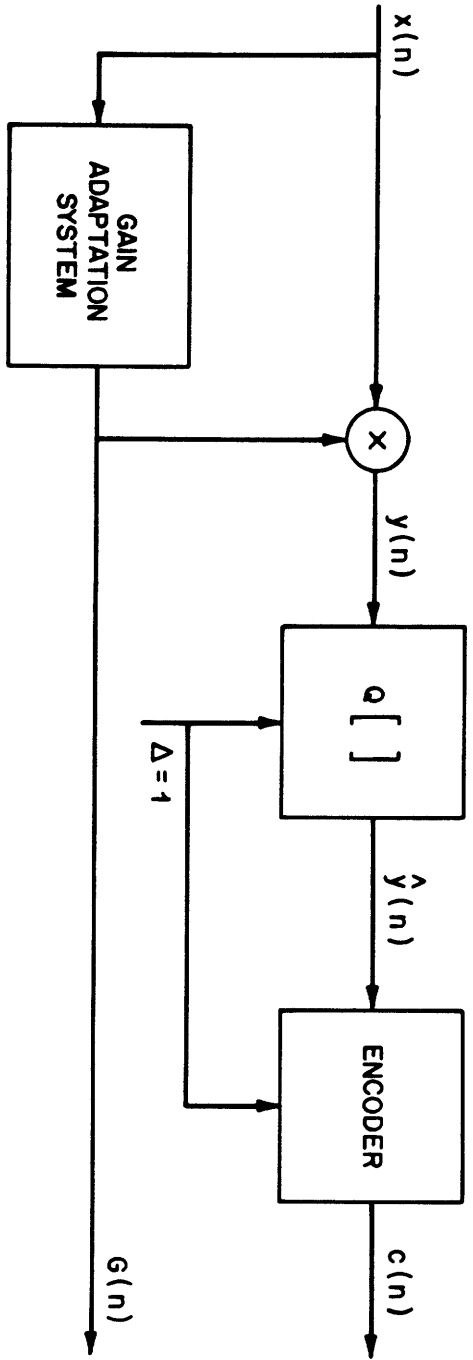


Fig. 5.1.1.1 General feed forward adaptive quantizer with a time-varying gain; (a) coder; (b) decoder. Rabiner and Schafer et al.: Digital Processing of Speech Signals.

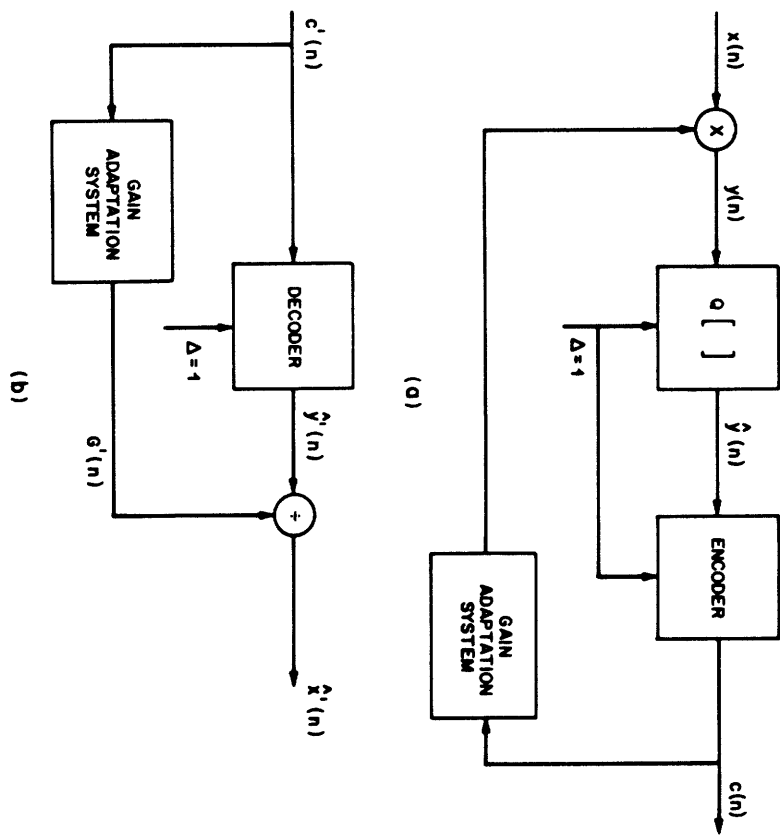


Fig. 5.1.1.2 General feedback adaptation of the time-varying gains; (a) coder; (b) decoder. Rabiner and Schafer et al.: Digital Processing of Speech Signals .

$$\Delta(n) = P \cdot \Delta(n-1) \quad (5.3)$$

where P , the step size multiplier, is a function of the magnitude of the previous codeword $|c(n-1)|$. If the codeword is one of the outer magnitude levels of the quantizer, a value of P greater than 1 is used to increase the step size of the quantizer for the next sample time. If the codeword is one of the inner magnitude levels, a value of P less than one is used to reduce the quantizer step size for the next sample time. Jayant has selected a set of 2^{B-1} step size multipliers which minimize the quantization error variance for normally distributed input signals. Clearly, this is a first order predictive technique whose success is based upon the relative amplitude stationarity of the input signal.

Crochiere has demonstrated the effectiveness of this technique for sub-band coding with two to five frequency bands [6]. For a sub-band coder with 32 bands, the critical sampling rate of the QMF analysis bank outputs is one thirty-second of the input sampling rate. At this decimation rate there is insufficient sample to sample amplitude correlation between successive outputs of a channel for predictive step size adaptation algorithms to be effective. Hence Jayant's technique cannot be extended to 32 band sub-band coding without significant loss of performance.

Croiser [33] has developed a feed-forward companding scheme which is neither instantaneous (where each coded sample contains its own companding information) or adaptive (where the range or scale factor to apply to the coder and decoder is derived from past history of the signal) in the strict sense. Rather than coding the samples one by one, a scale factor is chosen as a function of a whole block of samples according to a criterion. For example, the scale factor can be chosen so that the maximum sample amplitude in the block will not fall out of the coded range. After coding a block of data is formed for transmission comprised of the value of each sample and the common scale factor. In this scheme, the overhead bit rate is inversely proportional to the block length. Block companding has been successfully applied to sub-band coding with a small number of bands by Esteban and Galand [13]. This technique offers advantages of a very large dynamic range, limited error propagation, and no transient

clipping.

Extension of this technique for coding 32 sub-bands would require an inordinate amount of side information as each channel would require transmission of a scale factor. Since each band of the QMF analysis output filter bank is sampled once for every 32 samples of the input, long blocks (more than about 5 consecutive samples from any band) could not be exploited for overhead bit rate reduction as this would result in poor SNR over the block.

In transform coding, where there are many bands or transform coefficients (on the order of 128 to 256), adjusting the step sizes for quantizing each coefficient has been most successfully dealt with by using relatively complex feed-forward side information models. Two successful side information models are outlined here.

Tribolet and Crochiere have investigated one such model in which an LPC predictive analysis with pitch prediction is performed for each input speech frame [34]. The spectral side information consists of LPC predictor coefficients to model the spectral envelope, and pitch gain and pitch period terms to model the harmonic pitch structure. Both the bit allocation and the quantizer step sizes are determined on the basis of this side information model. Quantizer step sizes are determined according to the theory of Max [31] where for a given bit assignment $b(k)$, the step size $\Delta(k)$ is proportional to the estimated spectral level $|\tilde{x}(k)|$. Figure 5.2 illustrates this basic scheme.

It has been observed that as the dynamic range of the input spectrum becomes large, frequency domain aliasing occurs as a result of energy leakage from large energy bands to low energy bands. This effect was reduced by pre-emphasizing the input signal with an adaptive LPC inverse filter so as to obtain a spectrally flattened output prior to analysis/synthesis. This modified scheme is illustrated in figure 5.3. In principle this dynamic pre-emphasis corresponds to a division of the Discrete Cosine Transform spectral coefficients by the estimated speech spectrum, the result then being quantized using unit-variance uniform quantizers [35].

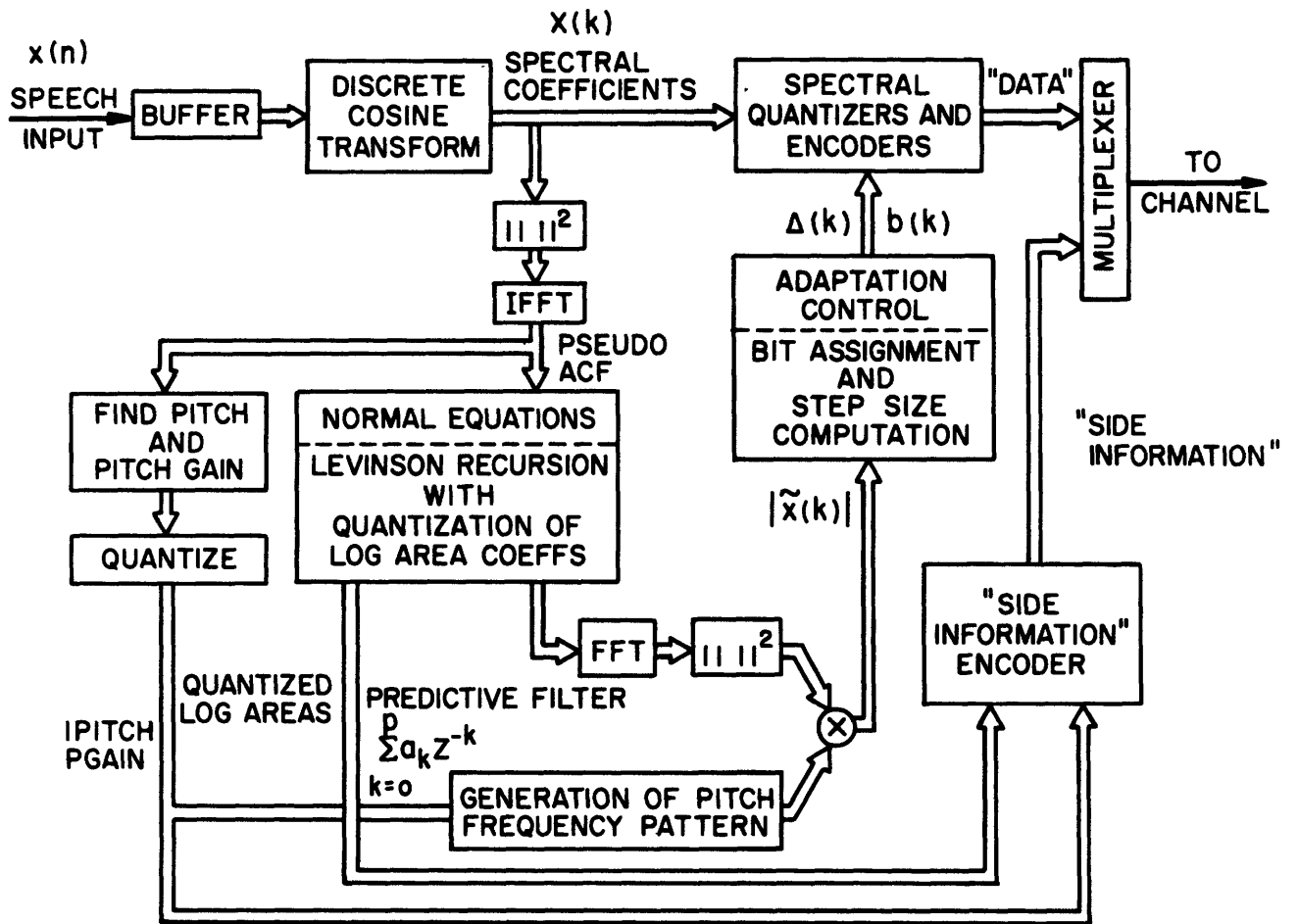


Fig. 5.2 Block diagram of LPC vocoder driven adaptive transform coder. Tribolet and Crochiere et al.: A Modified Adaptive Transform Coding Scheme with Post Processing-Enhancement.

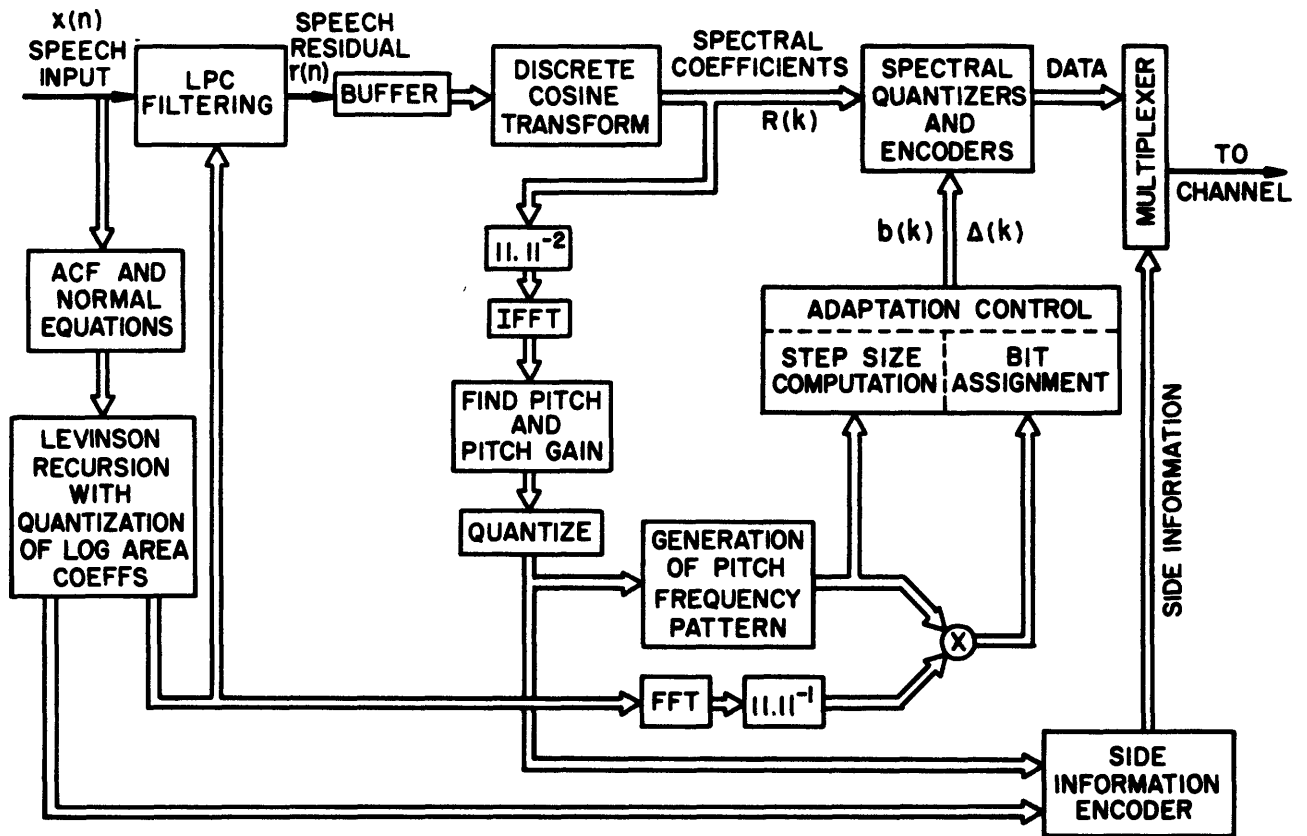


Fig. 5.3 Block diagram of a modified LPC vocoder driven adaptive transform coder. Tribolet and Crochiere et al.: A Modified Adaptive Transform Coding Scheme with Post Processing-Enhancement.

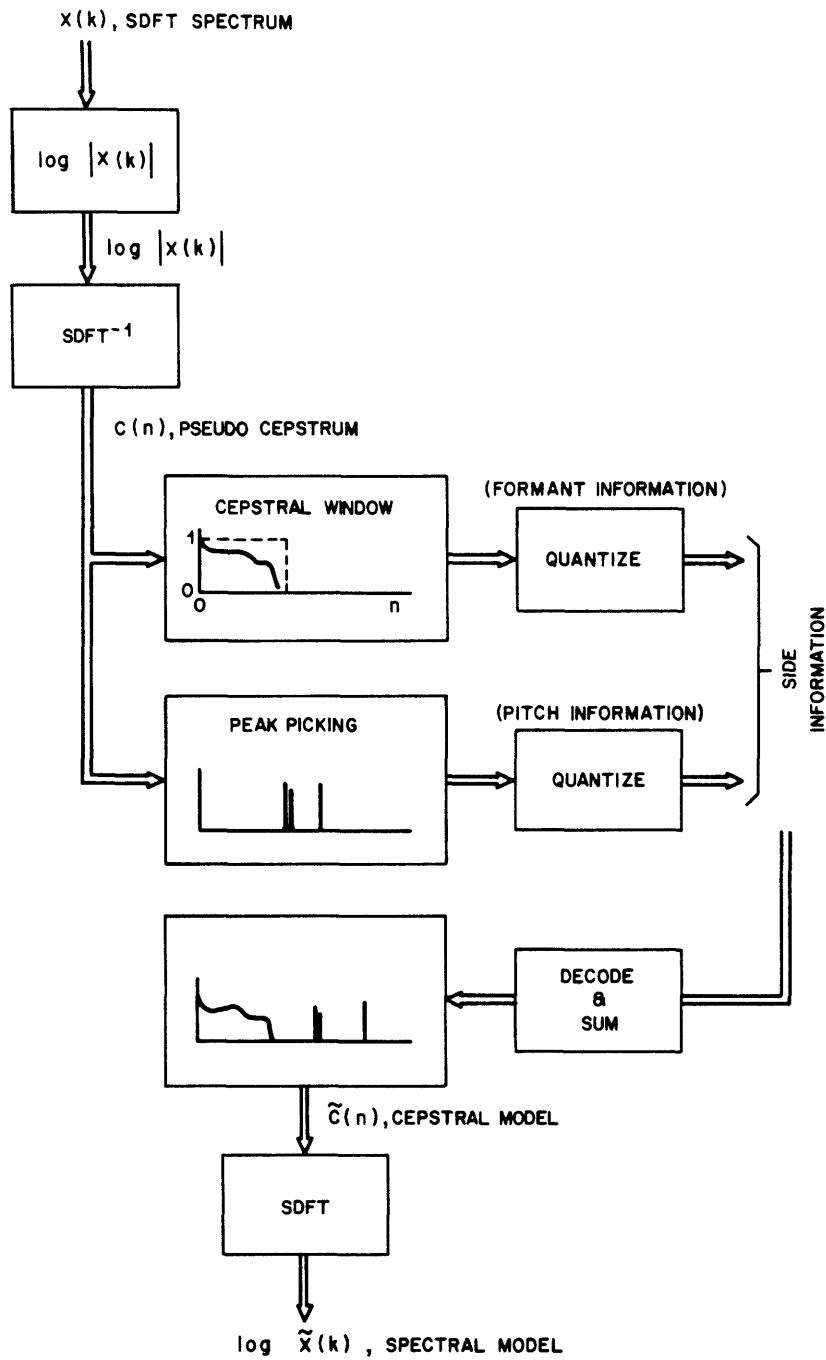


Fig. 5.4 Side information model for a homomorphic analysis.
Cox and Crochiere et al.: Real Time Simulation of Adaptive Transform Coding

Another successful spectral side information model is the homomorphic model which has been implemented in real time by Cox and Crochiere [3]. This side information model is outlined in figure 5.4. The formant spectral envelope is estimated by retaining the low-time portion of the cepstrum. The pitch structure is derived from peak-picking outside the low-time cepstral window. By retaining 10 to 14 cepstral coefficients for formant information and one to two pitch pulses for pitch information, this side information model requires between 2 and 3 kbs for transmission.

5.3 An Adaptive Quantization Scheme for Coding the Outputs of the 32-Channel Analysis Filter Bank

The problem of adapting the quantizers' step sizes for 32 band sub-band coding has been approached with a feed-forward adaptation scheme. Consider the method of figure 5.1.1 applied to coding the 32 channel outputs. As discussed in Chapter IV, the number of bits allocated for quantizing the i th channel is given by the bit assignment pattern corresponding to the LPC template employed for modeling the speech spectra in the current frame. The gain terms (sometimes referred to as inverse step sizes) are made inversely proportional to the estimate of the signal magnitude in this channel as provided by the vector quantization side information model of Chapter III by*

$$\sigma_k = \frac{\sqrt{\sigma_i}}{|A_i(\omega_k)|} \quad k = 1, 2, \dots, 31, 32 \quad (5.4)$$

where $1/|A_i(\omega_k)|$ is the LPC gain normalized spectral magnitude of the i th LPC template for the k th channel and $\sqrt{\sigma_i}$ is the LPC gain term developed in Section 3.3. This gain term was selected** so that the normalized channel outputs

* See equation III.3 of Appendix III.

** The gain term estimate $\sqrt{\sigma_i}$ was optimized by adjusting G of Eq. (3.5).

$$\frac{y(k)}{\left[\frac{\sqrt{\sigma_i}}{|A_i(\omega_k)|} \right]} \quad (5.5)$$

exhibited approximately unit variance.

In the first attempts at coding, eight, fourth order, LPC templates were used for bit assignment and step size adaptation. This number of templates and LPC order of analysis were chosen on the basis of the measurements described in Section 3.4.

In order to subjectively optimize the step sizes, bit assignments were calculated to achieve a spectrally flattened quantization noise signal. This condition is referred to as bit assignment without noise shaping (see figure 4.1 of Chapter IV).

For the first stage of subjective optimization the step sizes in band k satisfy the equation

$$C \cdot \frac{\sqrt{\sigma_i}}{|A_i(\omega_k)|} = \Delta(k) \cdot 2^{[b_k-1]} \quad (5.6)$$

where C is a constant chosen as 2.0, Δ is the step size, and b_k is the number of bits allocated to band k . This quantizing rule gives the gain term of figure 5.1.1 as*

$$G_n(k) = \frac{2^{[b_{k,n}-1]}}{C \cdot \left[\frac{\sqrt{\sigma_i}}{|A_i(\omega_k)|} \right]} \quad k = 1, 2, \dots, 32. \quad (5.7)$$

Quantization of the scaled signal $G_n(k) \cdot y(k)$ is accomplished with a uniform, unit variance, quantizer with mid-riser characteristics [28] when at least 1 bit is allocated to the quantizer. Otherwise the quantizer output signal is forced to zero.

The quantizing scheme described in Eq. (5.6) will be referred to as C signal loading. The reason for this terminology is that the largest signal that does not overload the quantizer has a magnitude of C standard deviations of the input.

* The subscript n is a reminder that the gain term is a function of time since the bit assignment B and template number i are inherently functions of time.

The major problem with this quantizing technique is that bands receiving only one or two bits have step sizes which are more often than not — too large. The dominant reason for this is that the LPC templates generally over estimate the magnitude of the spectrum in low amplitude regions. When there is no noise shaping, the number of bits assigned to a band is proportional to the amplitude of the template model in this band. Hence bands with a small number of bits correspond to low amplitude bands in the original speech. The problem is that we are trying to model the spectral magnitude of a signal which exhibits considerable dynamic range, with a small finite set of spectral models. Furthermore, since all-pole models are used, the spectral peaks are modeled more accurately than the low amplitude regions. The problem is further exacerbated since the dynamic range of the quantizers are proportional to the number of bits it receives. Hence quantizers receiving one or two bits do not have the dynamic range to capture the overestimated signal. Figure 5.5 gives a magnitude plot of the output range of the quantizers in each band (dotted lines) superimposed over the signal level in each band (the solid line). This illustrates the step size adaptation problem for a 8 template 4th order LPC side information model.

This problem is manifested by a trailing "noise shadow" which is present in the coded speech output. When the input to the quantizers in certain frequency bands lies outside the dynamic range of the quantizers a large amount of spectral error results in some channels. This spectral error manifests itself in the time domain as trailing noise due to the long (514 sample) impulse responses of the filter bank. This poor time resolution, caused by the time frequency duality principle, causes gross quantizing errors in frequency to be dragged out in time for the duration of the impulse response of the QMF filters.

Thus it must be concluded that in order to achieve major improvements in the coded speech quality the complexity of the spectral side information model must be increased. Considerable improvement has been realized by use of 32 10th order LPC templates. An increased number of templates allows less generality of the models, while an increased LPC order offers better resolution of spectral peaks and valleys. Figure 5.6 illustrates the increased accuracy of coding

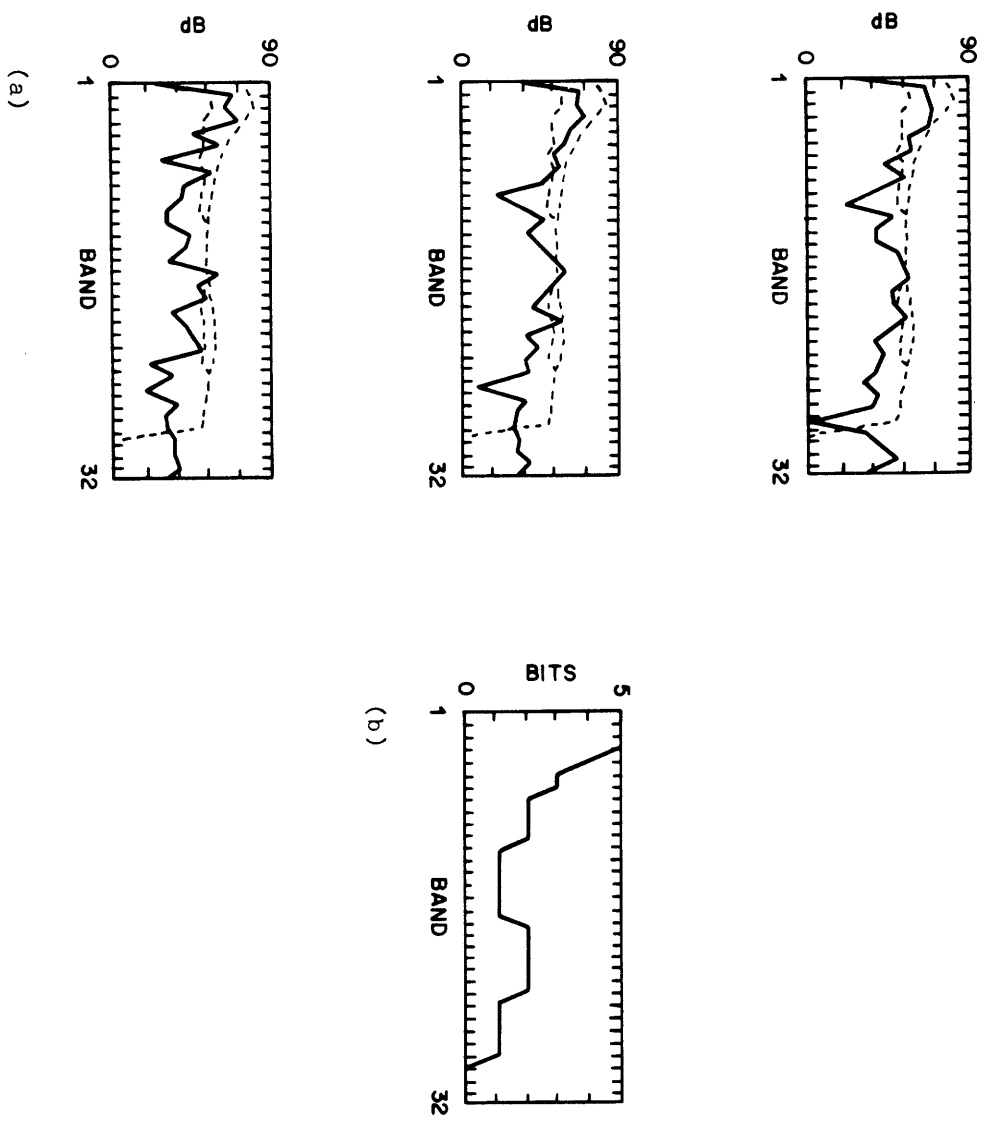
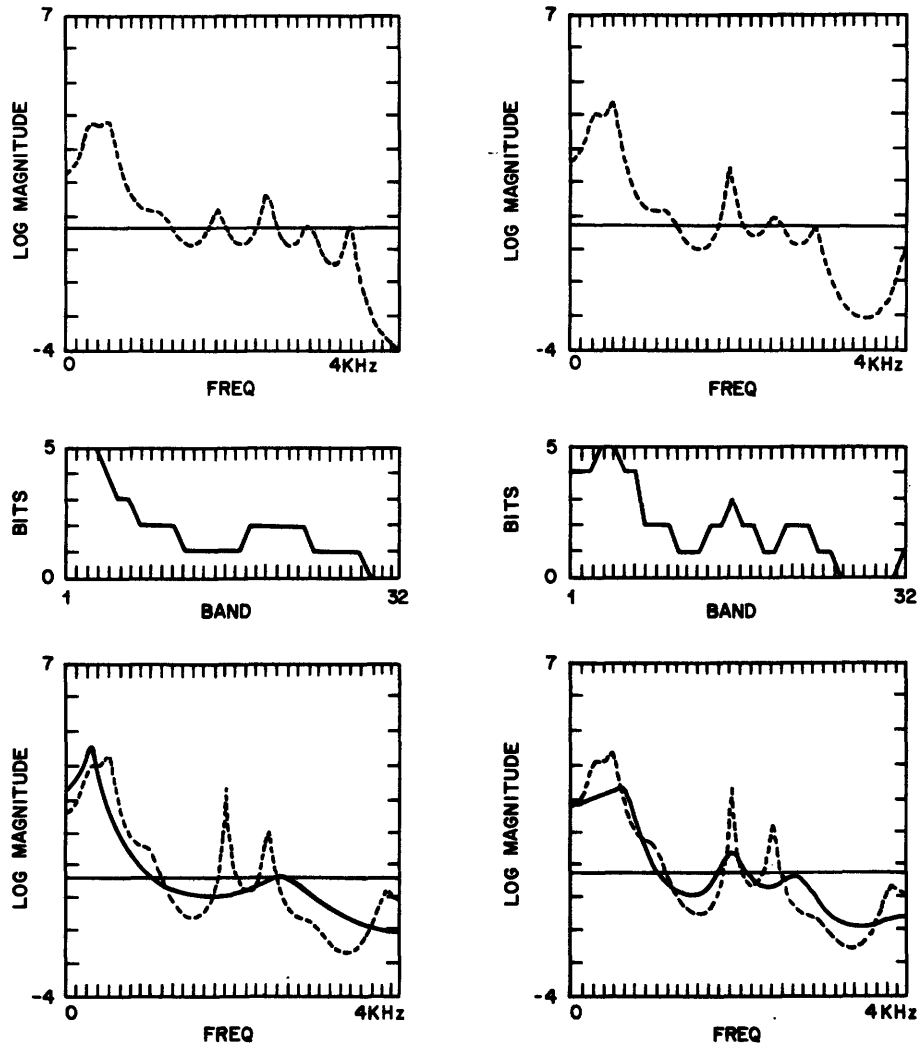


Fig. 5.5 (a) Successive 4ms frames of the QMF analysis filter bank output (solid line) superimposed over minimum and maximum quantizer levels, (b) the corresponding bit assignment.



(a) 8 template 4th order LPC analysis

(b) 32 template 10th order LPC analysis

Fig. 5.6 Figures illustrate from top to bottom the LPC spectrum of the coded output, the bit assignment, and the LPC input spectrum (dotted line) superimposed with the template LPC spectrum.

with 32 10th order templates. The figure includes a standard 14th order LPC analysis of the input and coded speech, the template used, and the derived bit assignment.

There is a practical limit to the amount of improvement which can be bought with additional templates and LPC order. Listening tests performed with 64 and 128 (10th order LPC) templates indicate only marginal improvement in subjective quality over using 32, 10th order LPC templates. The reason for this is that although more templates result in some improvement in the bit assignment patterns, there are never enough templates to do good modeling in 1 and 2 bit bands which correspond to low amplitude regions in the input spectra. Figure 5.7 illustrates this point for a 1024 template 10th order LPC analysis performed by B. H. Juang for LPC voice coding using vector quantization [19].

A fair amount of improvement in the quality of the coded speech results from reducing the sigma loading when quantizing with only one or two bits. This has the effect of proportionally decreasing the step sizes of these quantizers so they can better capture the input signal. The best results have been achieved by lowering the step sizes of 1 and 2 bit quantizers by approximately 9 and 5 dB respectively. This is implemented by changing C in Eq. (5.7) to .665 and 1.054 for 1 and 2 bit quantizers respectively.

By minimizing the quantizer error variance for the case of an equally spaced level quantizer with a normally distributed input signal, Max [31] found that the degree of sigma loading (the parameter C in Eq. (5.6)) should increase as the number of quantizer levels increase. As a final improvement to the step size adaptation scheme, quantizers receiving 3,4, or 5 bits used optimum step sizes according to Max. This was accomplished by using C parameters of 2.344, 2.682, and 3.009 for 3,4, and 5 bit quantizers respectively. This technique offers an increased amount of dynamic range in large amplitude portions of the spectra.

Figure 5.8 shows a magnitude plot of the quantizer output range (the dotted lines) superimposed over the signal level (the solid line) for each band using this final step size adaptation scheme. Comparison of figure 5.8 with figure 5.5 shows the improvement in

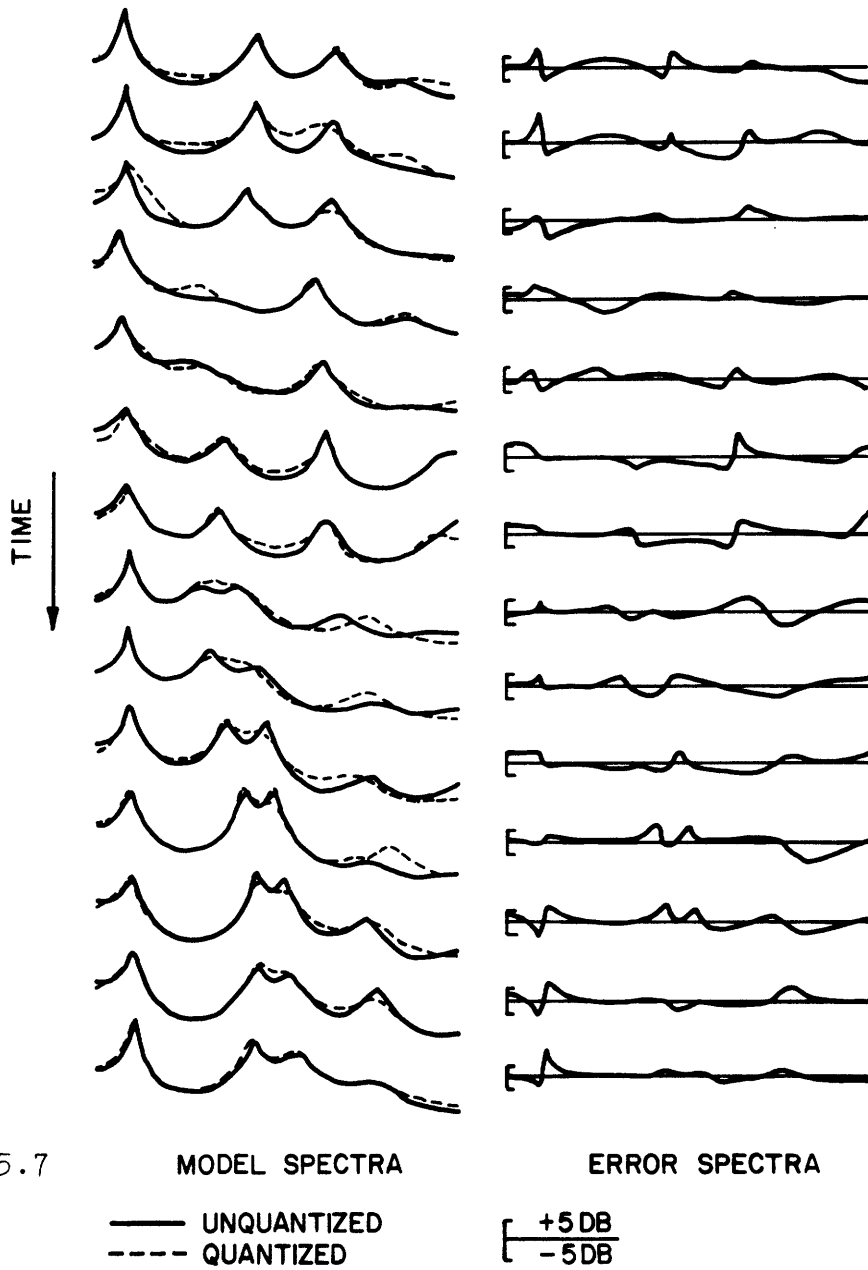


Fig. 5.7

Juang et al.: Distortion Performance of Vector Quantization for LPC Coding..

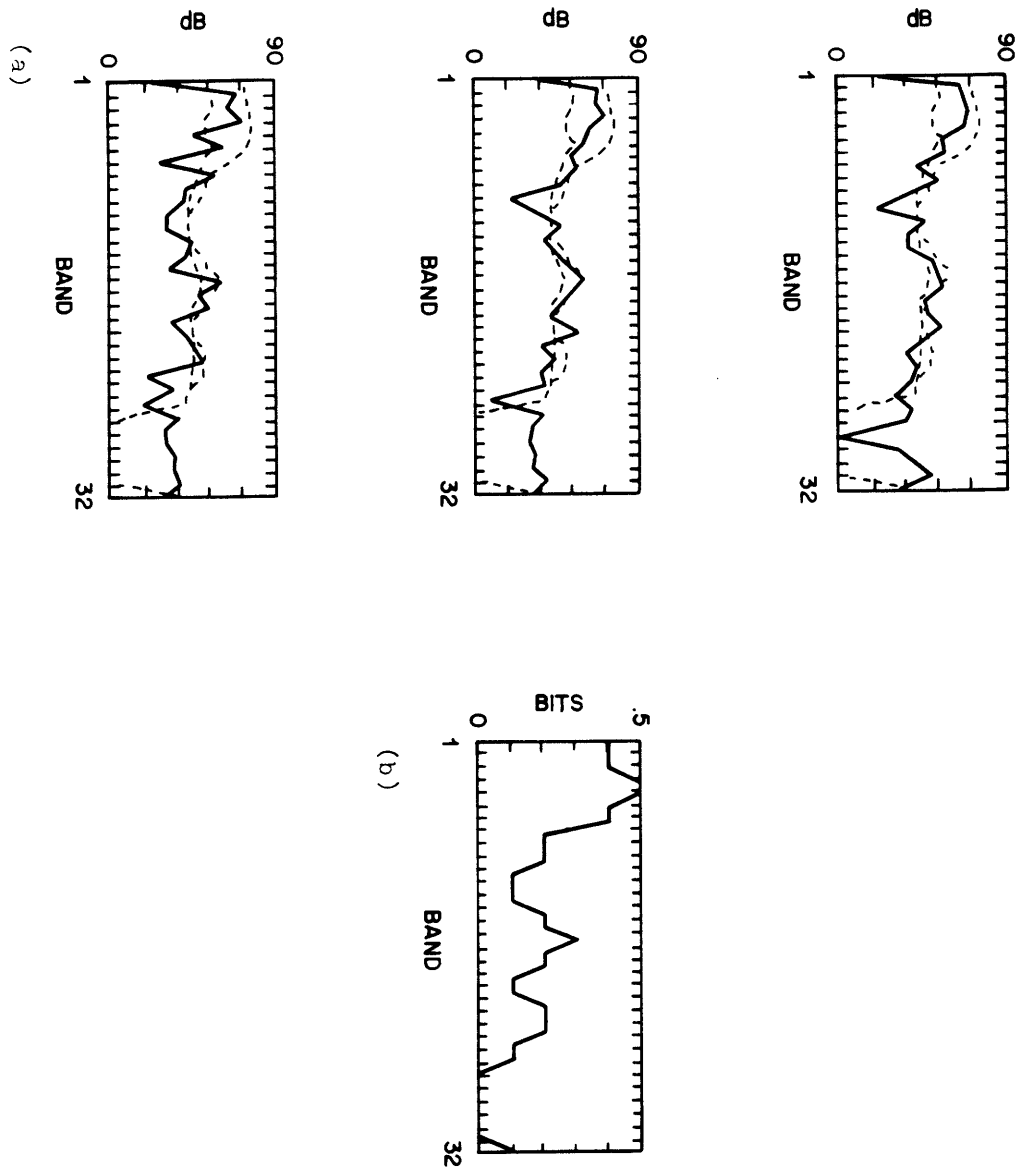


Fig. 5.8 (a) Successive 4ms frames of the QMF analysis filter bank output (solid line), superimposed with minimum and maximum quantizer output levels. (b) The corresponding bit assignment.

capturing the input signal resulting from:

1. More templates of higher LPC order.
2. Subjectively reducing the step sizes for quantizers receiving 1 or 2 bits.
3. Increasing the step size loading according to Max for quantizers receiving 3,4, or 5 bits.

5.3.1 Observations

As noted earlier in the discussion, all bit assignments were calculated without incorporating noise shaping to simplify the step size optimization procedure. Experimentation with the weighting function parameter γ of Chapter IV has indicated that in the best situations, perceptually sharp degradations, of durations on the order of the impulse response duration of the QMF filters, can be traded-off for increased noise levels throughout the utterance. The objective of noise shaping is to approach a spectrally flattened SNR by approaching a flat bit assignment in the channels. The problem with this is that a flat bit assignment (total noise shaping) at 16 kbs corresponds to allocating approximately 2 bits/channel.* Unfortunately, this reduces the dynamic range of the quantizers in channels with large spectral amplitudes and results in increased accuracy constraints on the spectral side information model in these channels. By allocating bits to channels previously starved of bits, noise shaping increases the number of low amplitude channels that are coded with 1 or 2 bits. Both situations result in additional spectral distortion (caused by overloading and underloading of quantizers in certain channels) which is not accounted for in the rate distortion equations in Chapter IV.

Spectral side information is transmitted every four, 4 mS frames without any noticeable degradation in coded speech quality. This scheme corresponds to twelve bits, five for the template number and 7 for the gain, transmitted every four frames leaving 61 bits for quantizing each 32-sample frame. This side information model requires 750 bits/sec. from the total 16 kbs coding rate.

* neglecting for the moment the issue of transmission of side information.

5.4 A Dynamic Pre-Emphasis/De-Emphasis Scheme for Adaptively Quantizing the Outputs of the 32-Channel Analysis Filter Bank

In the analysis/synthesis framework just discussed, large amounts of spectral error is introduced into some frequency bands where the signal amplitude lies outside the range of the quantizer outputs. This phenomena introduces a gross amount of distortion in some bands, in comparison with the distortion which normally results from quantizing a signal lying within the quantizer output range. One effect of this quantization error is to reduce the internal aliasing cancellation properties of the QMF filter bank.* The effect of uncanceled frequency aliasing in the filter bank — energy leakage from high energy bands to low energy bands — becomes more pronounced as the dynamic range of the spectrum becomes large.

In order to reduce the effects of energy leakage from large energy bands to small energy bands, an adaptive pre-emphasis filter is used to obtain a spectrally flattened output prior to analysis/synthesis. This pre-emphasis filter is the inverse LPC template filter $A_i(z)$ of figure 1.2 which best models the input speech in the current frame. The output of the QMF synthesis filter bank is filtered with the corresponding LPC synthesis template filter $1/A_i(z)$ in order to de-emphasize the coded signal. This modified system is illustrated in Figure 5.9.

The spectral side information model of figure 5.9 consists of 32 10th order LPC templates and incorporates the same template selection procedure as the previous section. The codeword or template number outputted by this procedure is used to update the coefficients of the pre-emphasis and de-emphasis filters. These coefficients are updated every 4, 4 mS frames along with the transmitted side information. As with the previous scheme, 5 bits for the templates number and 7 bits for the gain are transmitted every 4 frames leaving 61 bits for quantizing each 32-sample frame. This side information model requires 750 b/s from the total 16 kbs coding rate.

* See Eqs. (2.6) through (2.8).

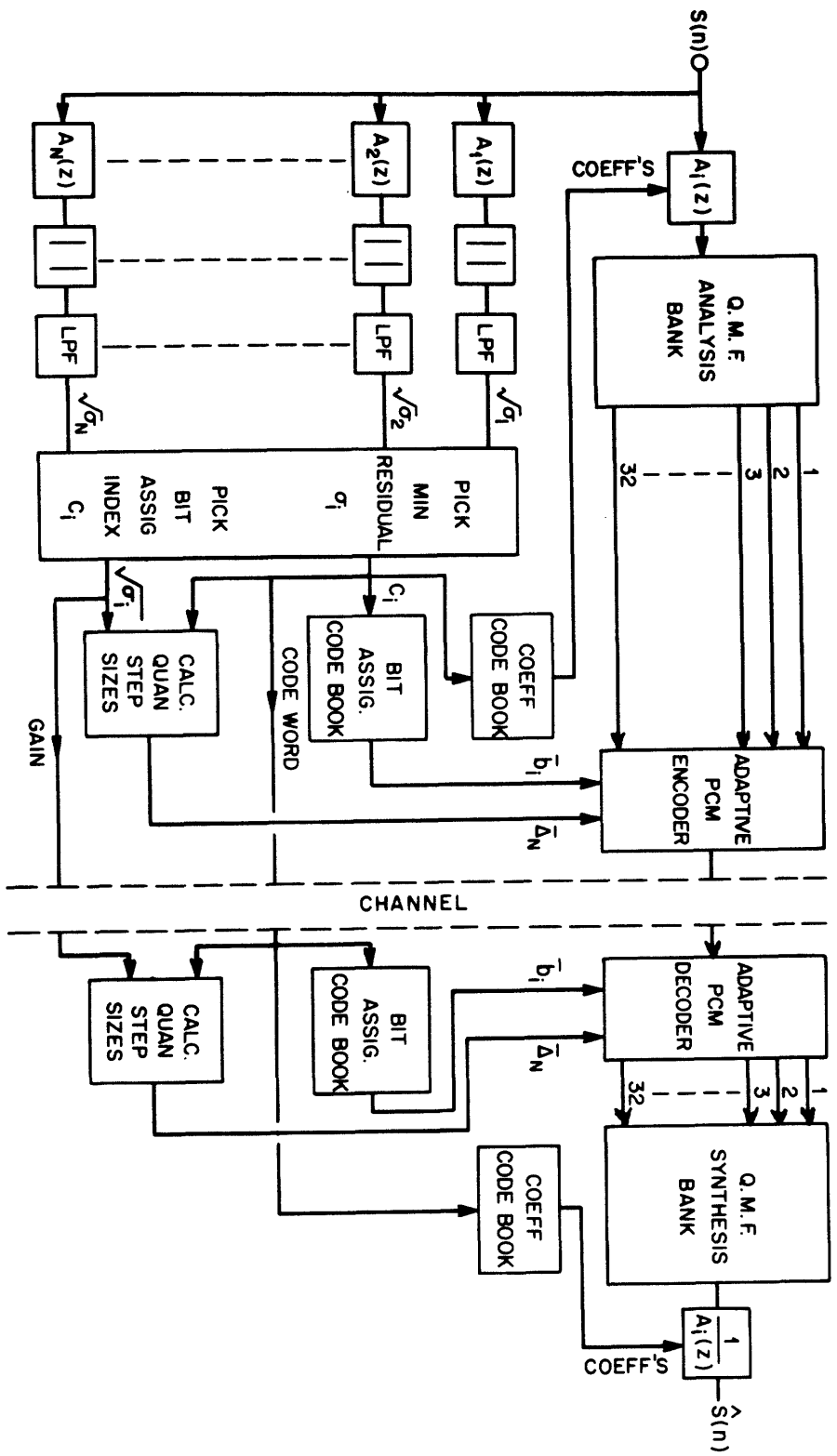


Fig. 5.9 32 band sub-band/transform algorithm with dynamic preemphasis.

The bit assignments are calculated without noise shaping as in the previous technique. Although the speech spectra was "flattened" before analysis, the number of bits assigned to a band is proportional to the logarithm of the template estimate of the spectral amplitude in that band. As before, the noise shaping parameter γ can be varied to tradeoff quantizing accuracy in the formant regions for the low amplitude regions of the speech spectrum.

For this residual coding scheme, the estimate of the pre-emphasized signal amplitude in each channel is the gain estimate $\sqrt{\sigma_i}$ developed in Section 3.3. This gain term is selected so that the normalized channel outputs*

$$\frac{y(k)}{\sqrt{\sigma_i}} \quad k = 1, 2, \dots, 31, 32 \quad (5.8)$$

exhibit approximately unit variance. The quantity $\sqrt{\sigma_i}$ is the local estimate of the standard deviation (RMS level) of the pre-emphasized input in each channel.

The quantizer step size adaptation scheme employed for residual coding is identical to the scheme developed in the last section. Specifically speaking, the forward adaptive gain term was computed as in Eq. (5.6) with $\sqrt{\sigma_i}$ substituted for the standard deviation of the quantizer inputs.

$$G_n(k) = \frac{2^{\lfloor b_{k,n} - 1 \rfloor}}{C \cdot \sqrt{\sigma_i}} \quad k = 1, 2, \dots, 32 \quad (5.9)$$

For 3, 4, and 5 bit quantization C was set according to Max [31] as 2.344, 2.682, and 3.009. One and two bit quantization was subjectively optimized with C values of .7096 and 1.4159 respectively. This corresponds to decreasing the quantizer step sizes by 9 and 3 dB respectively from the case of two sigma loading. Figure 5.10 shows a magnitude plot of the quantizer output range (the dotted lines) superimposed over the signal level (the solid line) in each band for this step size adaptation scheme.

* The gain estimate $\sqrt{\sigma_i}$ was optimized by adjusting G of Eq. (3.5).

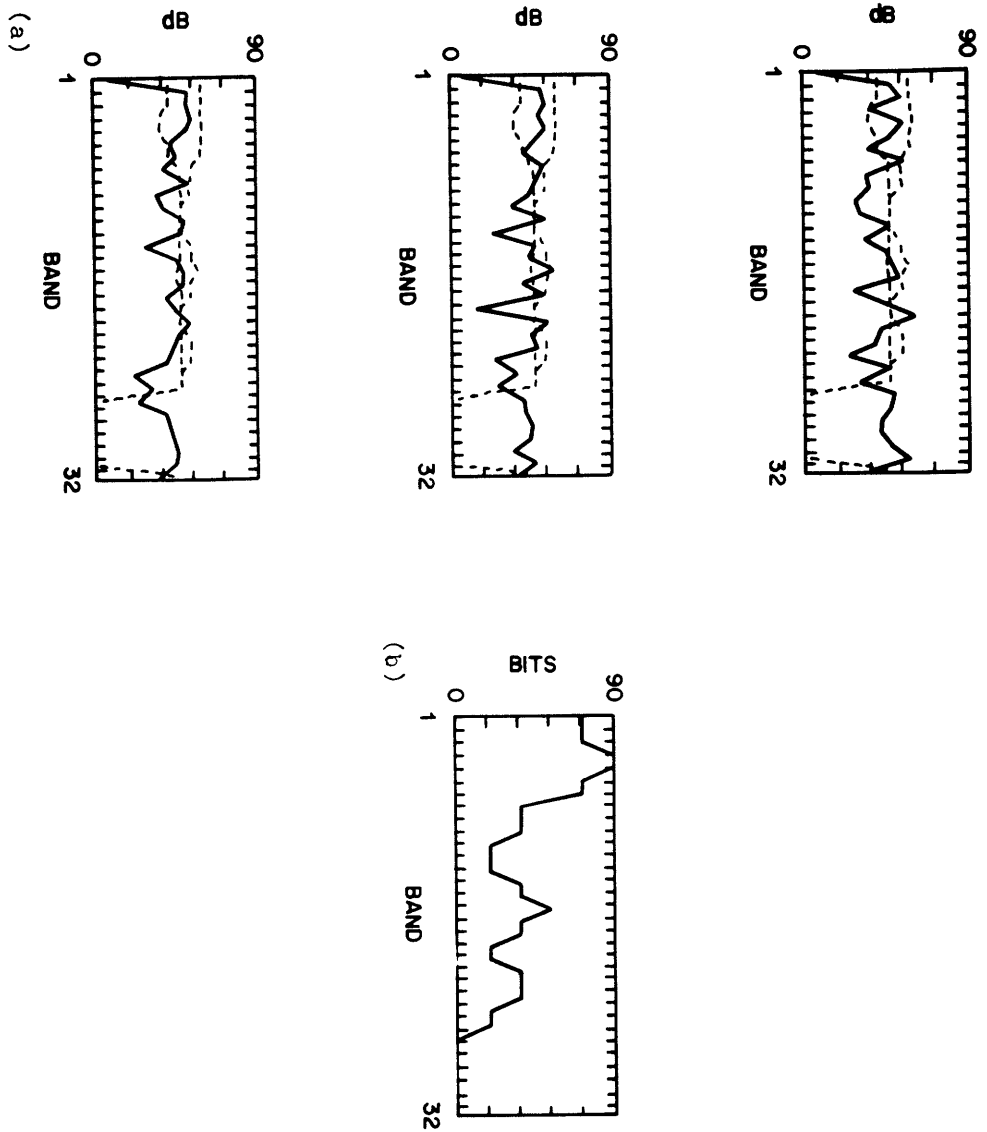


Fig. 5.10 (a) Successive 4ms frames of pre-emphasized QMF analysis filter bank output (solid line), superimposed over the minimum and maximum quantizer output levels (dotted line). (b) The corresponding bit assignment.

Experiments with dynamic pre-emphasis have shown that the perceptual effects of quantizer overloading (when the input level exceeds the maximum quantizer output level) are considerably worse than the perceptual effects of quantizer "underloading" (when the minimum quantizer output exceeds the input level). It is better to set the quantizer step sizes large enough to avoid overload at the cost of some "underloading" than to set the step sizes so that the amounts of underloading and overloading are about equal. This is suggested by the range of quantizer output levels shown in figure 5.10 for 16 kbs coding. The argument is better illustrated by using a flat bit assignment of 5 bits for each channel corresponding to a 40 kbs coder (neglecting side information). Figure 5.11 shows a magnitude plot of the quantizer output range (the dotted lines) superimposed over the pre-emphasized signal levels (the solid lines) in each band for the two output step size ranges described. In figure 5.11a the quantizer step sizes were set large enough to avoid overloading, while in figure 5.11b the step sizes were adjusted for roughly equal amounts of overloading and "underloading". The coded speech corresponding to figure 5.11a was "transparent" with the original while the coded output corresponding to figure 5.11b was considerably degraded.

5.4.1 Observations

In principle, incorporating dynamic pre-emphasis prior to the analysis/synthesis framework (such as in figure 5.9) is the time domain equivalent to a division of the un-emphasized outputs of the QMF analysis filter bank (see figure 1.2) by the estimated speech spectrum, then quantizing the result using uniform, unit variance quantizers [35].

For this reason the perceptual qualities of the speech coded with the dynamic pre-emphasis and de-emphasis technique are similar to those coded with the scheme of section 5.3. The quality of the two coding schemes remains similar across a wide range of complexities of the spectral side information model. In addition, experimentation with quantizer bit assignments incorporating various degrees of spectral noise shaping has yielded qualities similar to those obtained without dynamic pre-emphasis.

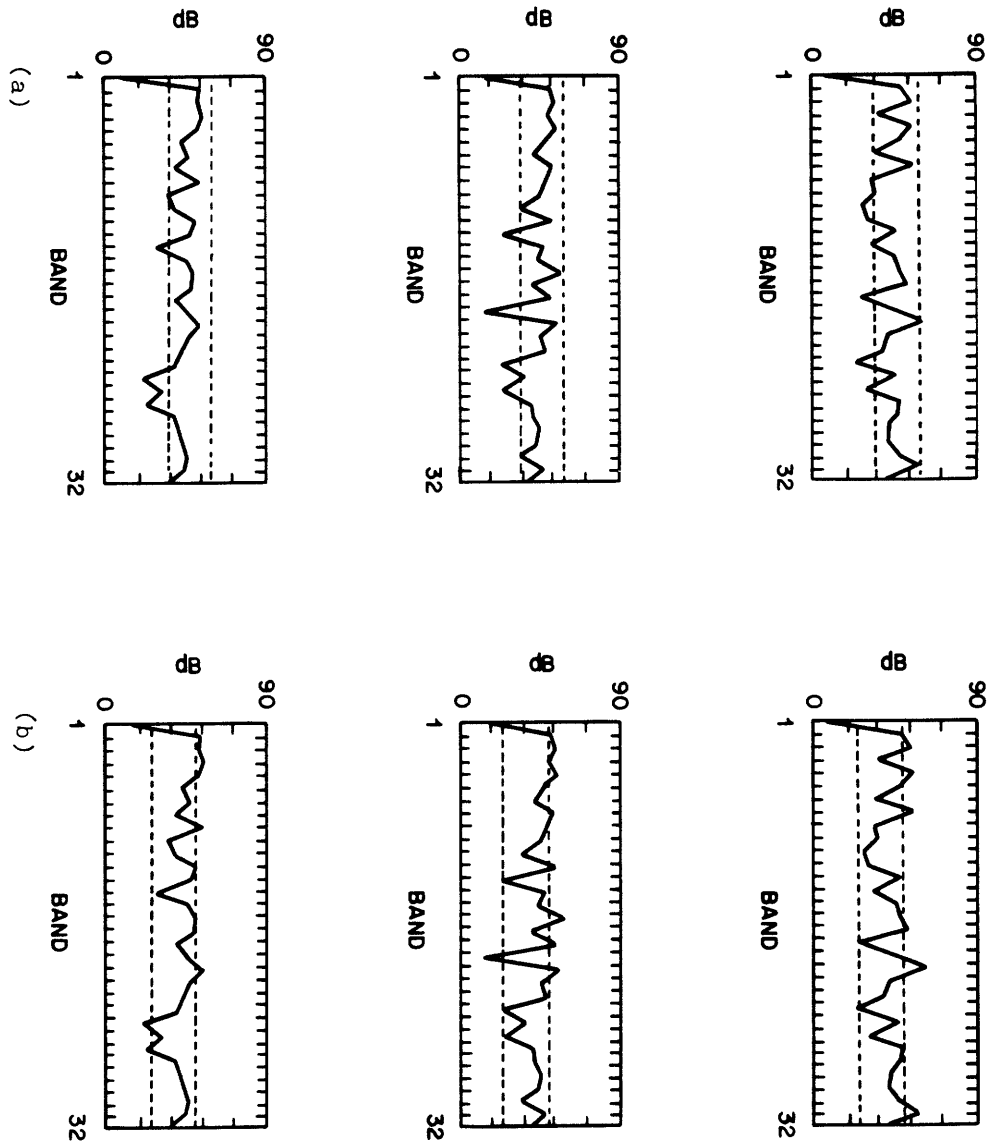


Fig. 5.11 Two cases of successive 4ms frames of preemphasized QMF analysis filter bank output (solid line), superimposed with minimum and maximum quantizer output levels (dotted line).

CHAPTER VI

6. AN ANALYSIS OF THE PERFORMANCE AND COMPLEXITIES OF BOTH 32 SUB-BAND/TRANSFORM CODERS

6.1 Introduction

In this chapter we investigate the performances and complexities of the 32 sub-band/transform coder designs relative to those of existing sub-band coding and adaptive transform coding techniques. The measure of performance is based on the results of an informal comparison test for quality whereas the measure of complexity is based on an estimate of the hardware requirements for real time implementation of the coders. The chapter concludes with an assessment of the performance versus complexity tradeoffs of the 32 sub-band/transform coders.

6.2 Results of an Informal A versus B Comparison Test

An informal comparison test for quality was performed to compare the effectiveness of both 32 sub-band coder designs presented in this thesis with sub-band and adaptive transform coding techniques. Four different frequency domain coding techniques were included: 1) the 32 sub-band algorithm of Section 5.3 without dynamic pre-emphasis at 16 kb/s, 2) the 32 sub-band algorithm of Section 5.4 with dynamic pre-emphasis at 16 kb/s, 3) a non-uniform four band sub-band coder algorithm [36] at 16 kb/s, 4) an adaptive transform coding algorithm using the homomorphic side information model of fig. 5.4 [3] at 16 kb/s. The numbers used to denote the various methods are listed at the bottom of Table 6.1.

Each coder was compared against all other coders and the source material in a forced *A* vs *B* decision for quality. The source material consisted of eight different phonetically balanced sentences. Two male and two female speakers were used in the test. A randomized mix of sentence material was used and not all of the sentences or speakers, were used to compare each coder to every other coder. However, each coder was compared against every other coder for at

least two different sentences. In addition, each *A* vs *B* comparison was accompanied by a corresponding *B* vs *A* comparison (in randomized order) to reduce any listener bias towards the first or second sentence of an *A-B* pair. A total of 24 listeners were used in the experiment. Two different randomized orders were used with 12 listeners each. Each listener made a total of 40 comparisons and each coder was compared against every other coder 4 times for each listener (yielding a total of 96 comparisons with every other coder).

Table 6.1 shows percentage listener preferences for the different *A* vs *B* comparisons. For example the lower right entry indicates that in comparing coder #4 to coder #3, 78 percent of the listeners chose coder #4 and 22 percent chose coder #3.

Table 6.2 shows a ranking of the coding algorithms according to the percentage of total possible votes that they could receive in the experiment (the total number of comparisons made in the experiment for each coder against all other coders or originals was 384).

TABLE 6.1

Percent Preference of Coders
in an *A* vs *B* Comparison

		<i>B</i>			
<i>A</i>		# 0	# 1	# 2	# 3
<i>A</i> vs <i>B</i>	# 0				
	# 1	1:99			
	# 2	5:95	36:64		
	# 3	3:97	19:81	38:62	
	# 4	6:94	52:48	70:30	78:22

CODER NUMBERS

- #0 — Original (uncoded)
- #1 — 32 Sub-band algorithm without dynamic pre-emphasis at 16 kb/s
- #2 — 32 Sub-band algorithm with dynamic pre-emphasis at 16 kb/s
- #3 — Non-uniform 4 band SBC [36] at 16 kb/s
- #4 — ATC algorithm using the homomorphic side information model of fig. 5.4 [3] at 16 kb/s.

TABLE 6.2

**Ranking of Coders According to
Percent of *A* vs *B* Votes Received**

Coder	Percent of Total Possible Votes Received
0	96
4	52
1	48
2	35
3	20

CODER NUMBERS

- #0 — Original (uncoded)
- #1 — 32 Sub-band algorithm without dynamic pre-emphasis at 16 kb/s
- #2 — 32 Sub-band algorithm with dynamic pre-emphasis at 16 kb/s
- #3 — Non-uniform 4 band SBC [36] at 16 kb/s
- #4 — ATC algorithm using the homomorphic side information model of fig. 5.4 [3] at 16 kb/s.

As seen in the table the original was distinctly preferred in terms of quality in 96 percent of its comparisons. This was followed by the ATC algorithm of [3] and the 32 sub-band algorithm without dynamic pre-emphasis. These two algorithms received 52 percent and 48 percent, respectively, of the total possible votes in their comparisons.

As shown by the overall preference ratings of table 6.2, the 32 sub-band scheme without dynamic pre-emphasis at 16 kbs is comparable in quality to the ATC algorithm of [3] at 16 kbs. In addition both 32 sub-band coders (with and without dynamic pre-emphasis) designed as part of this thesis were judged as having better quality than the four band SBC of [36].

Although the 32 sub-band coder without dynamic pre-emphasis scored 13 percent better in overall preference ratings than the 32 sub-band coder with dynamic pre-emphasis, both schemes sounded similar. Due to subtle differences in the distortion characteristics of the two coders people generally preferred the scheme without dynamic pre-emphasis.

Nevertheless, the fact that dynamic pre-emphasis did not improve the subjective performance of the 32 sub-band design indicates that this scheme is not worth the additional processing required. This would strongly suggest that the amount of internal frequency domain aliasing of the filter bank does not have a significant effect for the filter bank design of chapter two.

6.3 The complexity performance trade-offs

Now that we have addressed the performance of the 32 sub-band coders, something needs to be said about the complexities of these schemes relative to traditional sub-band and transform coding techniques. We can attempt to evaluate the relative complexity/performance trade-offs of the 32 sub-band algorithms by using results from current studies of coder quality by Daumer [37]; and real time speech coding hardware by Crochiere, Cox, and Johnston [7]. These studies include the 4 band SBC algorithm of [36] as well as the ATC algorithm using the homomorphic side information model of fig. 5.4 [3].

The measure of coder performance is based on the mean opinion score for listener ratings on a 1 to 5 scale (1= unsatisfactory, 5= excellent). The measure of coder complexity is based on a total count of required Bell Laboratories VLSI digital signal processing (DSP) chips [38]. A brief description of the DSP is given in Appendix IV.

If the QMF analysis and synthesis filter banks are implemented using the tree structure of figure 2.2 — for reduced coefficient storage — they could each be done in about 2 DSPs. The adaptive quantization scheme for the transmitter section of figure 1.2 including: a) the 32, 10th order LPC template side information model, b) the bit assignment codebook, c) the quantizer step size calculations, and d) the PCM encoding — could be done in about 2 DSPs. The quantizer step size calculations, the bit assignment codebook, and signal scaling operations — for the APCM decoder of the receiver — could be implemented in about 1 DSP. This means that about 4 DSPs are needed for the transmitter, about 3 for the receiver, plus a codec chip (see Appendix IV) for A/D and D/A conversion. This corresponds to a complexity factor of 8 (7 DSPs plus a codec) for the implementation of coder #1. Since the pre-emphasis and de-emphasis filtering operations of coder #2 (figure 5.9) correspond to an extra 10 tap IIR filtering operation for the receiver section (the FIR filtering can be shared with the template picking scheme since the required filtering of the input is performed there), coder #2 requires an additional fraction of 1 DSP of complexity.

Figure 6.1 [7] summarizes the assessment of coder performance versus complexity for the four algorithms included in the *A* vs *B* comparison test of the previous section. The vertical axis reflects the measure of coder performance. The horizontal axis reflects the measure of coder complexity based on the number of required DSPs plus the μ -law codec. This can be applied to all of the designs except ATC which requires an array processor. Each data point in the figure applies to the performance and complexity of one coder technique at a prescribed bit rate. The coder technique for each point is specified above the graph, e.g. the non-uniform 4 band SBC of [36] at 16 kb/s has a complexity factor of 3 (2 DSPs and 1 μ -law codec). The current speculation of coder performance versus complexity — from the study of [7] — is

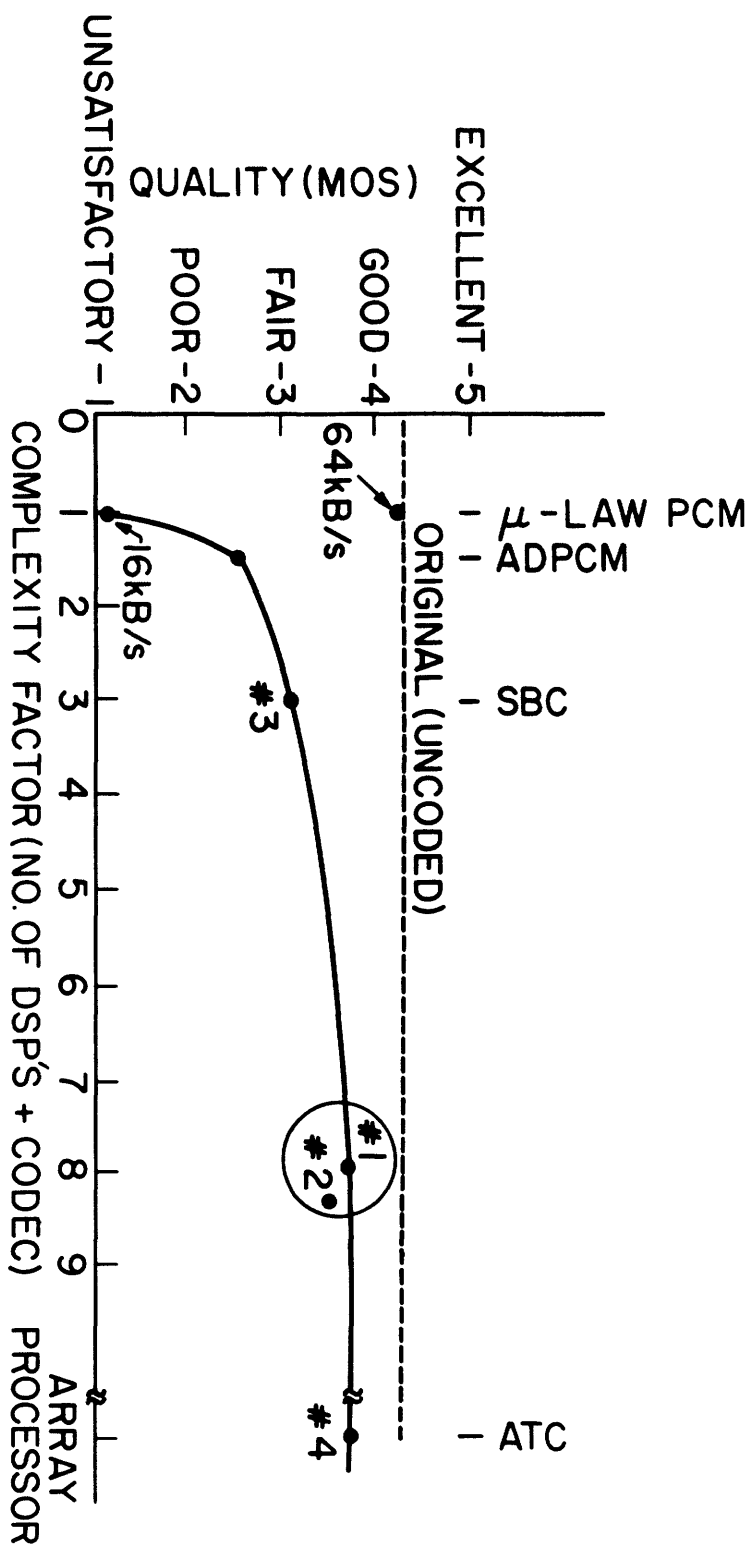


Fig. 6.1 Assessment of coder performance versus complexity.

indicated by the solid line. The upper dashed line corresponds to the mean opinion score of the original (uncoded) sentences of Daumer's study [37].

As seen from the results of this chapter, the 32 sub-band algorithm without dynamic pre-emphasis at 16 kb/s offers comparable performance to the ATC algorithm of [3] at 16 kb/s for about three times the complexity of the 4 band sub-band coding algorithm of [36]. This result is roughly in agreement with the current speculation of coder performance versus complexity [7].

CHAPTER VII

7. SUMMARY AND RECOMMENDATIONS FOR FURTHER RESEARCH

7.1 Summary

This thesis has attempted to explore techniques of frequency domain coding of digital voice at complexities and frequency resolutions which occupy the middle range between traditional sub-band and transform coding methods. Attention has focused on studying the performance of such systems operating at bit rates of 16 kb/s. Two new techniques for 32 sub-band/transform coding at 16 kb/s have been introduced. Dynamic bit assignment and quantizer step size adaptation has been accomplished with a spectral side information model consisting of a switched source of all-pole spectral templates in accordance with recent concepts of vector quantizing [17-19] and clustering methods [19,20,24,25]. Both coders have experimented with bit assignments for spectral shaping of the quantization noise in accordance with perceptual criteria [2].

The basic performance limitation of the 32 sub-band/transform coders has resulted, firstly, from the limited accuracy of the spectral side information model and, secondly, from the poor time resolution of the quadrature mirror filter (QMF) synthesis structure used for reconstructing the sub-band signals. The implications of these results regarding the performance of the basic algorithm for various complexities of the spectral side information model have been discussed in detail.

Preliminary results of simulations and informal subjective testing indicate that one of the new 32 sub-band/transform coder designs at 16 kb/s offers comparable performance with the 16 kb/s adaptive transform coder of [3]. This was achieved at roughly three times the algorithm complexity of the traditional sub-band coder of [36].

7.2 Suggestions for Further Research

In the discussion on performance of the new coders, we saw that the amount of internal

frequency domain aliasing of the QMF filter bank design of Chapter II was not perceptually significant. We also noted in Chapter V that the poor time resolution of the synthesis filter bank exacerbated the perceptual effects of quantizing errors resulting from sub-band signals which occasionally fall outside the range of the quantizer output levels. This would suggest that future filter bank designs should incorporate filters with shorter impulse responses. This would improve the time resolution of the filter bank at the cost of additional internal aliasing effects. In addition this would reduce the amount of computation required for implementing the analysis and synthesis filter banks. Incorporation of dynamic pre-emphasis filtering prior to analysis/synthesis [2,36] (discussed in Section 5.4) should reduce the perceptual effects of frequency domain aliasing for such a design.

Due to the difficulties cited in Chapter V of computing accurate local estimates of the variances of the sub-band signals necessary for quantizer step size adaptation, a 16 sub-band design might be considered. A 16 band design would offer wider sub-bands, additional sample-to-sample amplitude correlation in the sub-bands, and a smaller spectral dynamic range among the sub-bands. This would suggest that a coarser spectral side information model, with the advantage of fewer spectral templates of lower LPC order, could be used to obtain performances similar to the reported results of Section 5.5. In addition a 16 band design would offer better time resolution of the synthesis filter bank at a significant reduction in the overall complexity of the coder.

References

- [1] J. L. Flanagan, M. R. Schroeder, B. S. Atal, R. E. Crochiere, N. S. Jayant, J. M. Tribolet, "Speech Coding," IEEE Trans. Commun., Vol. COM-27, No. 4, pp. 710-737, April 1979.
- [2] J. M. Tribolet, R. E. Crochiere, "Frequency Domain Coding of Speech," IEEE Trans. Acoustics, Speech, and Signal Processing, Vol. ASSP-27, No. 5, pp. 512-530, October 1979.
- [3] R. V. Cox, R. E. Crochiere, "Real-time Simulation Of Adaptive Transform Coding," IEEE Trans. Acoustics, Speech, and Signal Processing, Vol. ASSP-29, No. 2, pp. 147-154, April 1981.
- [4] R. E. Crochiere, S. A. Webber, J. L. Flanagan, "Digital Coding of Speech in Sub-Bands," 1976 ICASSP, Philadelphia.
- [5] R. E. Crochiere, "An Analysis of 16 Kb/s Sub-Band Coder Performance: Dynamic Range, Tandem Connections, and Channel Errors," Bell Syst. Tech. J., Vol. 57, No. 8, pp. 2927-2952, October 1978.
- [6] R. E. Crochiere, "Digital Signal Processor Sub-Band Coding," Bell Syst. Tech. J., Vol. 60, No. 7, pp. 1633-1653, September 1981.
- [7] R. E. Crochiere, R. V. Cox, J. D. Johnston, "Real Time Speech Coding," IEEE Trans. Commun., Vol. COM-30, No. 4, April 1982.
- [8] A. J. Barabell, *An Analysis of Sub-Band Coding Techniques For Speech Communication*, MSEE Thesis, M.I.T., Cambridge, MA, October 1981.
- [9] J. D. Johnston and R. E. Crochiere, "An All-Digital 'Commentary Grade' Sub-Band Coder," Journal of the Audio Engineering Society, Vol. 27, No. 11, pp. 855-865, November 1979.
- [10] M. A. Krasner, *Encoding of Speech and Audio Signals Based on the Perceptual Requirements of the Auditory System*, PhD EE Thesis, M.I.T., Cambridge, MA, May 1979.
- [11] R. W. Schafer and L. R. Rabiner, "A Digital Signal Processing Approach to Interpolation," Proc. IEEE, Vol. 61, No. 6, June 1973.
- [12] R. E. Crochiere and L. R. Rabiner, "Interpolation and Decimation of Digital Signals — A Tutorial Review," Proc. IEEE, Vol. 69, No. 3, March 1981.
- [13] D. Esteban and C. Galand, "Application of Quadrature Mirror Filter to Split Band Voice Coding Schemes," ICASSP, Hartford, CT, pp. 191-195, May 1977.
- [14] D. Esteban and C. Galand, "Parallel Approach to Quasi Perfect Decomposition of Speech in Sub-Bands," Ninth International Congress on Acoustics, Madrid, April 1977.
- [15] D. Esteban and C. Galand, "Direct approach to quasi perfect decomposition of speech in sub-bands," Ninth International Congress on Acoustics, Madrid, April 1977.
- [16] J. D. Johnston, "A Filter Family Designed for Use in Quadrature Mirror Filter Banks," Proc. IEEE Int. Conf. ASSP (April 1980), pp. 291-4.
- [17] A. Buzo, A. H. Gray, Jr., R. M. Gray, and J. D. Markel, "Speech Coding Based Upon Vector Quantization," IEEE Trans. Acoustics, Speech, and Signal Processing, Vol. ASSP-28, No. 5, October 1980.
- [18] D. Y. Wong, B. H. Juang and A. H. Gray, Jr., "Recent Developments in Vector Quantization for Speech Processing," Proc. IEEE Int. Conf. ASSP (March 1981), pp. 1-4.

- [19] B. H. Juang, D. Y. Wong, A. H. Gray Jr., "Distortion Performance of Vector Quantization for LPC Voice Coding," *IEEE Trans. Acoustics, Speech, and Signal Processing*, Vol. ASSP-30, No. 2, pp. 294-304, April 1982.
- [20] L. R. Rabiner, Personal Communication.
- [21] A. H. Gray, Jr., and J. D. Markel, "Distance Measures for Speech Processing," *IEEE Trans. Acoustics, Speech, and Signal Processing*, Vol. ASSP-24, No. 5, pp. 380-391, October 1976.
- [22] R. E. Crochiere, J. M. Tribolet, and L. R. Rabiner, "An interpretation of the Log Likelihood Ratio As A Measure of Waveform Coder Performance," *IEEE Trans., Acoustics, Speech, and Signal Processing*, Vol. ASSP-28, No. 3, pp. 318-323, June 1980.
- [23] R. M. Gray, A. buzo, A. H. Gray, Jr., and Y. Matsuyama, "Distortion Measures for Speech Processing," *IEEE Trans., Acoustics, Speech, and Signal Processing*, Vol. ASSP-28, No. 4, pp. 367-376, August 1980.
- [24] L. R. Rabiner, and J. G. Wilpon, "Considerations in Applying Clustering Techniques to Speaker-Independent Word Recognition," *J. Acoust., Soc. Am.*, Vol. 66, No. 3, pp. 663-673, September 1979.
- [25] S. E. Levinson, L. R. Rabiner, A. E. Rosenberg, J. G. Wilpon, "Interactive Clustering Techniques for Selecting Speaker-Independent Reference Templates for Isolated Word Recognition," *IEEE Trans. Acoustics, Speech, and Signal Processing*, Vol. ASSP-27, No. 2, April 1979.
- [26] B. R. Boddie, J. D. Johnston, C. A. McGonegal, J. W. Upton, D. A. Berkley, R. E. Crochiere, and J. L. Flanagan, "Digital Signal Processor; Adaptive Differential Pulse-Code-Modulation Coding," *Bell Syst. Tech. J.*, Vol. 60, No. 7, pp. 1547-1561, September 1981.
- [27] J. L. Flanagan, J. D. Johnston, J. W. Upton, "Digital Voice Storage in a Microprocessor," *IEEE Trans. Commun.*, Vol. COM-30, No. 2, pp. 339-342, February 1982.
- [28] L. R. Rabiner, R. W. Schafer, "Digital Processing of Speech Signals," Prentice-Hall, Signal Processing Series, New Jersey 1978.
- [29] J. Huang and P. Schulthesis, "Block Quantization of Correlated Gaussian Random Variables," *IEEE Trans. Commun. Syst.*, Vol. CS-11, pp. 289-296, 1963.
- [30] R. E. Crochiere, L. R. Rabiner, N. S. Jayant, and J. M. Tribolet, "A Study of Objective Measures for Speech Waveform Coders," in 1978 Proc. Zurich, Switzerland, March 1978, pp. H1-H1.7.
- [31] J. Max, "Quantizing for Minimum Distortion," *IRE Trans. Inform. Theory*, Vol. IT-6, pp. 7-12, March 1960.
- [32] N. S. Jayant, "Adaptive Quantization With a One Word Memory," *Bell System Tech. J.*, pp. 1119-1144, September 1973.
- [33] A. Croisier, "Progress in PCM and Delta Modulation: Block-Companded Coding of Speech Signals," Proc. 1974, *Zurich Seminar on Digital Communications*, March 1974.
- [34] J. M. Tribolet and R. E. Crochiere, "A Modified Adaptive Transform Coding Scheme with Post-Processing-Enhancement," ICASSP, Denver, Colorado, pp. 336-339, April 1980.
- [35] M. Berouti and J. Makhoul, "An Adaptive-Transform Baseband Coder," Speech Communication Papers presented at the 97th Meeting of the Acoustical Society of America, MIT, Cambridge, MA, 12-16, June 1979.

- [36] R. E. Crochiere, "A DSP Implementation of Sub-band Coding for Low Bit Rate Digital Speech," *Submitted to B.S.T.J.*
- [37] W. R. Daumer, "Subjective Evaluation of Several 9.6-32 kb/s Coders in a Telephone Network Environment. IEEE Trans. Commun., Vol. COM-30, No. 4, pp. 655-662, April 1982.
- [38] J. R. Boddie, et. al., "Digital Signal Processor: Architecture and Performance," *B.S.T.J.*, 60, No. 7, Part 2, September 1981, pp. 1449-1462.
- [39] D. G. Marsh, B. K. Ahuja, T. Misawa, M. R. Dwarakanath, P. E. Fleischer, and V. R. Saari, "A Single Chip CMOS PCM Coder with Filters," *IEEE J. of Solid State Circuits*, Vol. SC-16, No. 4, August 1981, pp. 308-315.

APPENDIX I: QUADRATURE MIRROR FILTERING

The z -transform of the decimated sub-band signal $y_1(n)$ in figure 2.1 is given by

$$Y_1(z) = \frac{1}{2} [X(z^{\frac{1}{2}})H_1(z^{\frac{1}{2}}) + X(-z^{\frac{1}{2}})H_1(-z^{\frac{1}{2}})] . \quad (I.1)$$

The z -transform of $t_1(n)$ is found by interpolating $y_1(n)$ and filtering by $K_1(n)$

$$\begin{aligned} T_1(z) &= Y_1(z^2)K_1(z) \\ &= \frac{1}{2} [X(z)H_1(z) + X(-z)H_1(-z)]K_1(z) \end{aligned} \quad (I.2)$$

Similarly we obtain

$$T_2(z) = \frac{1}{2} [X(z)H_2(z) + X(-z)H_2(-z)]K_2(z) . \quad (I.3)$$

The z -transform of $s(n)$ is the sum of equations (I.2) and (I.3)

$$\begin{aligned} S(z) &= \frac{1}{2} [H_1(z)K_1(z) + H_2(z)K_2(z)]X(z) \\ &\quad + \frac{1}{2} [H_1(-z)K_1(z) + H_2(-z)K_2(z)]X(-z) . \end{aligned} \quad (I.4)$$

The second term of (I.4) represents aliasing effects due to decimation. If H_1 is a LPF and H_2 is the corresponding mirror image HPF then the following magnitude relation holds on the unit circle

$$|H_1(\omega)| = |H_2(\omega + \pi)| . \quad (I.5)$$

This can be accomplished by

$$H_2(\omega) = H_1(\omega + \pi) . \quad (I.6)$$

In which case

$$H_2(z) = H_1(-z) . \quad (I.7)$$

This gives the impulse response

$$h_2(n) = h_1(n)(-1)^n . \quad (I.8)$$

The second term of (I.4) can be cancelled by choosing

$$K_1(z) = H_1(z) \quad (\text{I.9})$$

$$K_2(z) = -H_2(z) = -H_1(-z) . \quad (\text{I.10})$$

Equation (I.4) now becomes

$$S(z) = \frac{1}{2} [H_1^2(z) - H_1^2(-z)]X(z) . \quad (\text{I.11})$$

If H_1 is chosen to be a symmetrical FIR filter, its Fourier transform can be expressed as

$$H_1(\omega) = H_{1M}(\omega) e^{-j \frac{(N-1)}{2} \omega} , \quad (\text{I.12})$$

where $(H_{1M}(\omega))^2 = |H_1(\omega)|^2$. Evaluating (I.11) on the unit circle and substituting in (I.12) yields

$$S(\omega) = \frac{1}{2} [|H_1(\omega)|^2 - |H_1(\omega+\pi)|^2 e^{-j(N-1)\pi}] \times e^{-j(N-1)\omega} X(\omega) \quad (\text{I.13})$$

Consider the case for N even, then

$$S(\omega) = \frac{1}{2} [|H_1(\omega)|^2 + |H_1(\omega+\pi)|^2] e^{-j(N-1)\omega} X(\omega) . \quad (\text{I.13b})$$

Perfect reconstruction of the signal is accomplished if

$$|H_1(\omega)|^2 + |H_1(\omega+\pi)|^2 = 1 , \quad (\text{I.14})$$

giving

$$S(\omega) = \frac{1}{2} e^{-j(N-1)\omega} X(\omega) . \quad (\text{I.15})$$

The signal is perfectly reconstructed (neglecting the factor of 1/2) with a delay of $N-1$ samples. Considering (I.13) for N odd, $S(\frac{\pi}{2}) = 0$, hence N must be even. To summarize, sufficient conditions for perfect reconstruction are:

1. H_1 is a symmetrical FIR filter of even order.
2. $H_2(z) = H_1(-z)$.
3. $K_1(z) = H_1(z)$.
4. $|H_1(\omega)|^2 + |H_1(\omega+\pi)|^2 = 1$

5. $K_2(z) = -H_2(z)$.

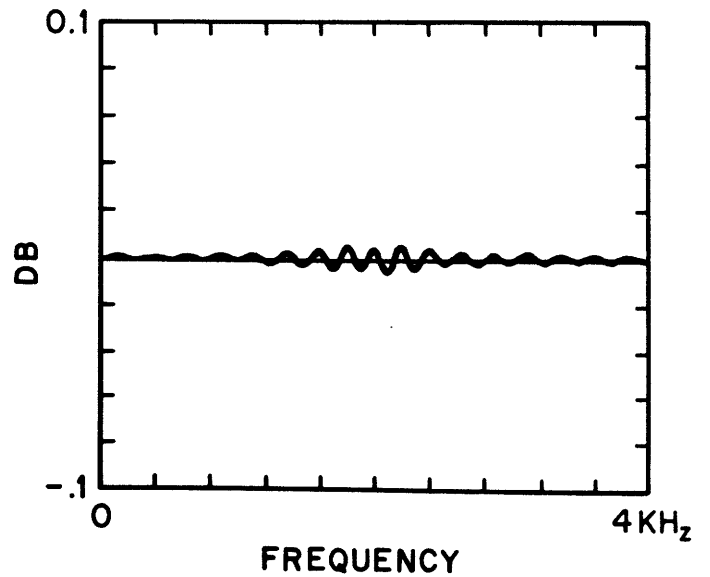
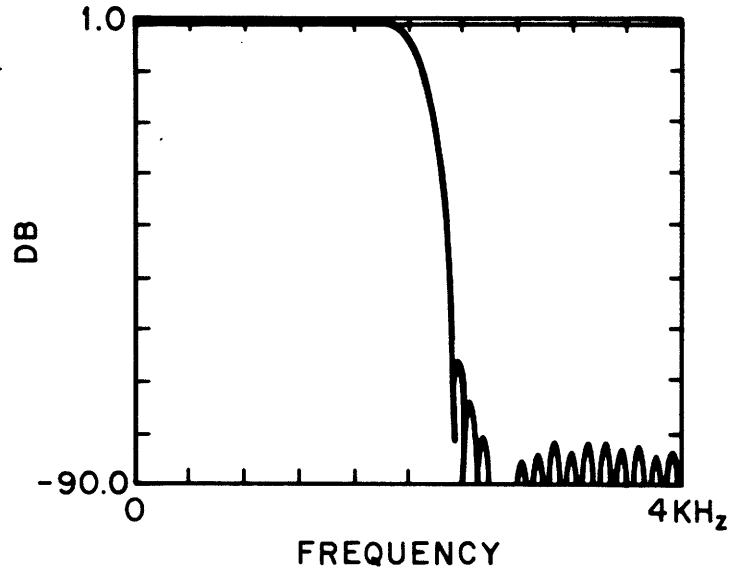
TABLE I.1: Z-Transforms of Analysis Filters

$$\begin{aligned}
F_1(z) &= F_{32}(-z) = H_1(z)H_2(z^2)H_3(z^4)H_4(z^8)H_5(z^{16}) \\
F_2(z) &= F_{31}(-z) = H_1(z)H_2(z^2)H_3(z^4)H_4(z^8)H_5(-z^{16}) \\
F_3(z) &= F_{30}(-z) = H_1(z)H_2(z^2)H_3(z^4)H_4(-z^8)H_5(-z^{16}) \\
F_4(z) &= F_{29}(-z) = H_1(z)H_2(z^2)H_3(z^4)H_4(-z^8)H_5(z^{16}) \\
F_5(z) &= F_{28}(-z) = H_1(z)H_2(z^2)H_3(-z^4)H_4(-z^8)H_5(z^{16}) \\
F_6(z) &= F_{27}(-z) = H_1(z)H_2(z^2)H_3(-z^4)H_4(-z^8)H_5(-z^{16}) \\
F_7(z) &= F_{26}(-z) = H_1(z)H_2(z^2)H_3(-z^4)H_4(z^8)H_5(-z^{16}) \\
F_8(z) &= F_{25}(-z) = H_1(z)H_2(z^2)H_3(-z^4)H_4(z^8)H_5(z^{16}) \\
F_9(z) &= F_{24}(-z) = H_1(z)H_2(-z^2)H_3(-z^4)H_4(z^8)H_5(z^{16}) \\
F_{10}(z) &= F_{23}(-z) = H_1(z)H_2(-z^2)H_3(-z^4)H_4(z^8)H_5(-z^{16}) \\
F_{11}(z) &= F_{22}(-z) = H_1(z)H_2(-z^2)H_3(-z^4)H_4(-z^8)H_5(-z^{16}) \\
F_{12}(z) &= F_{21}(-z) = H_1(z)H_2(-z^2)H_3(-z^4)H_4(-z^8)H_5(z^{16}) \\
F_{13}(z) &= F_{20}(-z) = H_1(z)H_2(-z^2)H_3(z^4)H_4(-z^8)H_5(z^{16}) \\
F_{14}(z) &= F_{19}(-z) = H_1(z)H_2(-z^2)H_3(z^4)H_4(-z^8)H_5(-z^{16}) \\
F_{15}(z) &= F_{18}(-z) = H_1(z)H_2(-z^2)H_3(z^4)H_4(z^8)H_5(-z^{16}) \\
F_{16}(z) &= F_{17}(-z) = H_1(z)H_2(-z^2)H_3(z^4)H_4(z^8)H_5(z^{16})
\end{aligned}$$

TABLE I.2: Filter coefficients, Frequency Responses, and QMF Ripple for the filters $H_1(z)$, $H_2(z)$, $H_3(z)$, $H_4(z)$, and $H_5(z)$.

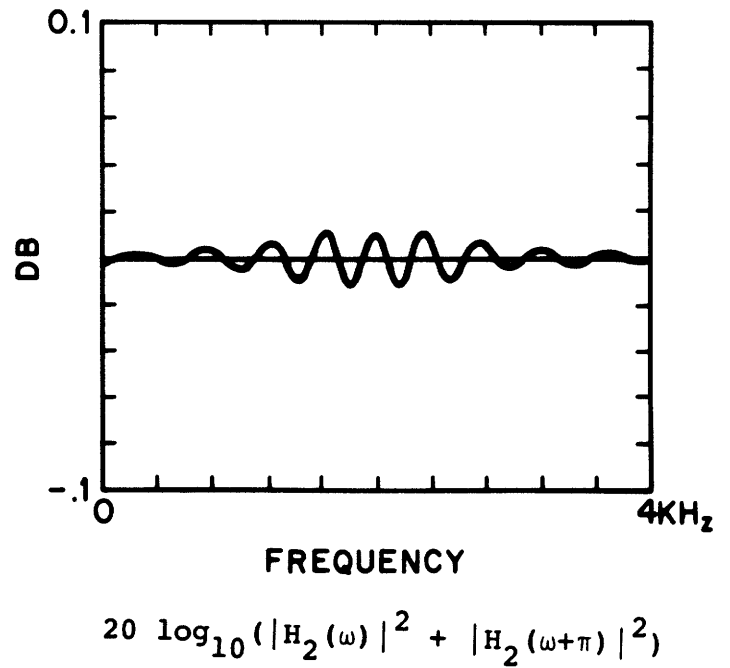
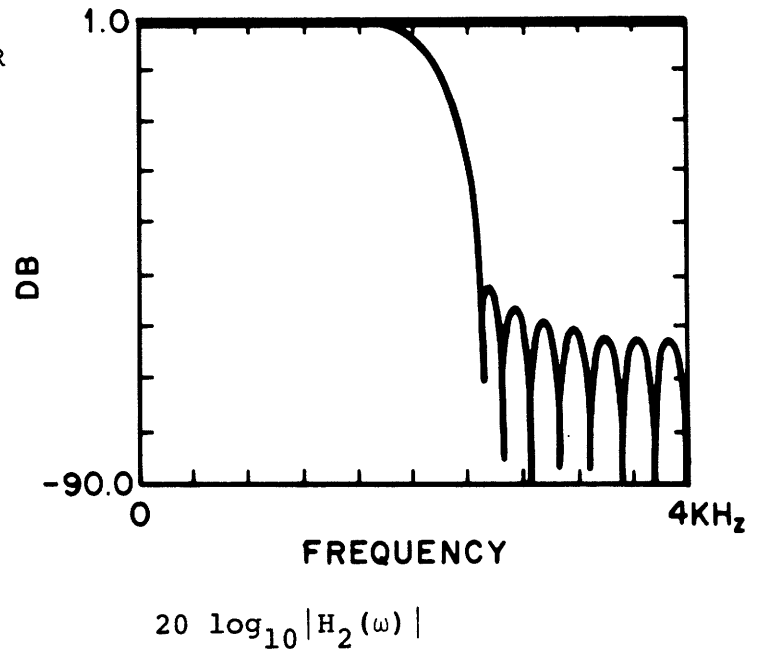
64 TAP DESIGN OF QM FILTER

$h_1(31)=h_1(32)=$.46009810E 00
 .13823630E 00
 -.97790960E-01
 -.50954870E-01
 .55432450E-01
 .26447000E-01
 -.37649730E-01
 -.14853970E-01
 .27160550E-01
 .82875600E-02
 -.19943650E-01
 -.43136740E-02
 .14593960E-01
 .18947140E-02
 -.10506890E-01
 -.48579350E-03
 .73671710E-02
 -.25847670E-03
 -.49891470E-02
 .57431590E-03
 .32358770E-02
 -.62437240E-03
 -.19861770E-02
 .53085390E-03
 .11382600E-02
 -.38236310E-03
 -.59535630E-03
 .22984380E-03
 .27902770E-03
 -.11045870E-03
 -.11235150E-03
 $h_1(0)=h_1(63)=$.35961890E-04



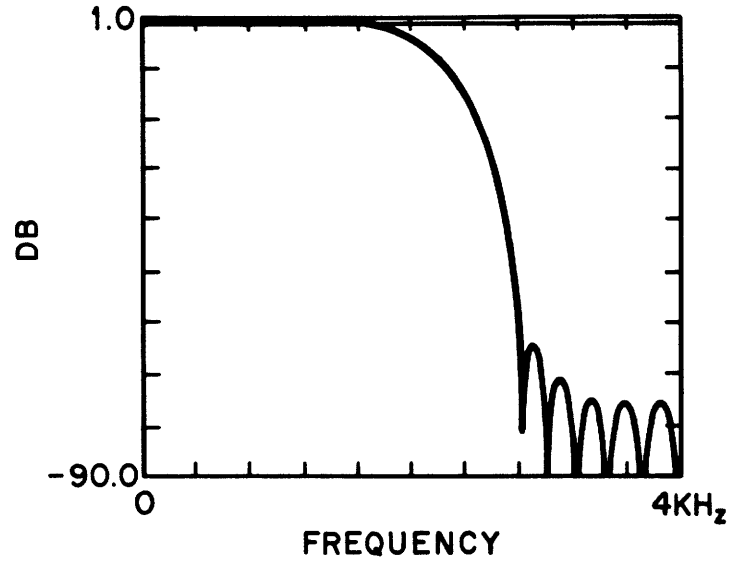
32 TAP DESIGN OF QM FILTER

$h_2(15)=h_2(16) = 4.6645830E-01$
 $1.2846510E-01$
 $-9.9800110E-02$
 $-3.9244910E-02$
 $5.2909300E-02$
 $1.4468810E-02$
 $-3.1155320E-02$
 $-4.1094160E-03$
 $1.7881950E-02$
 $-1.7219030E-04$
 $-9.3636330E-03$
 $1.4272050E-03$
 $4.1581240E-03$
 $-1.2601150E-03$
 $-1.3508480E-03$
 $h_2(0)=h_2(31) = 6.5064660E-04$

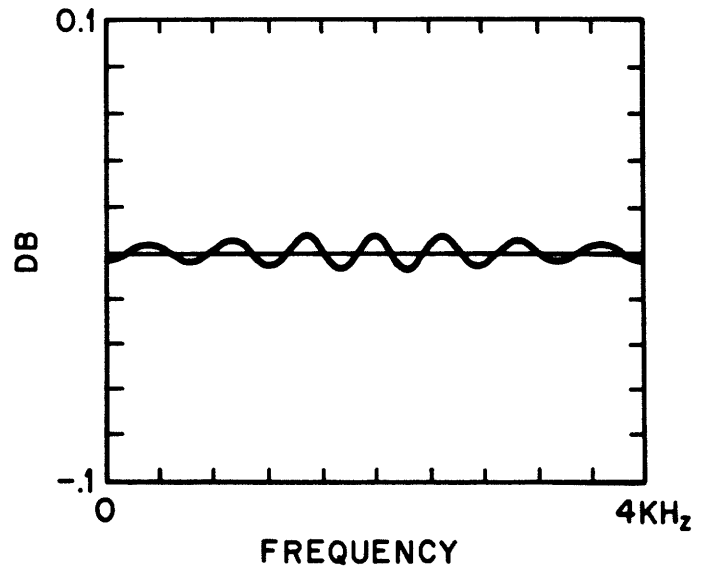


24 TAP DESIGN OF QM FILTER

$h_3(11)=h_3(12) = .47312890E\ 00$
 $.11603550E\ 00$
 $-.98297830E-01$
 $-.25615330E-01$
 $.44239760E-01$
 $.38915220E-02$
 $-.19019930E-01$
 $.14464610E-02$
 $.64858790E-02$
 $-.13738610E-02$
 $-.13929110E-02$
 $h_3(0)=h_3(23) = .38530960E-03$



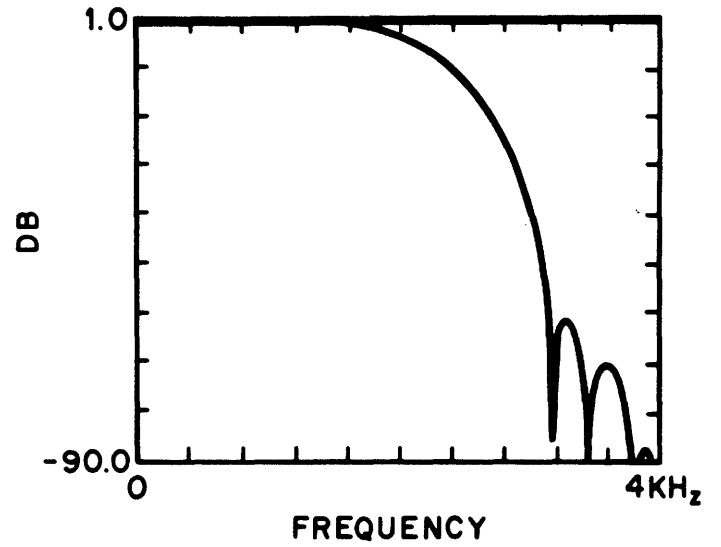
$$20 \log_{10} |H_3(\omega)|$$



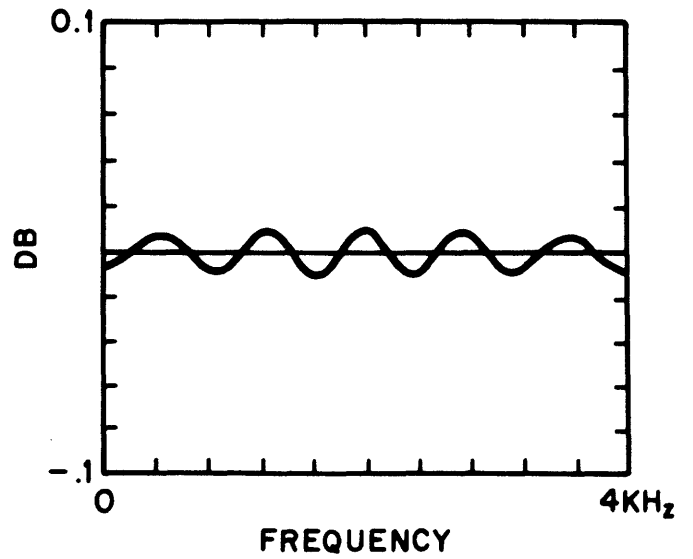
$$20 \log_{10} (|H_3(\omega)|^2 + |H_3(\omega+\pi)|^2)$$

16 TAP DESIGN OF QM FILTER

$h_4(7)=h_4(8) = .48102840E 00$
 $.97798170E-01$
 $-.90392230E-01$
 $-.96663760E-02$
 $.27641400E-01$
 $-.25897560E-02$
 $-.50545260E-02$
 $h_4(0)=h_4(15) = .10501670E-02$



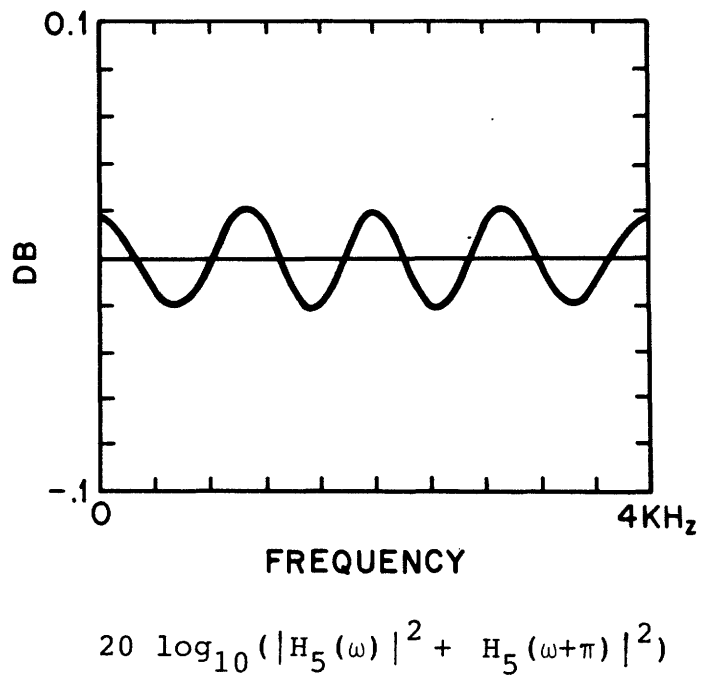
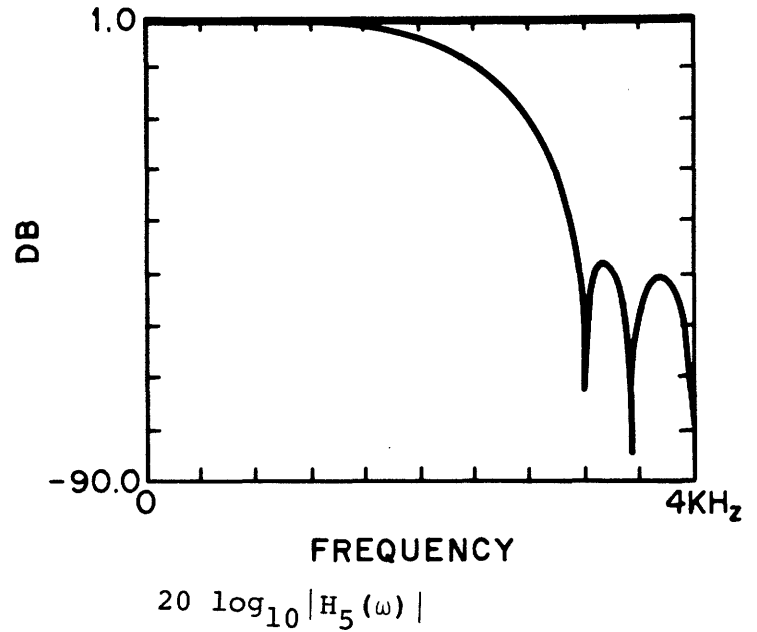
$$20 \log_{10} |H_4(\omega)|$$

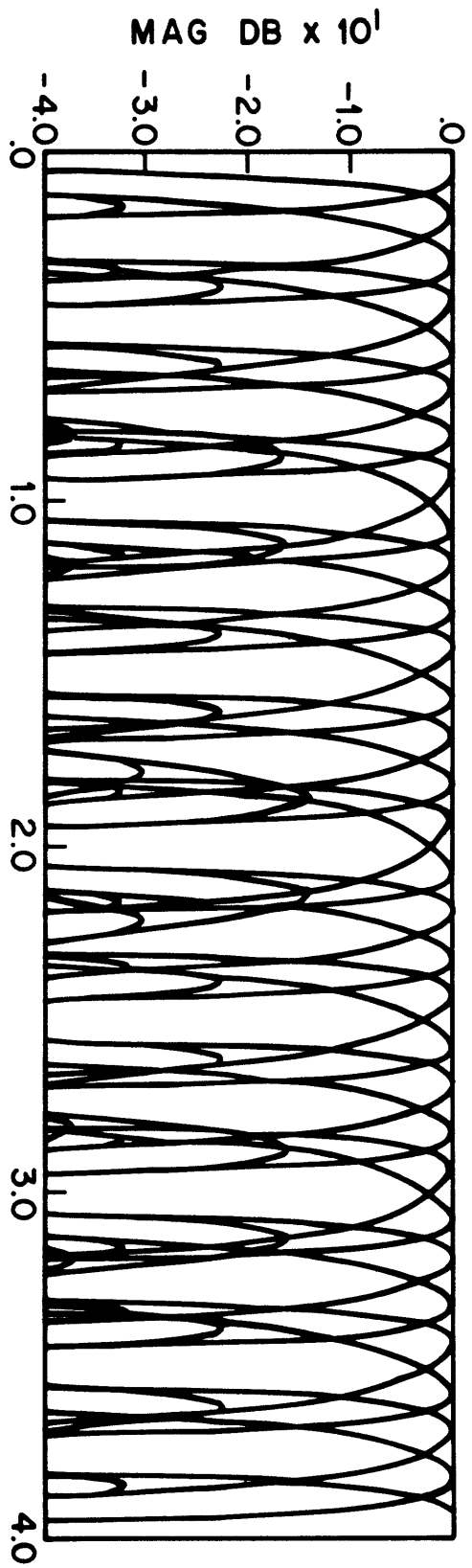


$$20 \log_{10} (|H_4(\omega)|^2 + |H_4(\omega+\pi)|^2)$$

12 TAP DESIGN OF QM FILTER

$$\begin{aligned}
 h_5(5) &= h_5(6) = .48438940E 00 \\
 &\quad .88469920E-01 \\
 &\quad -.84695940E-01 \\
 &\quad -.27103260E-02 \\
 &\quad .18856590E-01 \\
 h_5(0) &= h_5(11) = -.38096990E-02
 \end{aligned}$$





FREQUENCY (Hz) x 10³

Fig. I.1

Composite frequency response of the 32 band pass

$$\sum_{i=1}^{32} \text{QMF filters } |F_i(\omega)|$$

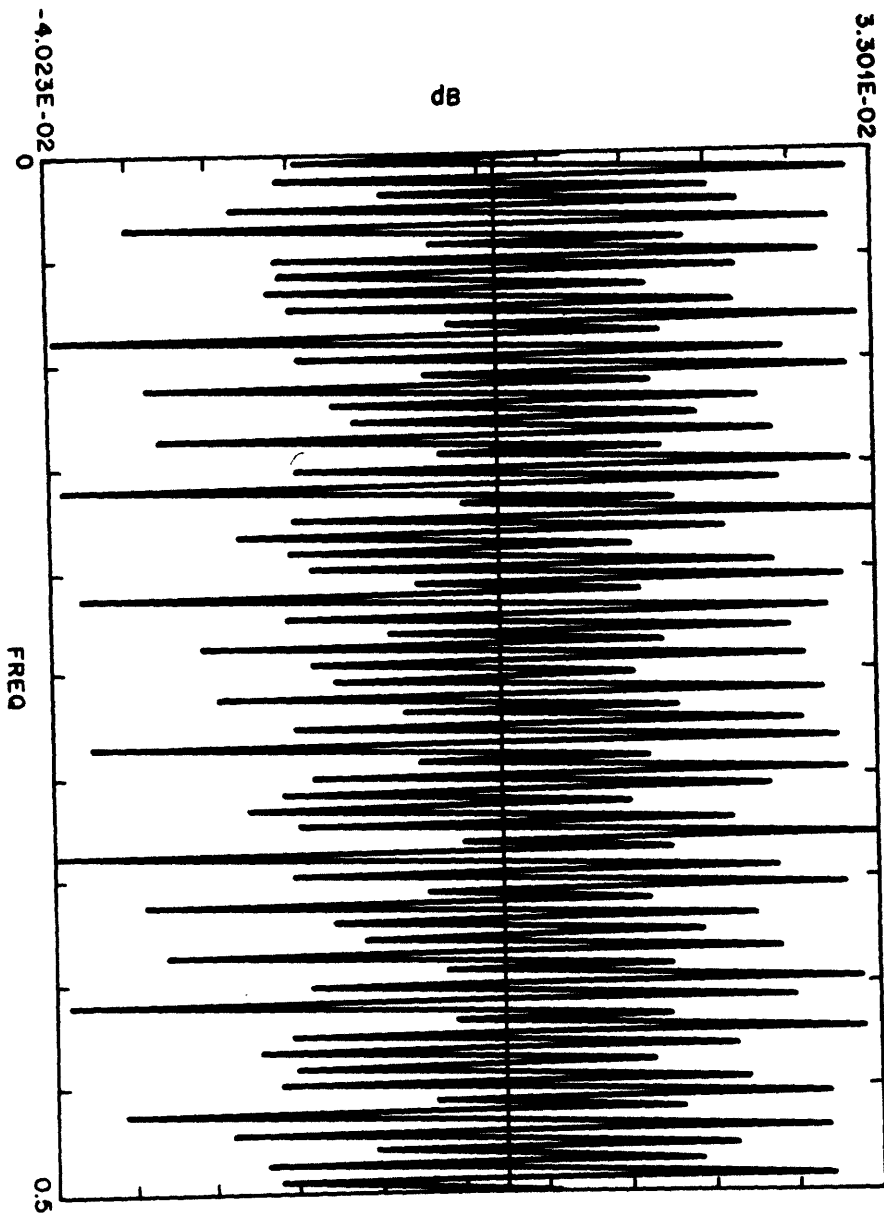


Fig. I.2 Magnitude ripple of the 32 band QMF analysis/synthesis filter bank.

APPENDIX II: FOURTH ORDER LPC TEMPLATES FOR 1,2,3,4, AND 5 BIT CODEBOOKS

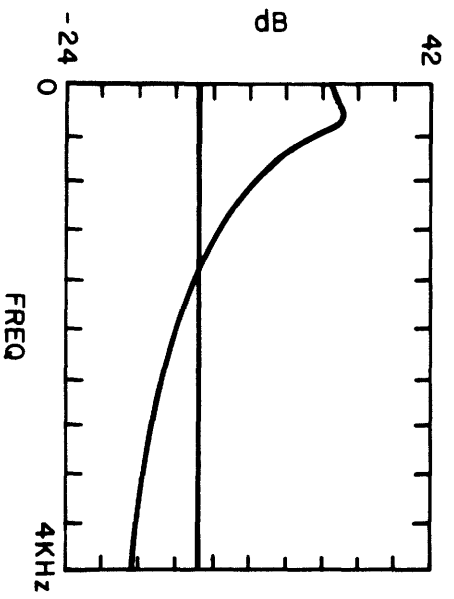
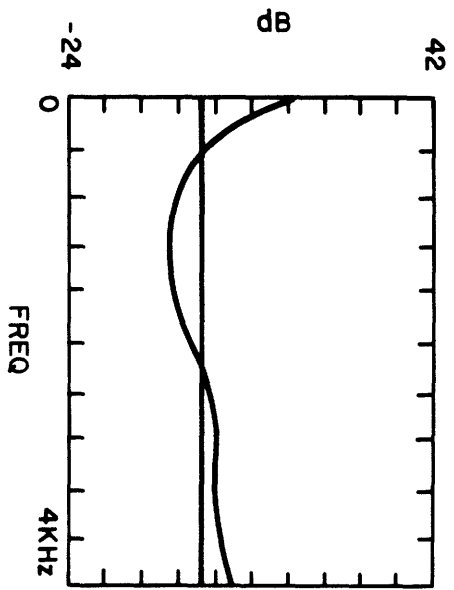


Fig. II.1a 1 bit template codebook.

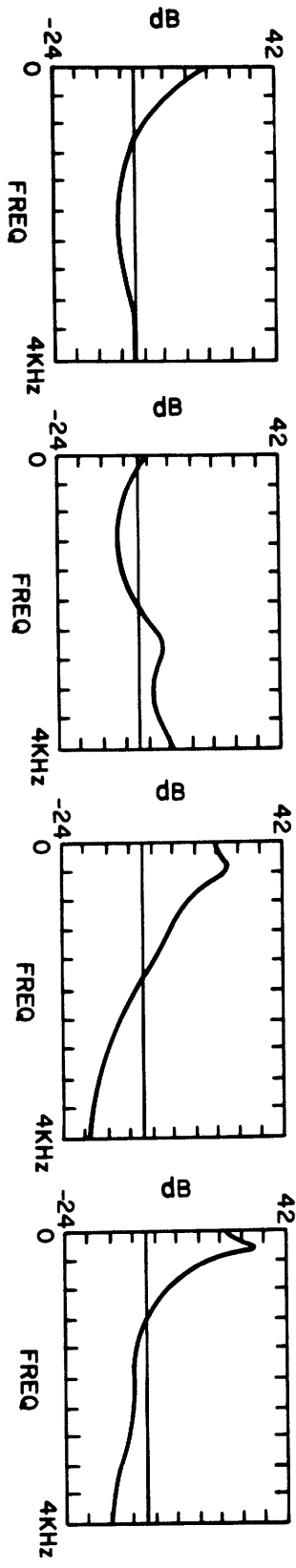


Fig. II.1b 2 bit template codebook.

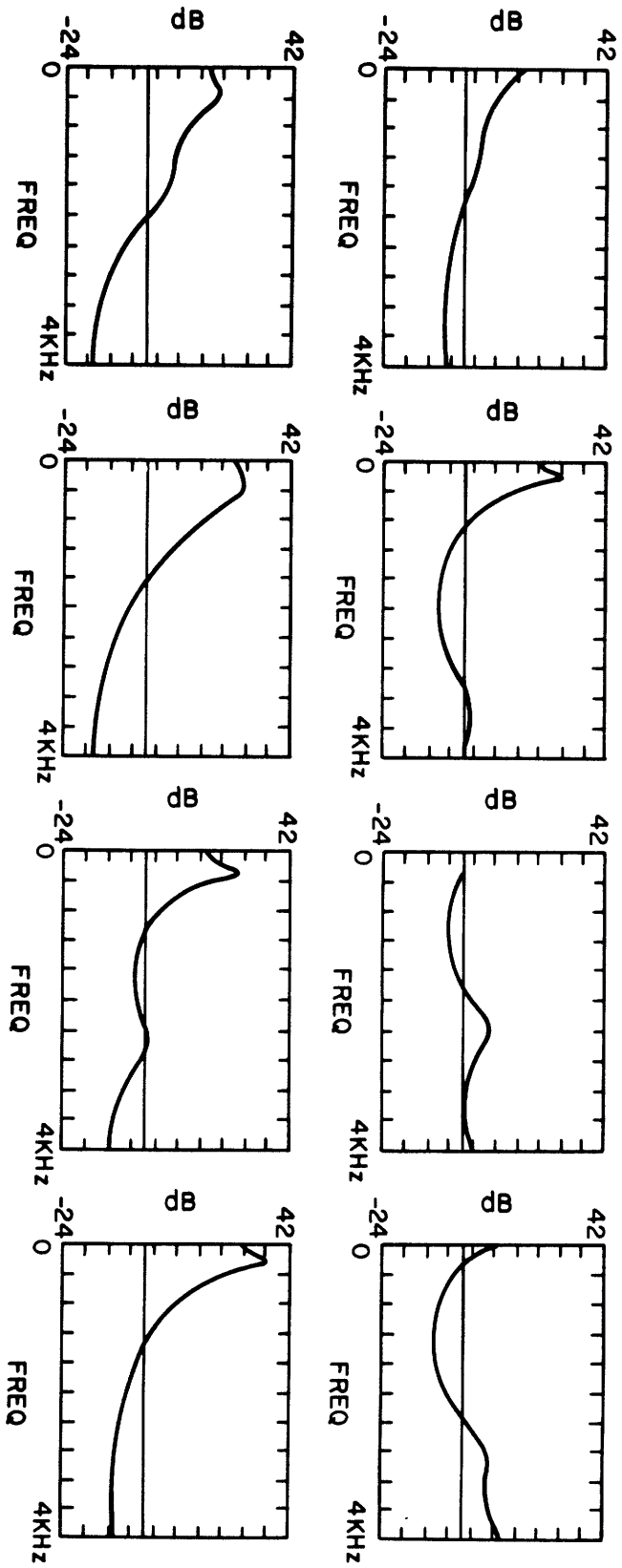


Fig. II.1c 3 bit template codebook.

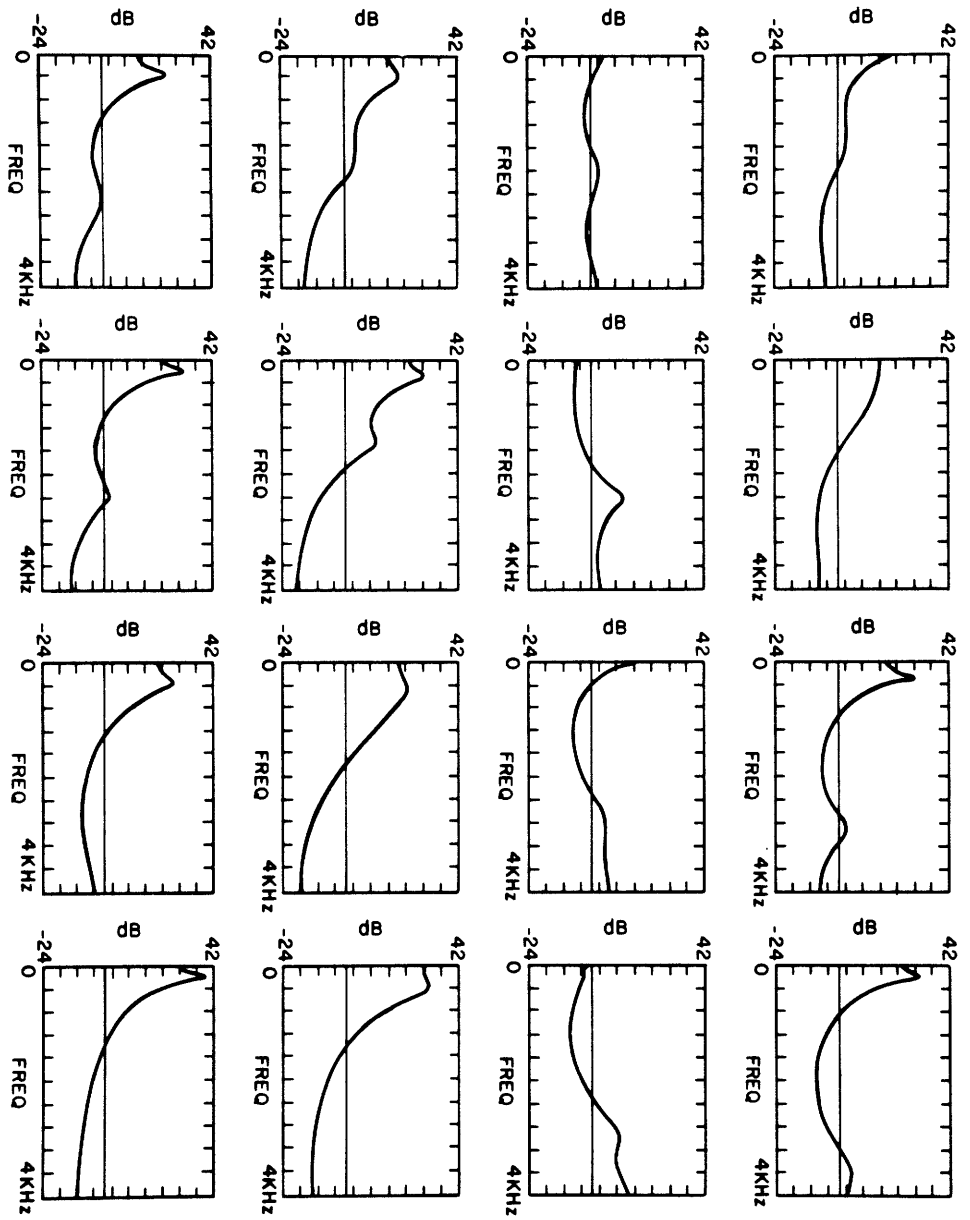


Fig. II.1d 4 bit template codebook.

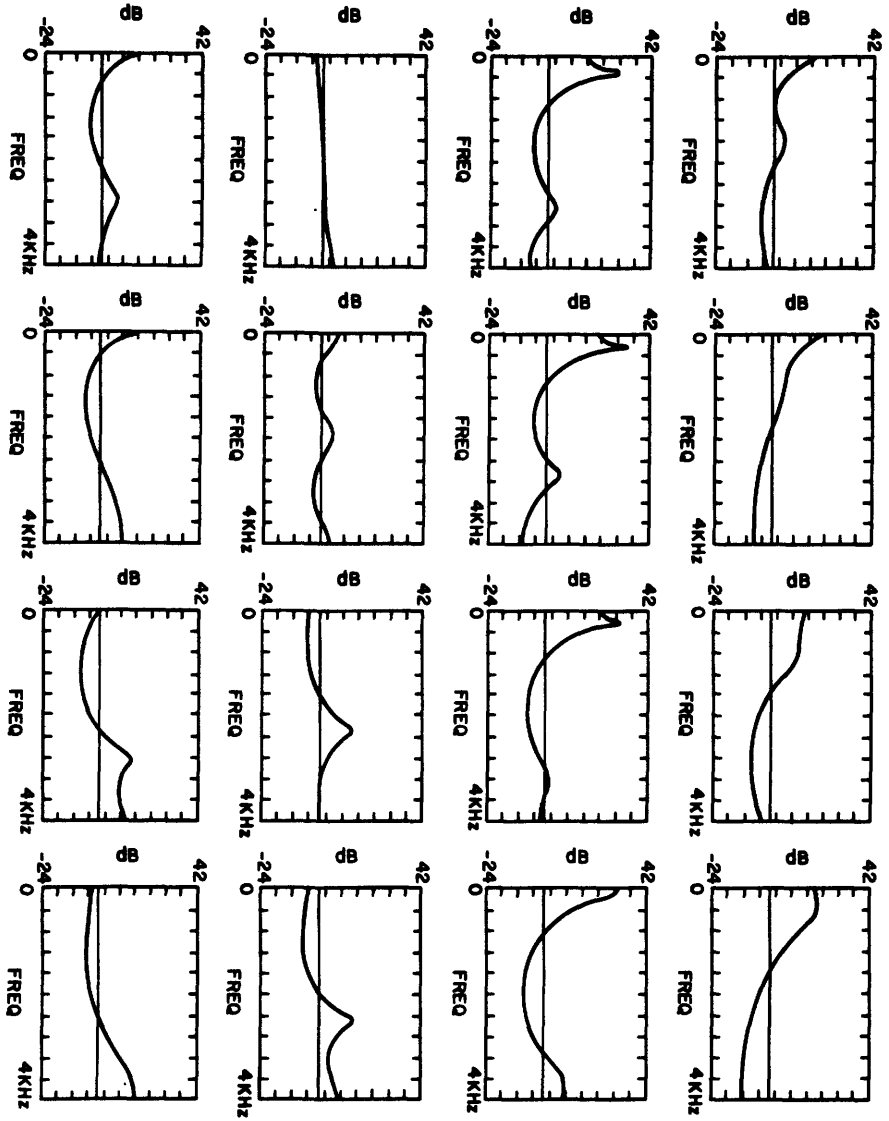


Fig. II.1e 5 bit template codebook.

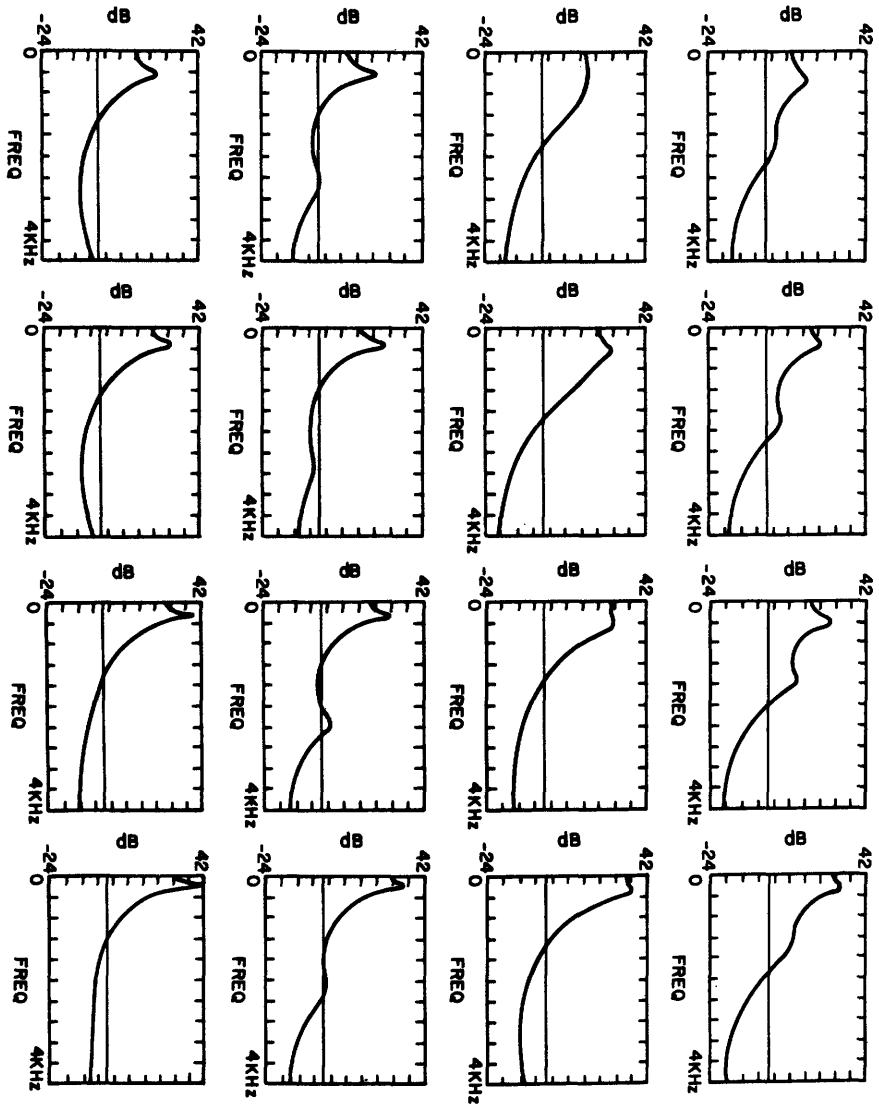


Fig. II.1e Con't.

**APPENDIX III: THE BIT ASSIGNMENT ALGORITHM USED FOR
GENERATING THE BIT ASSIGNMENT CODEBOOKS**

The bit assignment rule defined by Eqs. (4.3) and (4.4) is depicted by the flow chart in Figure III.1. Step 1 is to compute an estimate of D , the quantization noise in bits. Such an estimate has been given by Cox and Crochiere as [3]

$$D_1 = \frac{1}{32} \left[\sum_{i=1}^{32} (\log_2 \sigma_i) - B \right]. \quad (\text{III.1})$$

Steps 2 and 3 are direct implementations of Eqs. (4.4) and (4.3) respectively. If the estimated number of bits \tilde{B} is equal to the the B — the allowed number of bits/frame — the algorithm stops and b_i is the final bit assignment. If $\tilde{B} \neq B$ then D_1 is re-estimated as

$$D_1 = D_1 + \frac{\tilde{B} - B}{100} \quad (\text{III.2})$$

and the next iteration is performed. If the estimate \tilde{B} is too large the noise threshold D_1 is incremented by $(\tilde{B}-B)/100$. If \tilde{B} is too small the noise threshold D_1 is decremented by $(\tilde{B}-B)/100$.

As previously discussed, the magnitude spectrum of the input speech is modelled by a set of gain normalized LPC templates obtained by clustering techniques. Since each LPC template is associated with a unique bit assignment pattern, the terms σ_i in figure III.1 are derived from the templates. In general there are J templates each evaluated at the center frequency of each channel ω_i . For the J th template the RMS spectral magnitude estimate for each band is

$$\sigma_i = \left| \frac{1}{A(\omega_i)} \right| \quad i = 1, 2, \dots, 32 \quad (\text{III.3})$$

where $\frac{1}{A(\omega_i)}$ are derived from the LPC templates $\frac{1}{A(z)}$.

Since the purpose of an LPC template is to model the signal as seen by the quantizers for each channel, the magnitude of the template at the center of each channel frequency is obtained by filtering the template (obtained through clustering) with the appropriate QMF

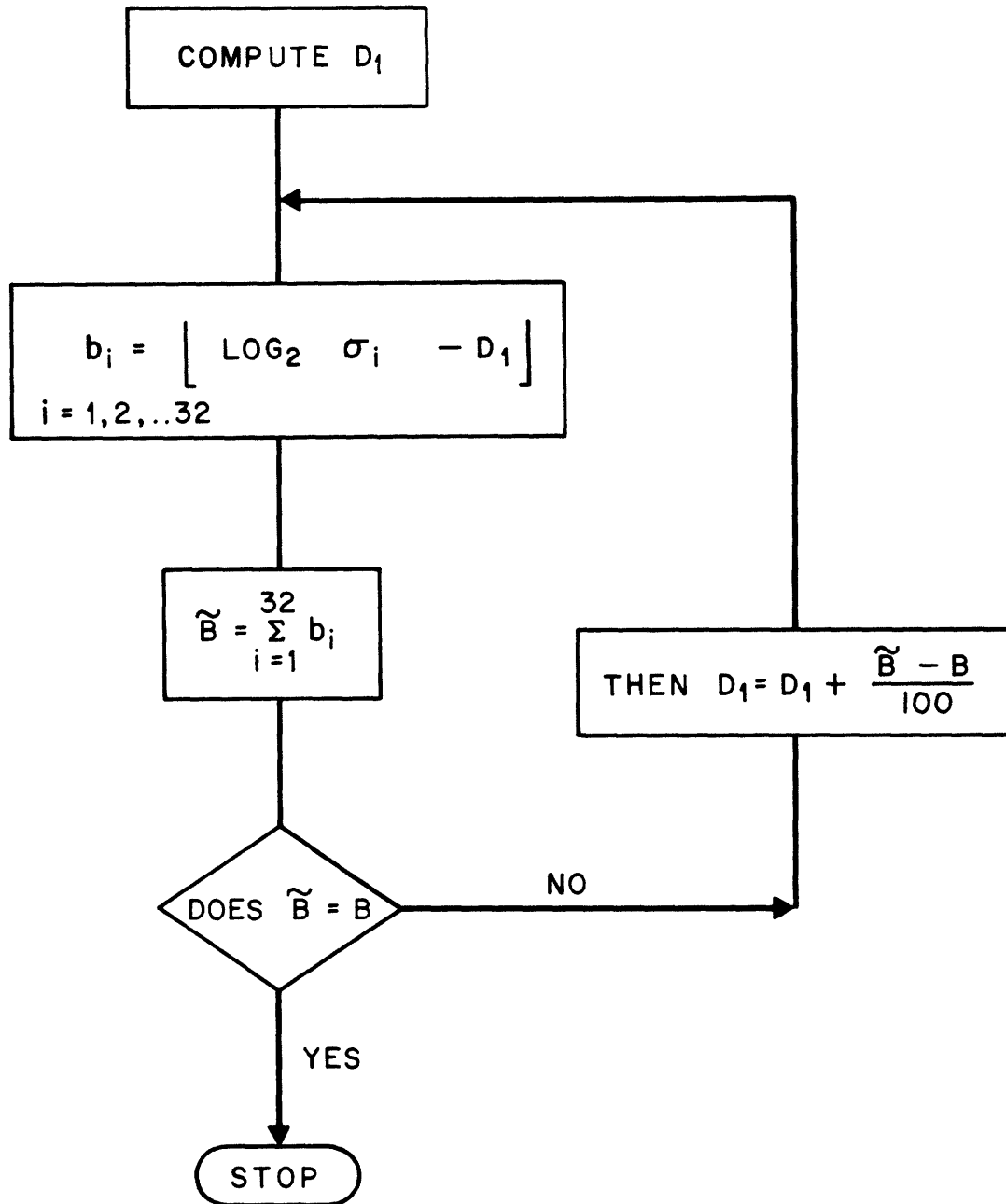


Fig. III.1 Flowchart of the bit assignment rule for a flat noise spectrum.

analysis filter $F_i(z)$ for that channel, then averaging to arrive at a modified template magnitude for the channel. This "template shaping" was achieved as follows for the i th channel:

1. Perform a 1024 pt DFT on the finite sequence $a(n) = Z^{-1}[A(z)]$ yielding

$$A(k) = A \left| (\omega)_{\omega = \frac{2\pi}{1024} k} \right. \text{ for } 0 \leq k \leq 1023.$$

2. Similarly compute a 1024 pt DFT on $f_i(n) = Z^{-1}[F_i(z)]$ to form $F_i(k) = F_i \left| (\omega)_{\omega = \frac{2\pi}{1024} k} \right.$

for $0 \leq k \leq 1023$.

The modified template magnitude for the i th channel is then.

$$\frac{1}{\hat{A}(\omega_i)} = \left[\frac{1}{513} \sum_{k=0}^{512} \left| \frac{1}{A(k)} \right|^2 \left| F_i(k) \right|^2 \right]^{1/2} \quad (\text{III.4})$$

Equation III.4 is the square root of the average energy of the LPC template in band i .

APPENDIX IV: THE D.S.P.

The DSP is a powerful, single chip, microprocessor that is especially suited for performing digital signal processing operations. A block diagram of this processor is given by figure IV.1. The DSP contains a) a 1024×16 bit ROM for storage of the program, tables, and coefficients, b) a 256×20 bit RAM for storage of state variables and dynamic data, c) a main arithmetic unit (AU) with provision for multiplication, full product accumulation, rounding and overflow protection, d) an address arithmetic unit (AAU) with address registers for controlling memory access and provision for updating these addresses, e) an I/O unit to control serial data transmission in and out of the chip, and f) a control unit which provides instruction decoding and synchronization. The analog-to-digital conversion for the DSP, including the lowpass filters, is done by a single μ -law PCM codec chip, also developed at Bell Laboratories [39]. A special instruction set in the DSP handles the conversion between μ -law and linear PCM.

The processor operates with an 400 nsec machine cycle time. In one machine cycle it can perform all of the following functions: a) fetch and decode an instruction, b) fetch data and perform a 16×20-bit multiplication, c) accumulate the output products from the multiplier, d) store data in memory and e) modify memory address under program control.

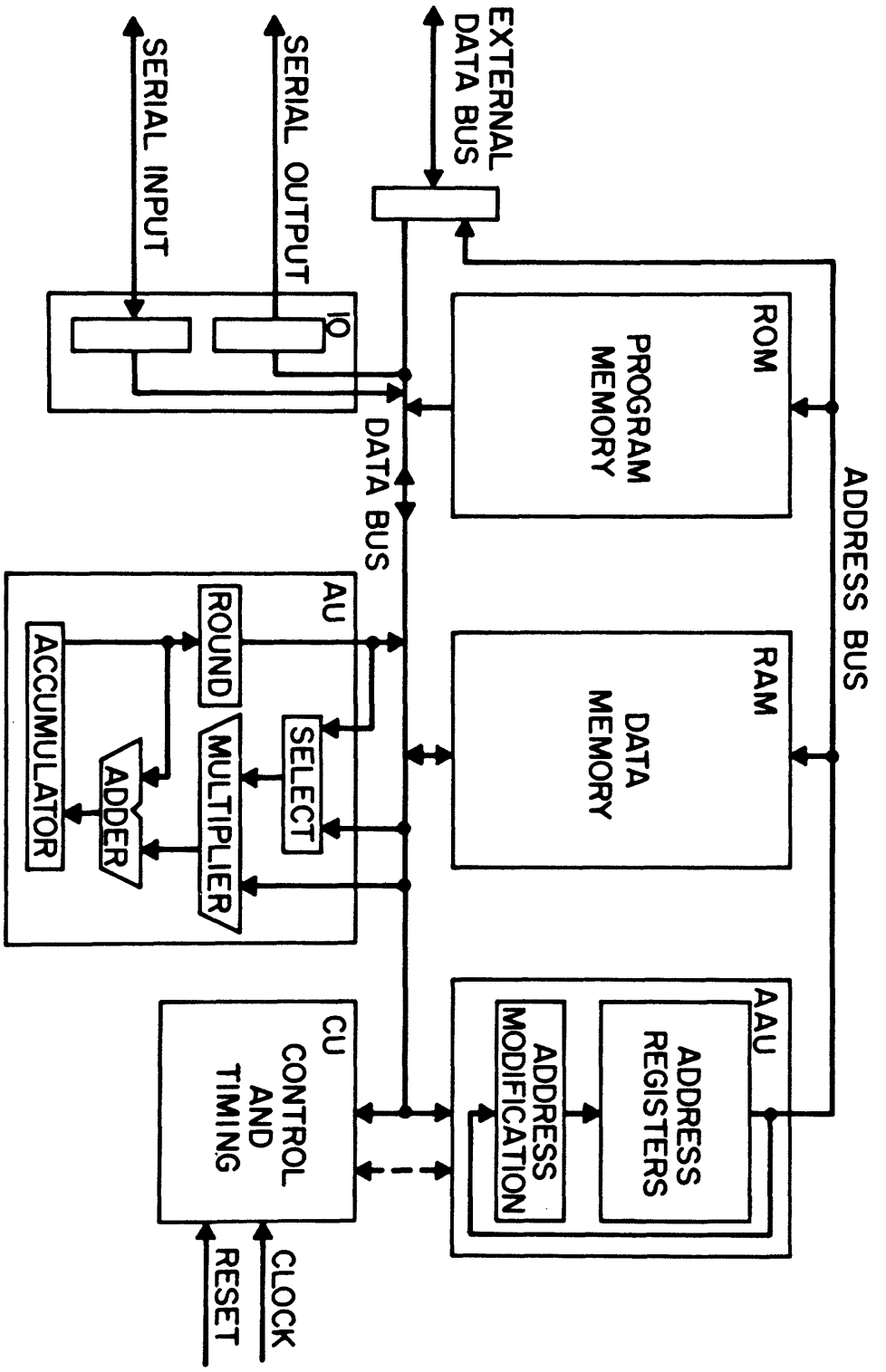


Fig. IV.1 Block diagram of the digital signal processor.

BIOGRAPHICAL NOTE

Courtney D. Heron was born in New York, New York, on May 20, 1959. He is a candidate for the degrees of Bachelor of Science and Master of Science in Electrical Engineering at the Massachusetts Institute of Technology. As an undergraduate at M.I.T., he belonged to Tau Beta Pi, Eta Kappa Nu, and the IEEE. He has been the recipient of a National Merit Scholarship, The Bell Telephone Laboratories Engineering Scholarship, and is a GEM Fellow in the National Consortium for Graduate Degrees for Minorities in Engineering. He is the first author of "A 32 Band Sub-band/Transform Coder Incorporating Vector Quantization for Dynamic Bit Allocation" (co-authored by R. E. Crochiere and R. V. Cox of the Acoustics Research Department at Bell Laboratories) which will be presented at the 1983 IEEE International Conference on Acoustics, Speech, and Signal Processing. His Master's thesis was done at Bell Telephone Laboratories where he worked under the M.I.T. 6-A Cooperative Program for three years.